Dissertation

Submitted to the
Combined Faculties for the Natural Sciences and for Mathematics of
the Ruperto-Carola University of Heidelberg, Germany for the degree
of Doctor of Natural Sciences

presented by
Ramón Leonardo Serrano, M.S.
Tovar, Mérida, Venezuela

Oral examination: 9th July, 2003

Structural and Functional Characterization of GAPR-1, a Mammalian Plant Pathogenesis-related Protein in Lipid-enriched Microdomains of the Golgi Complex

Referees: Prof. Dr. Felix T. Wieland
Prof. Dr. Wilhelm Just

Table of content

Abbreviations

AA(aa)	Amino acid
ARF	ADP-ribosylation factor
ATP	Adenosine tri-phosphate
BCA	Bicinchonic acid
BFA	Brefeldin A
bp	base-pair
BSA	Bovine serum albumin
CHAPS	3-[(3-cholamidopropyl1)dimethylammonio]-1-propanesulfonate
CHO	Chinese hamster ovary
CNBr	Cyanogen bromide
COP	Coat-protein
DMSO	Dimethyl sulfoxide
DRM	Detergent-resistant membranes
DTT	Dithiothretiol
EDTA	Ethylendiaminetetraacetic acid
ER	Endoplasmic reticulum
GDP	Guanosine di-phosphate
GPI	Glycosylphosphatidylinositiol
GTP	Guanosine triphospahte
hr	hour
IF	Immunofluorescence
IP	Immunoprecipitation
kDa	Kilo-Dalton
min	Minute
mut	Mutant
MOPS	Morpolinepropanesulfonic acid sodium salt
NP-40	Nonidet® P40 (Nonylphenylpolyethylene glycol)
NRK	Normal rat kidney
nt	Nucleotides
PBS-T	Phosphate buffer saline + Tween 20

PCR	Polymerase chain reaction
PI	Phosphatidylinositiol
PIPES	Piperazine-1,4-bis(2-ethanesulfonic acid)
PMSF	Phenylmethulsulfonyl fluoride
PR	Plant Pathogenesis-related
rpm	Revolutions per minute
sec	Second
SDS-PAGE	Sodium dodecyl sulfate-polyacrylamide gel electrophoresis
SNARE	Soluble N-ethylmaleimide sensitive factor attachment protein receptor
TCA	Trichloroacetic acid
TEMED	N, N, N', N'-Tetramethylethylenediamine
v-ATPase	vacuolar ATPase
wt	wild type

Abstract

During the characterization of lipid-enriched microdomains at the Golgi (GICs) (Gkantiragas, I. *et al.* 2001), a protein with an apparent molecular mass of 17 kDa was identified. Cloning and preliminary biochemical characterization identified a novel protein, GAPR-1, belonging to the superfamily of PR proteins. Based on the primary amino acidic sequence of this protein, some potentially interesting characteristics were identified. It contains a consensus sequence for myristoylation, a putative caveolin-binding domain, a coiled-coil structure, and an isolelectric point (pI) of 9.4, suggesting that GAPR-1 is a highly hydrophilic protein (Eberle, H. B. *et al.* 2002).

In this thesis, this structural information, was used to i) study the interaction of GAPR-1 with membranes, ii) to obtain structural information on the protein, and iii) to identify proteins that interact with GAPR-1.GAPR-1 was shown to be myristoylated and to interact with Caveolin-1. Myristoylation, together with protein-protein or electrostatic interactions at physiological pH could explain its strong membrane association. The crystal structure of GAPR-1 showed strong structural similarities to other plant pathogenesis-related proteins. Substitution of the most conserved amino acids in GAPR-1 (His54, Glu65, Glu86 and His103) in the putative active center changed the protein behavior in solution. Size exclusion chromatography revealed that the major population of GAPR-1 mutant migrated as a dimer, whereas GAPR-1 wild type behaves predominantly as a monomer. The tendency of GAPR-1 to form dimers was confirmed by crosslink experiments and by the yeast two hybrid system. By affinity chromatography, GAPR-1 was shown to interact with three proteins: Nucleolin, Template activating factor α (TAFIα) and HSAPRIL. In the yeast two hybrid system, the interaction of GARP-1 with Nucleolin was confirmed and shown to be dependent on the most conserved amino acid residues in GAPR-1. The interaction between GAPR-1 and Nucleolin may represent a new mechanism of regulation of innate immunity in mammalian cells.

Introduction

Cell membranes are dynamic and fluid structures and their molecules are able to move in the plane of the membrane. A membrane provides a two-dimensional fluid support for proteins as well as a hydrophobic barrier to separate compartments. It is believed that a cell or plasma membrane similar to those of today's cells defined the boundary of the first cell nearly 4 billion years ago. Since then, cells have evolved in such a way that the plasma membrane and intracellular membranes now perform many functions: as a barrier to keep the contents of the cell together, allowing nutrients to pass in but keeping out many harmful substances; as a signaling platform to relay information about the surroundings of the cell to the inside and vice versa; as a scaffold to provide places where enzymes can be arranged in an assembly-line fashion; and as a compartmentalizing structure to separate different parts of the cell with different functions.

1 Microdomains in biological membranes

Progress in identifying and characterizing the constituents of membrane bound compartments has revealed a distinct level of cellular and sub-cellular compartmentation. Proteins and lipids are not uniformly distributed in the membrane of a given organelle as domains are formed by a combination of hierarchical assembly processes and protein and lipid segregation. This implies that membranes should not be considered as a random ocean of lipids (Singer, S. J. Nicolson, G. L. 1972), but rather the existence of domain structures in the bilayer is acknowledged that impose an organization on the distribution of proteins. One of the important features of these domains is that the composition and physical properties differ from the overall properties of the membrane (Brown, D. 2002). Lipid-based structures within the membranes have been designated as lipid microdomains or lipid rafts. These heterogeneous structures in membranes were postulated by Simons and van Meer (1988). The first experimental evidence for the existence of lipid-enriched microdomains was obtained by the finding that in non-ionic detergents (*i.e.* Triton X-100) in the cold, certain lipids such as cholesterol and sphingolipids are detergent-insoluble. In addition, due to the enrichment of

lipids, these detergent-insoluble complexes have a low density as observed by flotation experiments in 5-30% linear sucrose gradients (Brown, D. A. Rose, J. K. 1992). Thus, the term raft refers to a domain in intact membranes, whereas the term detergent-resistant membrane (DRM) refers to the structure isolated by detergent insolubility. Due to their presence in the DRMs, many proteins are believed to be associated with lipid rafts, *e.g*. GPI-anchored proteins, transmembrane proteins, and dual acylated proteins such as tyrosine kinases (Src family) (reviewed in Simons, K. Ikonen, E. 1997). A wide variety of detergents other than Triton X-100 have been used to isolate low density detergent-insoluble membrane fractions, such as NP40, octylglucoside, CHAPs, lubrol and Brij96 (Ilangumaran, S. *et al.* 1999; Roper, K. *et al.* 2000; Bagnat, M. Simons, K. 2002; Drevot, P. *et al.* 2002). Detergent-free preparations of lipid microdomains and microdomain preparations in the presence of low TX-100 concentrations have also been reported (Song, K. S. *et al.* 1996).

Lipid rafts or lipid-enriched microdomains can be defined as subdomains of the plasma membrane, containing high concentrations of cholesterol and sphingolipids (sphingomyelin and glycosphingolipids). In these domains, cholesterol condenses the packing of sphingolipid molecules by occupying the spaces between the saturated chains. Thus, a separate liquid-ordered phase (l_o) is formed, which is dispersed in the liquid disordered phase (l_c), the latter representing a freely packed fluid matrix of the membrane (Fig. 1). How the exoplasmic arrangement of sphingolipids and cholesterol is linked to the underlying cytoplasmic leaflet is currently not known. Lipid rafts incorporate distinct classes of proteins (Brown, D. A. London, E. 1998), such as glycosylphosphatidylinositol (GPI)-anchored proteins, dual acylated peripheral membrane proteins, cholesterol-linked proteins (Caveolin), and selected transmembrane proteins (Fig.1). Little is known about the targeting of proteins to lipid-enriched microdomains. A number of these proteins containing a combination of covalently attached fatty acids (myristate and palmitate) at their N-termini (Galbiati, F. *et al*. 1999b; Melkonian, K. *et al*. 1999; van't Hof, W. Resh, M. 1997). This suggests that two saturated acyl chain can cause partitioning of proteins into lipid microdomains. Other reports show that a single prenyl group or myristate group alone can be sufficient to target a

protein to lipid microdomains (Song, K. S. *et al.* 1996). In these cases, N-terminal acylation, coupled with protein-protein interactions or protein-lipid interactions, can cause partitioning of a protein to DRMs (McCabe, J. B. Berthiaume, L. G. 2001).

While there is abundant evidence that such microdomains exist and that they perform important functions, it has proven very difficult to obtain experimental evidence for their existence *in vivo*, including a description of their properties in terms of size, composition and dynamics. As mentioned above, the existence of different types of membrane (micro)domains adds to the difficulty in understanding their properties. For instance, Caveolae are one type of microdomain at the plasma membrane (Fig. 1). They are small (50-70nm in diameter) flask-shaped invaginations with an abundant membrane protein, Caveolin, associated with their structures (Kurzchalia, T. V. Parton, R. G. 1999). Caveolae can also be flat within the plane of the membrane, or be present as vesicles. These structures are cholesterol-rich, and when cells are treated in the cold with non-ionic detergents (*i.e.* Triton X-100), caveolae resist detergent-solubilization and can be recovered in low-density fractions on density gradients. Caveolae are enriched in molecules that play crucial roles in intracellular signal transduction. These molecules include the heterotrimeric G proteins, receptor tyrosine kinases, components of the MAP kinases pathway, and nitric oxide synthase (reviewed in Smart, E. *et al*. 1999). As a consequence, caveolae function as preassembled signaling complexes or chemical relays for integrating signal transduction. Interestingly, caveolae are only a minor fraction within DRMs (Kurzchalia, T. V. Parton, R. G. 1999) and the existence of large amounts of non-caveolar (glycosphingolipids(GSL)-enriched) domains in the plane of the membrane (Iwabuchi, K. *et al*. 1998) adds to the complexity of lateral organizations in the plasma membrane for complex activities such as signal transduction (Anderson, R. 1998) (Vincent, J. 2003).

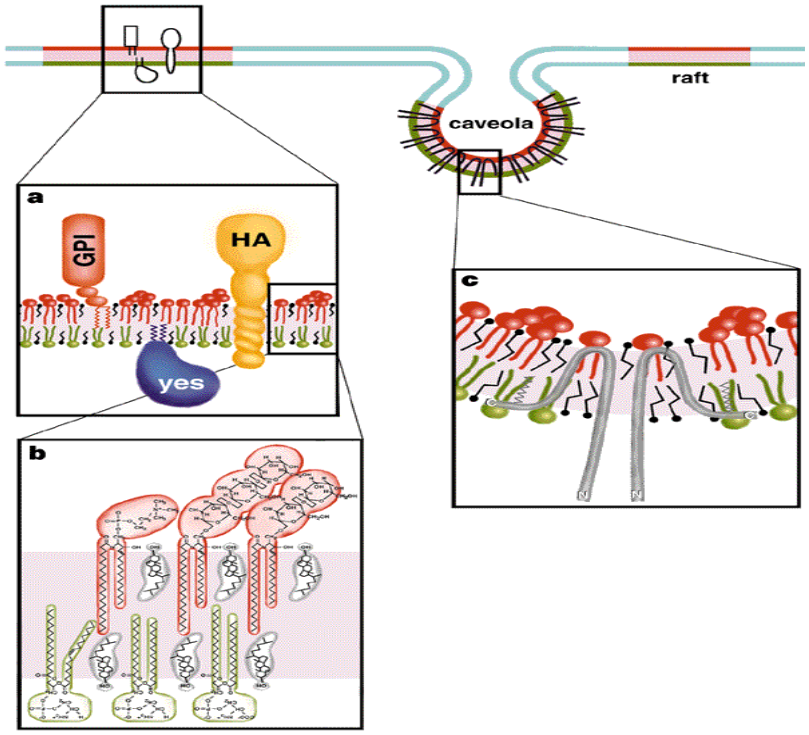

***Figure 1*. Model of a lipid-enriched domain at the plasma membrane.** (**a**). A GPI-anchored protein is attached to the exoplasmic leaflet, and a doubly acylated Src-kinase to the cytoplasmic leaflet or a transmembrane protein (HA). Lipids in the raft are shown as red and green, and the lipids in the liquid disordered phase as blue. (**b**) The lipid bilayer in rafts is asymmetric with sphingomyelin (red) and glycosphiongolipid (red) enriched in the exoplasmic leaflet and phospholipids (green) e.g phophatidylserine and phosphatidylethanolamine. Cholesterol (grey) is present in both faces of the membrane filling the space under the head groups of sphingolipids (**c**) Caveolae formed by caveolin molecules making a hairpin lop in the membrane, and the interaction with rafts may be mediated by binding of cholesterol and acylation of C-terminal cysteines. (Picture taken from Simons, K. and Ikonen, E. 1997).

1.1 Lipid microdomains and signal transduction

Experimental evidence suggests that there are several different mechanisms through which lipid microdomains may control cell signaling. Lipid rafts may contain complete signaling pathways that are activated when a receptor or other required molecule is recruited into the raft. In this view, rafts serve to co-localize the prerequisite components, facilitating their interaction and supporting signaling. Thus, receptors, coupling factors, effector enzymes and substrates would all be co-localized in a single microdomain, and specificity of signaling could be enhanced by restricting receptor localization to a particular class of microdomains that contains a specific subset of signaling components (Cary, L. Cooper, J. 2000). This restriction would limit access of the receptor to components of other signaling pathways and prevent non-specific signaling

(Langlet, C. *et al*. 2000 (Oh, P. Schnitzer, J. E. 2001;Prior, I. A. *et al.* 2001). In this model, microdomains could also contain a nearly complete signaling pathway that would be activated when a receptor or other require molecule, that is normally localized in the non-raft portion of the membranes, is recruited to the rafts (Roy, S. *et al.* 1999). As an alternative how rafts may control cell signaling, rafts could also limit signaling, either by physical sequestration of signaling components to block non-specific interactions or by suppressing the intrinsic activity of signaling proteins present within rafts (Mueller, G. Frick, W. 1999; Mettouchi, A. *et al*. 2001). In these scenarios, microdomains may provide regulation *via* compartmentalization of proteins that could otherwise interact, leading to unregulated activation of a pathway. Many receptor tyrosine kinases including the EGF receptor, the PDGF receptor, and the insulin receptor have been reported to control cell signaling by modulating their intrinsic activities due to lipid microdomain localization (Mineo, C. *et al*. 1996, Anderson, G. 1998). The involvement of lipid rafts in the function of proteins has been studied by different approaches such as depleting cells of cholesterol. Lipid rafts are held together via interactions between cholesterol and sphingolipids and the integrity can be disrupted by treatment with methyl-β-cyclodextrin that removes cholesterol (Kilsdonk, E. *et al*. 1995; Pike, L. Miller, J. 1998). Cholesterol depletion *e.g.* impairs the ability of receptor tyrosine kinase to signal, diminishes insulin-stimulated phosphorylation of its receptor, or affects insulin-stimulated glucose uptake and oxidation (Vainio, S. *et al*. 2002; Parpal, S. *et al*. 2001).

1.1.1 Lipid microdomains and their potential role in immune cell activation

One of the best described examples on the involvement of lipid rafts in cellular signaling processes are T cells. Cells of both the innate and adaptive immune systems express a variety of receptors that allow them to respond to the presence of foreign macromolecules in a highly discriminating and sensitive fashion. Multichain immune recognition receptors (MIRRs) in lymphocytes, for instance, are surface receptors formed by the association of immunoglobulin-like subunits (recognition subunits) and transducing subunits. The TCR, BCR and FcεRI are among the best studied MIRRS in terms of signal transduction mechanisms (Dykstra, M. *et al.* 2003). These molecules are activated through

phosphorylation by the Src family protein tyrosine kinases such as LcK, Fyn or Lyn. Membranes lipid microdomains are enriched in Src proteins (Resh, M. D. 1999) and upon activation of Lyn and Lck, engagement of FcεRI (Field, K. *et al*. 1995) and TCR (Horejsi, V. *et al*. 1999) in membrane rafts is observed. This implies that microdomain location is crucial for downstream signaling events. In the case of the TCR, upon ligand engagement, the microdomain-associated receptor complexes are highly enriched in hyperphosphorylated p23 ζ chains (Montixi, C. *et al*. 1998) and TCR-CD3 associated complexes. This supports the idea that MIRRs directly transmit information via membrane rafts upon ligation. MIRR signaling in a restricted area of the membrane therefore permits a quick and efficient connection to signaling cascades upon receptor engagement. Still the implications of protein sequestering into lipid rafts are not completely clear. Membrane proteins in the lipid rafts could favor the formation and stabilization of supramolecular complexes by e.g. sequestering some proteins away from the endocytic pathway. This could promote sustained signaling, a mechanism considered of vital importance during immune response (Langlet, C. *et al*. 2000). During the adaptive and innate immune response, microdomains could also be involved to establish functionally distinct signaling domains during antigen recognition.

1.2 Membrane domains in the secretory pathway

The primary function of the Golgi apparatus is the stepwise modification and sorting of cargo synthesized in the endoplasmic reticulum (ER) and destined for different cellular and extracellular locations (Rothman, J., Wieland, F. 1996). Many hypotheses have been proposed to understand the general concept of transport. Golgi anterograde transport may require vesicles, tubules and cisternal-mediated transport (reviewed in Marsh, B., and Howell, K. 2002). In the case of vesicular transport, a heptameric cytosolic protein complex called COPI (coatomer), in conjunction with the GTP binding protein ARF1, forms an electron-dense coat on Golgi membranes, facilitating membrane budding and fission events associated with Golgi membrane traffic (Nickel, W., Wieland, F. 1998). Recruitment of COPI onto Golgi membranes requires ARF1, which, like all GTPases, cycles between a GDP-bound, inactive, and a GTP-bound, active form. ARF-1-GTP assembles COPI onto

Golgi membranes, whereas GTP hydrolysis is thought to trigger membrane release of COPI into the cytosol (Donaldson, J. *et al*. 1992). This makes COPI available for repeated cycles of coat assembly and disassembly. ARF1 thus operates as a switch to control COPI assembly onto membranes and therefore to regulate its function (Rothman, J., Wieland, F. 1996; Helms, J. and Rothman, J. 1992; Donaldson, J. G. *et al.* 1992). The binding of ARF and coatomer onto membranes creates a local domain, involved in sorting of cargo and budding of vesicles. Coatomer binds to the C-terminal KKXX motif of transmembrane proteins that cycle between the Golgi and ER interface (Sohn, K. *et al.* 1996). This carboxyl-terminal peptide functions as ER retrieval sequence (Nilsson, T. *et al*. 1989). By interaction of COPI-subunits with cytoplasmic tails of cargo proteins, resident proteins displaying the K(X)KXX-like sequence are recognized directly by the coat, and sorted into budding vesicles which then returns the resident proteins to earlier compartments in the pathway. COPI-coats therefore collect cargo into transport vesicles and mediate cargo sorting (Cosson, P. Letourneur, F. 1994). In addition to the KKXX sequence, many lumenal ER resident proteins contain a carboxyl terminal peptide with a KDEL-sequence, which functions also as retrieval signal returning lost ER proteins from as far away as the trans-Golgi network. Both motifs are capable to retain certain molecules in the ER through constant retrieval from post ER compartments.

Many of the proteins going through the Golgi complex become modified by the action of enzymes present within the Golgi, followed by the sorting of the final product to its final destination. In mammalian cells, the Golgi is comprised of a ribbon of flattened stacks of cisternae that are interspersed by opening of various sizes, through which tubules project and vesicles can move (Ladinsky, M. S. *et al.* 1999). Proteins enter the stack at one face, the cis-Golgi network and eventually exit the stack at the other face, the trans-Golgi network. It has been recognized that individual cisternae include different set of proteins and that the lipid composition changes from one side of the Golgi stack to the other. For instance, the *cis*-Golgi contains the O-linked oligosaccharide-modification enzyme, N-acetylgalactosamine transferase; the medial Golgi contains N-aceylglucosamine transferase I; whereas the TGN contains sialyl-transferase. In addition to the segregation of

enzyme activities between cisternae, each individual cisterna is segregated into domains by the assembly of transport vesicles: vesicles form exclusively at the cisternal rims and not in the middle of cisternal structures. The Golgi must retain resident proteins in one domain and catalyze vesicle formation in another (Warren, G. Malhotra, V. 1998; Shorter, J. Warren, G. 2002). Thus, as is postulated for the ER (see below), vesicle formation may represent a mechanism by which membrane domains are generated. When an ER retention signal is attached onto one of two medial Golgi enzymes, it was found that ER retention of one medial Golgi enzyme led to ER accumulation of the other untagged (Nilsson, T. Warren, G. 1994). In contrast, ER retention of a trans Golgi enzyme had no effect on the distribution of the medial Golgi enzymes (reviewed in Ward, T. H. *et al.* 2001). This suggests that the two medial Golgi enzymes are in domains as well, possibly a Golgi matrix.

A detergent-insoluble Golgi matrix was identified that binds specifically to medial-Golgi enzymes and contains the protein GM130 (Shorter, J. Warren, G. 2002). GRASP65, a *cis*-Golgi surface protein required for stacking of Golgi cisternae *in vitro* (Barr, F. *et al*. 1997) binds to GM130, and GM130 binds to the vesicle docking protein p115 and to Rab1, a GTPases needed for ER to Golgi transport. P115 also interact with Rab1 (Nakamura, N. *et al*. 1997). Thus a *cis*-Golgi matrix, comprised minimally of GRASP65 and GM130, exists as an independent unit that can be recognized by vesicle docking and tethering machinery constituents (Rab1 and p115). Therefore, these proteins represent a mechanism in which the Golgi matrix could play a role for incoming vesicles recognizing the compartment at the Golgi and delivering the secretory cargoes.

The Golgi apparatus is also the major site of sphingolipid biosynthesis within the cell and acts as a buffer between the glycerolipid-rich ER and the sterol/sphingolipid-rich plasma membrane (van Meer, G. 1989). In the Golgi a gradient of cholesterol exists across the cisternae, with higher levels in the *trans* side (Pagano, R. E. *et al.* 2000). To explain this gradient, it was proposed that cholesterol-rich membrane domains are selectively transported forward through the Golgi toward the plasma membrane (Bretscher, M., Munro, S. 1993). Lipid rafts could also be involved in maintenance of the

distinct lipid compositions of the plasma membrane and organelles of the secretory pathway that are maintained in the face of membrane traffic in both directions (Mukherjee, S. Maxfield, F. 2000).

The importance of membrane microdomains in trafficking (Simons, K. Ikonen, E. 1997; Pfeffer, S. 2003) was shown at late stages of the secretory pathway and in the endocytic pathway. Membranes of the Golgi, TGN, and endocytic pathway can contain significant amounts of cholesterol and sphingolipid that may partition in microdomains as observed at the plasma membrane (Brown, D. A. London, E. 1998).Sorting of cargo proteins can be coupled to lipid sorting if proteins partition preferentially into lipid rafts (Simons, K. Ikonen, E. 1997). ER to Golgi transport of GPI-anchored proteins, for instance, is selectively retarded when sphingolipid synthesis is inhibited (Skrzypek, M. *et al*. 1997), suggesting that lipid microdomains form in the ER and that GPI-anchored proteins must partition into these domains for efficient transport (Sütterlin, C. *et al*. 1997). However, GPI-anchored proteins are detergent-soluble when present in the ER and only become detergent-insoluble in the medial-Golgi during biosynthetic transport (Brown, D. A. London, E. 2000). Maybe microdomains in the ER are only held together by weak interactions that are disrupted by addition of Triton X-100.

1.3 Golgi apparatus as a signaling platform

Coatomer and Cdc42 interact at the Golgi apparatus and this interaction affects both secretory traffic and cellular growth control. This raises the possibility that the Golgi functions as a scaffold for cell signaling (reviewed in Donaldson, J. Lippincott-Schwartz, J. 2000). It is likely that mammalian cells have exploited Golgi membranes and their unique cellular setting to regulate several key cellular processes during evolution. The Golgi is situated between the ER and the plasma membrane (PM), at the intersection of a variety of membrane trafficking pathways. A variety of signaling molecules associate with Golgi membranes, including heterotrimeric G proteins, PI(3)kinase, eNOS and Cdc42 (McCalllum, S. *et al*. 1998; Garcia-Cardena, G. *et al.* 1997); Godi, A. *et al*. 1999). Golgi membranes also interact with a variety of motor and cytoskeletal proteins, including p200/myosin II, myosin I, V, and VI, dynein, spectrin, and ankyrin (De Matteis, M. A. Morrow, J. S. 1998) that

facilitate the Golgi's spatial control of membrane traffic but also might help to coordinate signaling pathways.

Signaling cascades at the Golgi complex may be regulated by lipid-enriched microdomains as well. The presence of such domains at this organelle is supported by several lines of evidence.

First, Lipid microdomains have been identified at several organelles along the late secretory pathway and endocytic pathway (including endosomes (Nichols, B. *et al*. 2001)), caveosomes (Pelkmans, L. *et al.* 2001) and phagosomes (Dermine, J. F. *et al.* 2001). Via membrane trafficking pathways, the Golgi complex is connected to these organelles and evidence exists that also raft components travel between the Golgi and these compartments. Proteins such as TGN38 and STxB travel from the plasma membrane to the Golgi complex. They are taken up via clathrin-coated pits into transferrin-positive recycling endosomes and sorted for subsequent delivery to the Golgi complex (Gosh, R. *et al*. 1998; Mallard, F. *et al*. 1998). The folate receptor, a GPI-anchored protein, also recycles via this pathway and the recycling efficiency appears to depend on raft partitioning (Mayor, S. *et al*. 1998). Other rafts markers *en route* to the Golgi are, however, separated from the pathway followed by transferrin (Nichols, B. *et al*. 2001), implying that certain lipid microdomains continuously circulate between plasma membrane and Golgi pools, possibly via caveosomes.

Second, it has been observed that cholesterol is essential for the biogenesis of secretory vesicles from the TGN, suggesting that this process requires the formation of lipid rafts (Wang, Y. *et al*. 2001). At the TGN, assembly of glycosphingolipids together with cholesterol into lipid microdomains suggests a means of packaging glycosphingolipids into the curved lumenal membrane side of secretory vesicles. In this model, lipid rafts coincide with secretory vesicle formation, and this has been suggested for the formation of constitutive secretory vesicles to the apical membrane (Röper, K. *et al*. 2000). Lipid rafts in the TGN may contribute to the driving force for the formation of secretory vesicles.

Third, microdomains have been isolated from early Golgi compartments (Gkantiragas, I. *et al.* 2001). These microdomains contain a unique subset of proteins and lipids as compared to other membrane rafts. These detergent-insoluble complexes in the Golgi have been denominated as GICs (Golgi-derived detergent-insoluble complexes). Similar to other types of DRMs, it reveals an enrichment of sphingolipids and cholesterol. This lipid-scaffold seems to be required for GICs integrity (Gkantiragas, I. *et al.* 2001). Interestingly, GIC proteins and lipids are segregated for COPI vesicles, suggesting that they are not involved in the budding of COPI-vesicles at the early Golgi complex. Since the core complex travels through the early secretory pathway, an as yet unknown and distinct mechanism must exist by which GICs are transported. The presence in GICs of heterotrimeric G proteins (α and β subunits) opens the possibility that these microdomains are involved in signal transduction at the Golgi complex. GICs are composed of ten major proteins (Fig. 2): 1) Caveolin-1, which has been implied in regulating the function of heterotrimeric G proteins (Okamoto, T. *et al.* 1998) and which localizes predominantly to detergent-resistant complexes at the plasma membrane; 2-3) α and β subunits of heterotrimeric G proteins, implicated in signal transduction (Moffet, S. B., Deborah; Linder, Maurine. 2000), membrane fusion (Helms, J.B. *et al.* 1998) and maintenance of Golgi structure (Jamora, C. *et al.* 1997; Yamaguchi, T. *et al.* 2000); 4-7) 4 subunits of the V1 domain of the vacuolar H^+ -ATPase, possibly involved in luminal pH regulation by association/dissociation of V1 and V0 subunits and in membrane fusion (reviewed in Gkantiragas, I. *et al.* 2001); 8) Flotillin-1, described as a component of DRMs (Volonte, D. *et al.* 1999) and as a component involved in insulin signaling by association with CAP-Cbl complex, directing the complex to the plasma membrane microdomain (Christian A. Baumann, V. R., Makoto Kanzaki, *et al.* 2000); 9) GREG (referred to as p45 in Gkantiragas, I. *et al.* 2001), a GPI-anchored protein at the Golgi (Xueyi Li unpublished data), and involved in maintenance of the Golgi structure. GREG may also be responsible for the structural organization of GICs, and 10) GAPR-1. Cloning of GAPR-1 (Eberle, H. B. *et al.* 2002) allowed its classification as a mammalian homologue of plant pathogenesis-related proteins (PR proteins). Biochemical characterization revealed some unique features not seen for any other family member, such as intracellular

localization, myristoylation, membrane localization, and microdomain association. Its association to the microdomains and relationship to the immune response could help to understand and clarify its role in the cell as well as to understand the function of GICs in the Golgi apparatus.

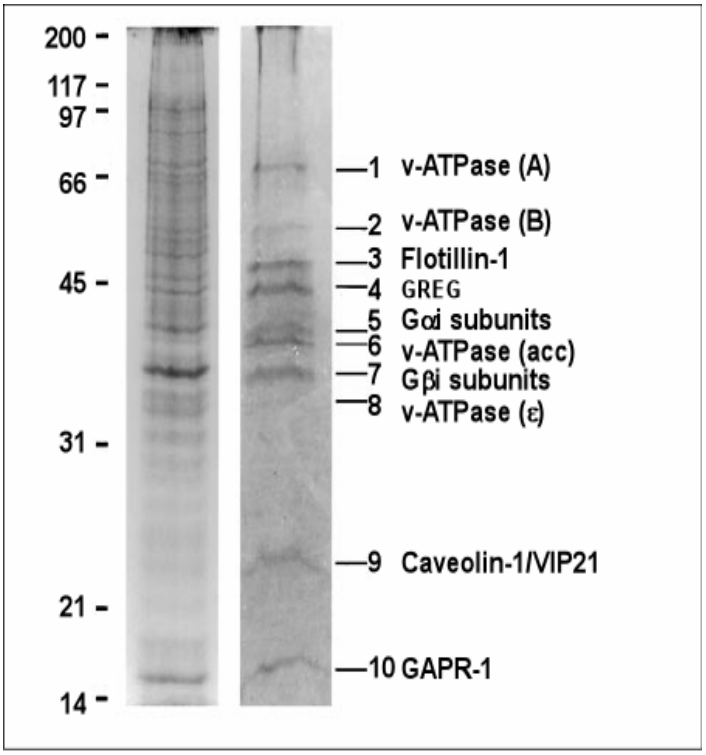

Figure 2. **Comparison of the protein components of DRM and GICs**. GICs and total-DRM were isolated from CHO Golgi membranes and total cell lysates, respectively, as described in MATERIALS AND METHODS. Proteins were analyzed by SDS-PAGE (12%) gel and stained with Coomassie blue. Proteins identified in GICs are shown on the right (Gkantiragas, I. *et al.* 2001).

2 Plant pathogens and integrated defence responses to infection

The homology of GAPR-1 to the superfamily of PR proteins, group 1, suggests a possible role of GAPR-1 in the immune system. In plants, PR proteins have been implied in the immune system, which is reminiscent of the innate immune system in mammals. Innate immunity is an ancient form of defense against microbial infection that is shared by plants, insects and vertebrates. The discrimination of many potential pathogens from self is a formidable task for the innate immune system. Many plants respond to local attack by pathogens with a production of compounds reducing or inhibiting

further attack. Responses occur at the site attacked but also at distal parts. At the site of attack, the responses include an oxidative burst, leading to cell death. In this way the pathogen is killed and is prevented from spreading from the site of initial infection. Further local responses in the surrounding cells include changes in cell wall composition, *de novo* synthesis of phytoalexins and pathogenesis-related proteins (PR). PR proteins were detected and defined as being absent in healthy plants but accumulating in large amount after infection (Heil, M. Bostock, R. M. 2002). More than 17 protein families have been assigned to this superfamily of proteins (http://www.bio.uu.nl/~fytopath/PR-families.htm). PR-1 proteins play a central role in the defense system in plants during the manifestation of systemic acquired resistance (SAR). Fig. 3 shows the NMR structure of one member of the PR-1 group, p14a tomato, which exhibits a 35% amino acid sequence identity with the human glioma pathogenesis-related protein (GliPR). Comparison of both proteins led to the identification of a common, partially solvent-exposed cluster of four amino acid residues in GLiPR-1 (His69, Glu88, Glu110, and His127) that is well conserved in all known plant PR proteins group 1 (Szyperski, T. *et al.* 1998). This could indicate the existence of a common active site for these proteins. In P14a, due to the arrangement of the amino acid residues at the potential active cluster, a possible role as a Zn protease has been suggested. However, a Zn^{2+} ion did not localize to the pocket of p14a when crystals were grown in presence of Zn^{+2} (Szyperski, T. *et al.* 1998). It has also been suggested that the arrangement of the two histidines at the active center represents the active site of a ribonuclease, but biochemical assays to detect such activity could not confirm this (Szyperski, T. *et al.* 1998). Interestingly, the same cluster of amino acid residues is observed in GAPR-1, which is the object of study in this experimental work.

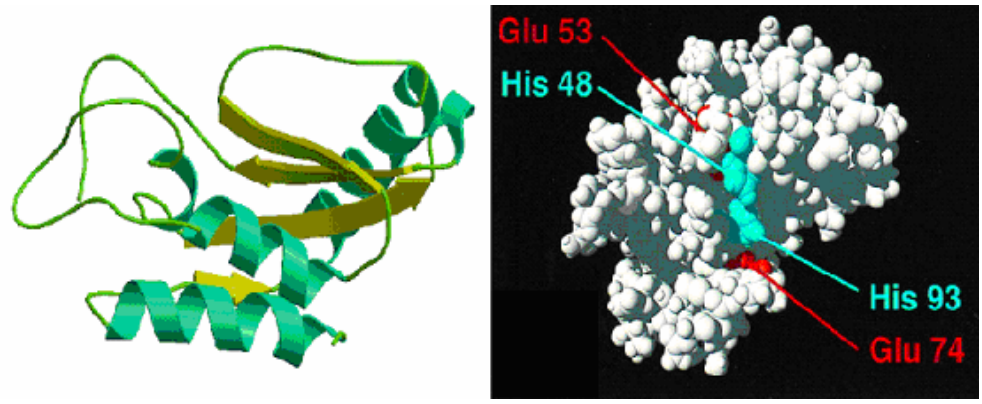

Figure 3*. P14a tomato drawing based on NMR information. *Left view. Representation of structural elements in p14a, containing four α-helices, and four β-strands. Ribbon structure of p14a obtained by Dr. Matthew Groves using MolScript® (Kraulis, P. 1991), Raster3D® (Bacon, D. Anderson, W. 1988). A similar structure has been described for Ves v5 from Vespula vulgaris (PDB 1QNX) and GAPR-1 isolated from GICs microdomains (see Discussion). ***Right view***. Space-filling representation of P14a, showing the putative active site with histidinyl and glutamyl residues depicted in blue and red, respectively (Szyperski, T. *et al.* 1998).

2.1 Systemic acquired resistance (SAR)

Secondary to the responses at the site of infection, long range responses are induced to protect distal parts of the plants. These responses are described as systemic resistance of plants against pathogens (Hammerschmidt, R. 1999) or systemic acquired resistance (SAR). Many components associated with SAR, *e.g.* PR proteins, are expressed in response to a first infection, but the mechanisms of this response are not fully understood (Conrath, U. *et al.* 2002). For instance, salicylic acid (SA) in plants is a critical signaling molecule in the pathway(s) leading to local and systemic resistance and SA is synthesized in response to infection both locally and systematically (Thomma, B. *et al.* 1998). Thus, the actual sites of *de novo* production of SA in non-infected plant might therefore contribute to induction of SAR (Meuwly, P. *et al.* 1995). NO has been implicated in the activation of plant defenses as well. The immune response of plants also depends on reactive oxygen intermediaries (ROI) and reactive nitrogen intermediaries (RNI) for signaling and apoptosis, and possibly for necrosis and direct antimicrobial actions (Klessig, D. F. *et al.* 2000).

In mammalian cells, salicylates are potent scavengers of NO and its derivatives, and salicylates inhibit the activity and transcription of iNOS

(Farivar, R. S. Brecher, P. 1996). NO has previously been shown to serve as a key redox-active signal for the activation of various mammalian defense responses, including the inflammatory and innate immune responses (Schmidt, H. H. Walter, U. 1994;Mannick, J. B. *et al.* 1994; Stamler, J. S. 1994). Infections, microbial products, and cytokines readily induce expression of NO synthase in tissue macrophages from rodents. Reactive nitrogen intermediaries (RNI) are critical in host defense not only because they can damage pathogens but also because they are immunoregulatory (Bogdan, C. *et al*. 2000). For instance, RNI can inhibit G proteins, activate or inhibit kinases, caspases, metalloproteases, transcription factors, and DNA methyltransferase, inhibit lymphocytes proliferation, alter cytokine and postaglanding production, and either cause or prevent apoptosis of the host cells (reviewed in Nathan, C. Shiloh, M. U. 2000).

Resistant plants often develop a hypersensitive response (HR), in which necrotic lesions form at the site(s) of pathogen entry (reviewed in Klessig, D. F. *et al.* 2000). This localized cell death associated with the HR may help prevent the pathogen from spreading to uninfected tissues. Just before or concomitant with the appearance of a HR, an increased synthesis of several families of pathogenesis-related (PR) proteins is observed (Schneider, D. S. 2002). It has been proposed that the HR response by activation of R (resistance) genes is responsible for controlling the entire intracellular environment such as guarding the secretory apparatus (Schneider, D. S. 2002).

The function of PR proteins in both SAR and HR is not known. By looking for similarities between the immune responses in plant and animal cells, likely the innate immune system in mammals is the one that resembles HR-producing infections in plants. The similarities are not only based on molecular mechanisms of action, but also on other levels such as monitoring endosomal traffic and activation of programmed cell death if traffic is disrupted. These considerations may be important for defining a role for PR proteins in general and for GAPR-1 specifically. GAPR-1 as potential regulator in the innate immune response may monitor the integrity of the Golgi apparatus due to its location at this organelle.

2.2 Mammalian PR-1 family members

Since the identification plant PR-1 proteins, secretory proteins with a significant sequence homology have been identified in various other organisms including fruiting body proteins in fungi that are expressed during infection (Schuren, F. H. *et al.* 1993), insect allergens (Lu, G. *et al.* 1993; Schreiber, M. C. *et al.* 1997), mammalian CRISP proteins possibly involved in sperm maturation or sperm-egg fusion (Kratzschmar, J. *et al.* 1996), human GliPR/RTVP-1, specifically expressed in glial tumors (Murphy, E. V. *et al.* 1995; Rich, T. *et al.* 1996), and in snake or lizard venoms, reported to block ryanodine receptors or cyclic nucleotide-gated ion channels (Morrissette, J. *et al.* 1995; Brown, R. L. *et al.* 1999). Together with plant PR-1 proteins, these proteins constitute a large PR-1 protein superfamily. Despite the diversity within this superfamily, very little is known about the function of the individual members and the plant PR proteins, described above, remain the most intensely studied family members.

3 Purpose of this thesis

During the characterization of lipid microdomains at the Golgi (GICs) (Gkantiragas, I. *et al.* 2001), a protein with an apparent molecular mass of 17 kDa was identified. Cloning and preliminary biochemical characterization identified a novel protein, GAPR-1, belonging to the superfamily of PR proteins. Based on the primary amino acidic sequence of this protein, some potentially interesting characteristics were identified (Fig. 4). It contains i) a consensus sequence for myristoylation (grey box); ii) a putative caveolin-binding domain (red box); iii) a coiled-coil structure (green box) and iv) an isolelectric point (pI) of 9.4, suggesting that GAPR-1 is a highly hydrophilic protein. Further characterization of GAPR-1 showed that the protein is differentially expressed in various tissues (Eberle, H. B. *et al.* 2002). For instance, GAPR-1 is highly expressed in immunocompetent organs and cells such as in lungs, spleen, and lymphocytes, but is absent in e.g. liver, heart, and brain. Here, this basic information was used to study the interaction of GAPR-1 with membranes (Section 1), to obtain structural information on the protein (in collaboration with Prof. Dr. Irmgard Sinning at the EMBL/BZH-

Heidelberg) (Section 2), and to identify proteins that interact with GAPR-1 (Section 2.4).

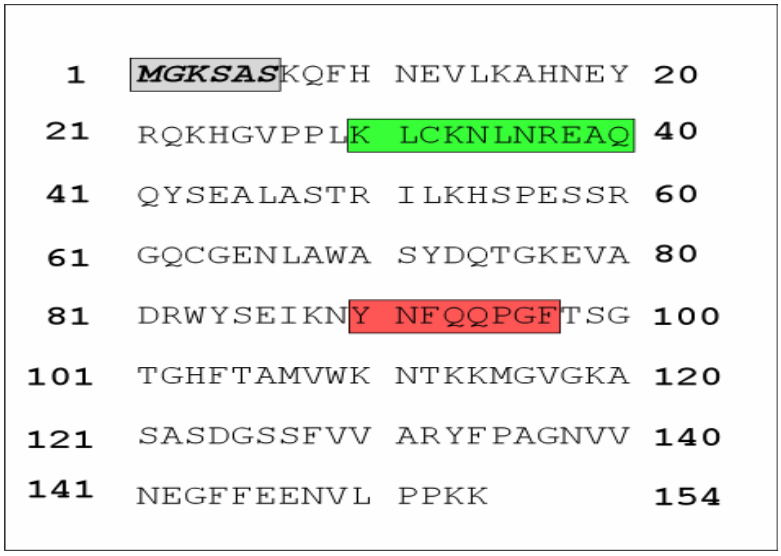

Figure 4. **cDNA-derived sequence of GAPR-1**. The consensus sequence for *N*-myristoylation is indicated by the grey box. The potential protein-protein interacting sites, i.e. a coiled-coil region and a caveolin-interacting region are indicated in green and red, respectively.

Results

1 Membrane association of GAPR-1

1.1 *N*-myristoylation of GAPR-1 in *Escherichia coli*

The enzymology of the myristoylation reaction is well understood. Proteins that are destined to become myristoylated contain the N-terminal sequence: Met-Gly-X-X-X-Ser/Thr (for a review see Resh, M. 1999). The initiating methionine is removed co-translationally by methionine amino-peptidase, and myristate is linked to Gly-2 via an amide bond by an *N*-myristoyl transferase. To investigate whether the consensus sequence for N-myristoylation in GAPR-1 (Fig. 4) is a substrate of myristoyl-CoA:protein N-myristoyl-transferase (NMT1), an *E .coli* strain was used that contained two plasmids for simultaneous expression of GAPR-1 (expression vector pQE60, Eberle, H. B. *et al.* 2002) and yeast NMT1 (in expression vector pBB131 Duronio, R. J. *et al.* 1990) (Fig. 5 panel A). The vectors were designed so that they could be simultaneously maintained as stable episomal plasmids and that independent induction of transcription of their heterologous DNA sequences was possible. The expression of NMT was placed under the control of the isopropyl-β-D-thiogalactopyranoside (IPTG)-inducible *tac* promoter, and GAPR-1 under the control of the T5 promoter. The various plasmid combinations were compared for the efficiency of GAPR-1 myristoylation during expression of proteins upon induction with IPTG. To determine myristoylation efficiency of GAPR-1, [^{3}H]-myristic acid was added during the overexpression. Subsequently, lysates were prepared from the *E. coli* cultures, and subjected to SDS-PAGE (Fig. 5, *middle* panel B). Autoradiography showed that in the presence of NMT1 and GAPR-1, a labeled band of 17 kDa was observed and indicated that the radiolabel is readily incorporated into GAPR-1 (Fig. 5, lane 1, *bottom* panel C). Labeling of GAPR-1 was absolutely dependent on the presence of NMT1. *E. coli* that expressed NMT1 but lacked GAPR-1, or *E. coli* that lacked NMT1 but expressed GAPR-1, failed to label the 17 KDa protein with the tritiated fatty acid (Fig. 5, panel B and C, lanes 5 and 3, respectively).

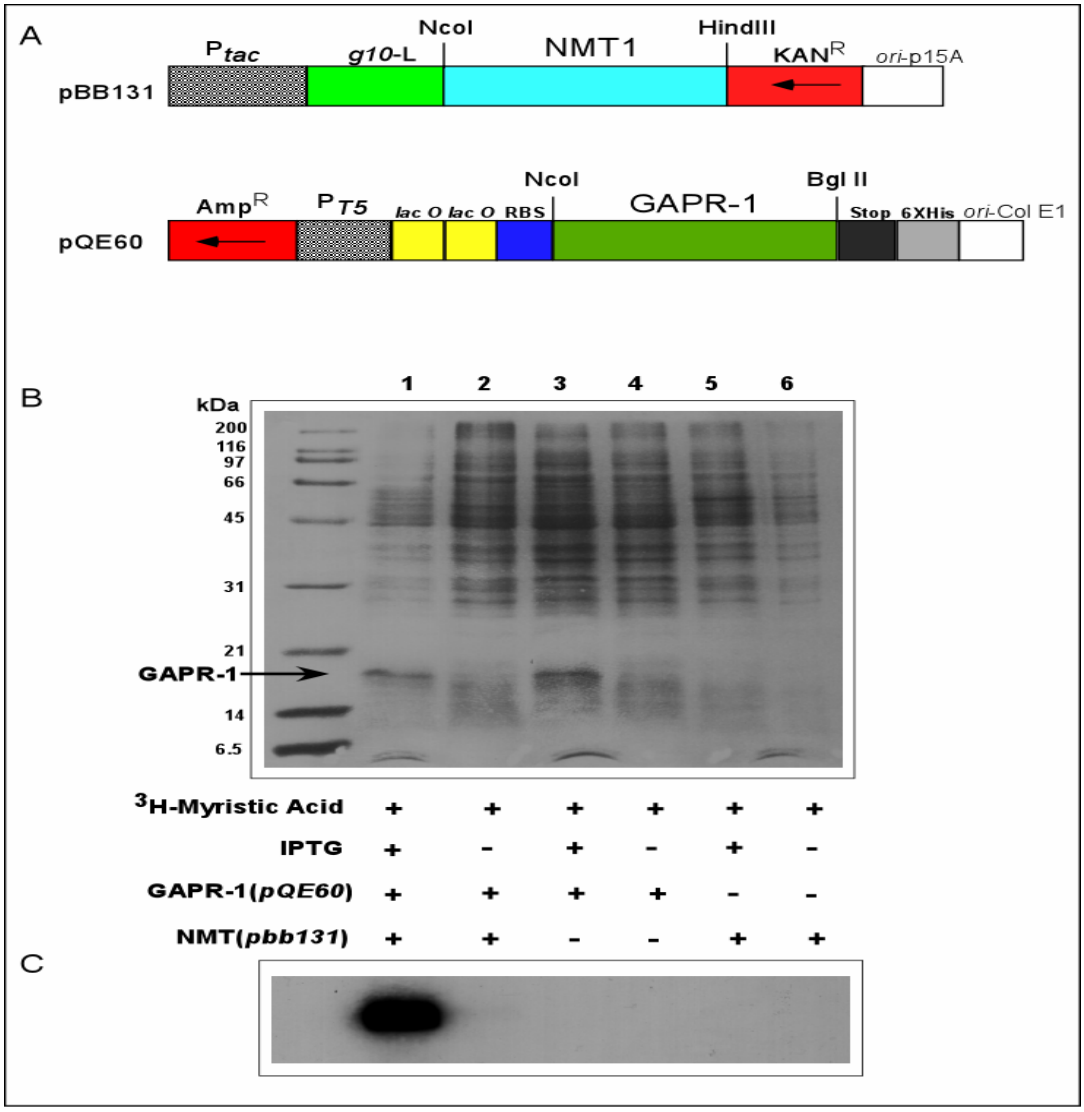

Figure 5. **[^{3}H]-Myristate-labeled GAPR-1 in *E. coli*.** (A) Schematic presentation of plasmid constructs used to express NMT1 and GAPR-1 in *E. coli.* KAN^R, gene for kanamycin resistance; AMP^R, gene for ampicilin resistance. (B) The radiolabeling conditions were compared for induced (IPTG) and non-induced bacteria, containing distinct plasmid combinations: transformed bacteria with GAPR-1 and NMT1 (lanes 1 and 2) were induced (lane 1) or not induced (lane 2) with IPTG (1mM) in the presence of [^{3}H] myristic acid (50µCi/ml culture). Cells were lysed in SDS-gel loading buffer 1, heated for 5 min at 95^o C, and after centrifugation (5 min, 14000 rpm), an aliquot of the supernatant (lysate) (20µl) was mixed with (5µl) SDS-gel loading buffer 2 (5X), and analyzed by SDS-PAGE (14% acrylamide). After staining with Coomassie Blue, the dried gel was exposed to a film. Lysates from bacteria containing only pQE60 (GAPR-1) (lanes 3 and 4) or pBB131 (NMT1) (lanes 5 and 6) were induced or not induced with IPTG (as indicated in figure) and analyzed as described above.

1.2 *N*-myristoylation of GAPR-1 *in vivo*

To determine whether the consensus sequence for N-myristoylation also results in myristoylation of GAPR-1 *in vivo*, proteins from a large-scale preparation of Golgi-derived detergent-insoluble complexes (GICs) were separated by SDS-PAGE. After staining the gel with Coomassie Blue, the protein band at 17 kDa was excised from the gel and digested with trypsin. The resulting peptides were analyzed by electrospray ionization mass spectrometry (ESI-MS) (Fig. 6). Trypsinization of the GAPR-1 band generated 21 major peptides (Fig. 6A, *upper* panel). If native GAPR-1 is myristoylated, then a myristoylated dipeptide [myrGK] with a theoretical [M+H]+ signal at m/z 414.33 is expected to be present. The survey spectrum of the tryptic digest of GAPR-1 showed a signal at m/z 414.327 (Fig. 6A, *lower* panel), consistent with the calculated m/z value for the myristoylated fragment. Also the isotopic ^{13}C-peak at m/z 415.33 could be detected. The ion at m/z 414.327 was further analyzed by ESI tandem mass spectrometry, and the products obtained from this ion by fragmentation are displayed in Fig. 6B. All major fragment ions in this spectrum can be assigned to the myrGK sequence, as indicated in Fig. 6B (insert) and Table 1. In particular the fragment ion triplet at 211, 240 and 268 is indicative of the myrG structure. In summary, mass spectroscopic data show that native GAPR-1 is myristoylated at the N-terminus. All the ESI-MS data were obtained and analyzed in collaboration with Dr. Andreas Schlosser and Dr. Wolf Lehmann at the Cancer Center Heidelberg (DKFZ).

Table 1. Summary of positive nanoESI product ion spectrum of expected and calculated MS/MS signals for myrGK fragment of GAPR-1.

ion type	calc. mass	exp. Mass
$[M+H]^+$	414.333	414.332
y_1	147.113	147.111
y_2	204.135	lock mass
b_0	211.206	211.207
a_1	240.209	240.235
b_2	268.204	268.232

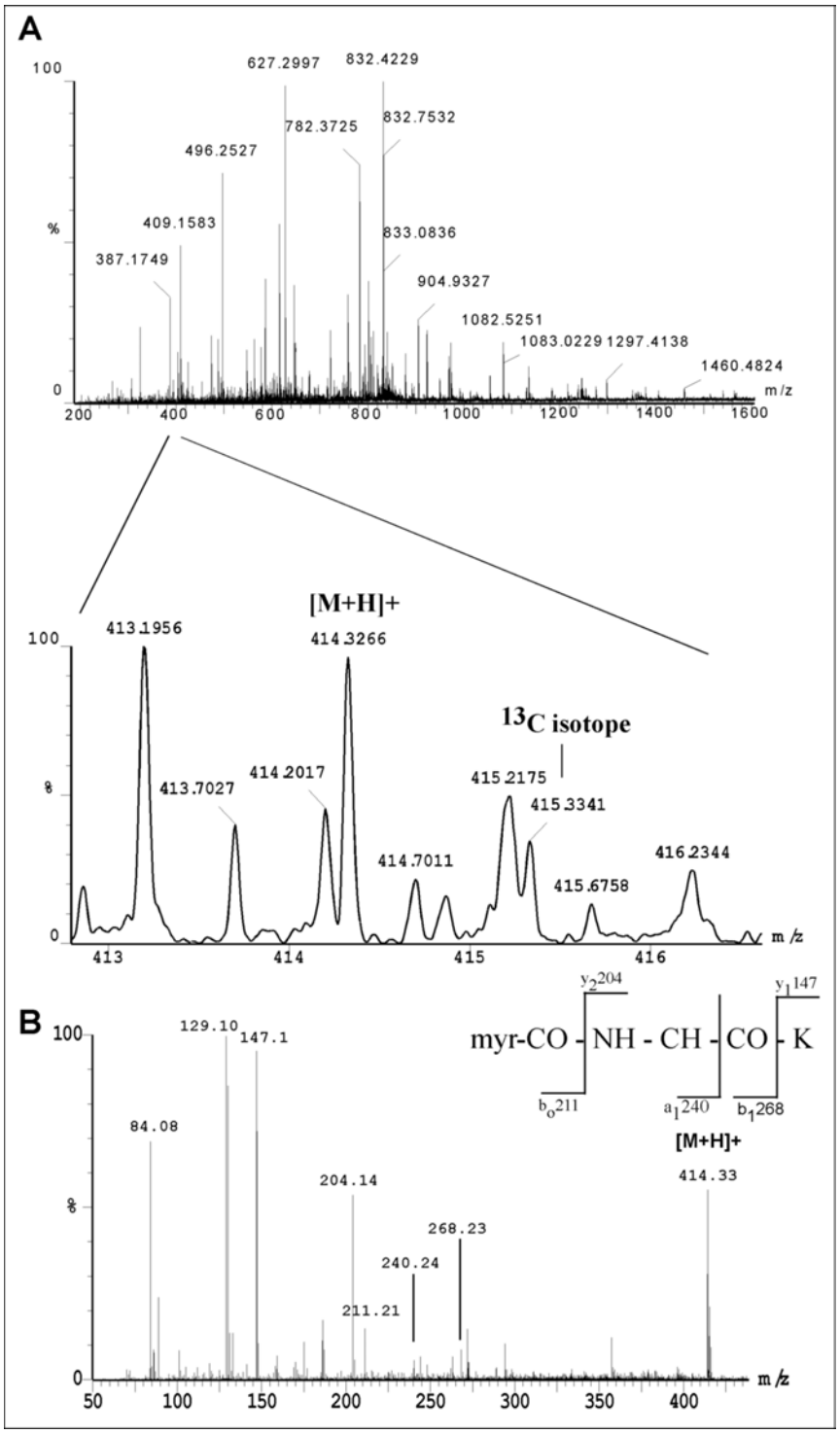

***Figure 6*. In vivo myristoylation of GAPR-1**. (A) Positive nanoESI spectrum of peptides derived from an in-gel digest of native GAPR-1. The top panel shows the complete survey spectrum, and the lower panel the expanded view from m/z 413 to 417, showing the singly protonated molecular ion of the T1 fragment including the ^{13}C isotope peak. (B) Positive nanoESI product ion spectrum of m/z 414.33. The spectrum shows the key fragments for the myrG structure at m/z 211, 240 and 268 and sequence–specific fragment ions, which identify the peptide as T1 fragment myrGK of GAPR-1. Data obtained and analyzed by Dr. Andreas Schlösser and Dr. Wolf Lehmann (DKFZ-Heidelberg).

1.3 Association of GAPR-1 with Golgi membranes

Myristoylation is necessary but not sufficient for membrane binding of myristoylated proteins (Peitzsch, R. M. McLaughlin, S. 1993). A second signal for stable membrane binding of *N*-myristoylated proteins has been defined as either a polybasic cluster of amino acids or a palmitate moiety (Resh, M. D. 1999). GAPR-1 is tightly associated with Golgi membranes, which is reflected by the absence of GAPR-1 from the cytosolic fraction: GAPR-1 could not be detected by immunoprecipitation from large amounts of cytosol (Fig. 7A). When the Golgi structure is disrupted with Brefeldin A and GAPR-1 is dispersed in the cell (Eberle, H. B. *et al.* 2002), GAPR-1 remains associated with the membrane fraction of these cells as determined by efficient immunoprecipitation the total membrane fraction. This indicates that GAPR-1 is absent from the cytosol (see, however section 1.6). The characteristics of this tight membrane association of GAPR-1 were further investigated by incubation of isolated Golgi membranes under various conditions. As shown in Fig. 7B, treatment of Golgi membranes with 1 M KCl did not strip GAPR-1 off the membranes, whereas NSF, a peripheral Golgi membrane protein (Block, M. R. *et al.* 1988) is affected by this treatment. Alkaline treatment of the membranes, which causes the dissociation of most peripheral membrane proteins, did affect the membrane binding of NSF and GAPR-1 (Fig. 7B). As a control, p23, a type I transmembrane protein of the Golgi complex (Sohn, K. *et al.* 1996), remains present in salt or alkaline-treated membranes (Fig. 7B). Biophysical studies have established that the binding energy provided by myristate is relatively low (with a K_d of 10^{-4} M) (Peitzsch, R. M. McLaughlin, S. 1993) and not sufficient to stably anchor a protein to a lipid membrane (Moffet, S. B. *et al*. 2000). To determine whether the myristoyl moiety of GAPR-1 contributes to the salt-resistant membrane binding, purified non-myristoylated GAPR-1 was bound to isolated Golgi membranes (Fig. 7C). Upon salt treatment of the membranes, most of the non-myristoylated GAPR-1 is stripped again from the membranes. These data indicate that native GAPR-1 is bound to Golgi membranes not only by ionic interactions, but also through the myristoyl moiety, which affects membrane anchoring of the protein. The primary structure of GAPR-1 shows the presence of

basic residues in the N-terminal region. An amino-acidic stretch at the N-terminus (21 amino acids) has a theoretical pI 9.8, containing five positively charged amino acids [Arg-Lys]. The ^{151}LPKK^{154} sequence at the C-terminus represents another potential positive structure that may play a role on membrane interaction. The high overall pI of GAPR-1 suggests that a contribution of several positively charged regions together with the myristoyl moiety allows the protein to bind strongly to the membrane.

1.4 GAPR-1 interaction with Caveolin-1

A number of studies support the hypothesis that caveolin provides a direct mean for proteins to be sequestered within lipid-enriched microdomains (Oh, P. Schnitzer, J. E. 2001). Many proteins that interact with caveolin, including G-protein α subunits, Ha-Ras, Src family tyrosine kinases, endothelial NOS, 1 EGF-R and related receptor tyrosine kinases, and protein kinase C isoforms (Okamoto, T. et al. 1998) do so via an interaction with a common putative caveolin-binding motif (Fig. 4, ΦXΦXXXXΦ, where Φ is aromatic amino acid Trp, Phe, or Tyr). GAPR-1 also contains this putative caveolin-binding motif (***Y****n****F****qqpg****F***), which might contribute to its strong membrane-binding. To determine a direct interaction between caveolin-1 and GAPR-1, co-immunoprecipitation studies were carried out. Under native conditions using various detergents caveolin could not be co-immunoprecipitated with GAPR-1 or vice versa (data not shown). For that reason, co-immunoprecipitation studies were performed after chemical crosslinking of proteins in Golgi membranes. As shown in Fig. 7D, crosslinking with N-Hydroxylsulfosuccinimidyl-4-azidobenzoate resulted in an irradiation-dependent crosslink product of caveolin-1 at 40-45kDa (Fig. 7D left panel).

When GAPR-1 was immunoprecipitated from similar incubations (10 fold upscale of incubations), caveolin-1 was found to co-immunoprecipitate with GAPR-1 in a crosslink product of 40-45kDa (Fig. 7D, lane 3). Co-immunoprecipitation of crosslinked Golgi membranes with Caveolin-1 antibody produced a similar result. GAPR-1 was co-immunoprecipitated in a crosslinked product that runs at 40-45kDa (Fig. 7D, lane 6), corresponding to a similar product observed for co-

immunoprecipitation with GAPR-1. These results indicate a direct interaction of GAPR-1 with caveolin-1. The crosslink products at high molecular weights (HMW) (Fig. 7D, lane 6) appeared only when immunoprecipitations were performed with caveolin-1 antibodies and western-blotting was performed with a GAPR-1 antibody. This indicates that GAPR-1 can interact with caveolin-oligomers.

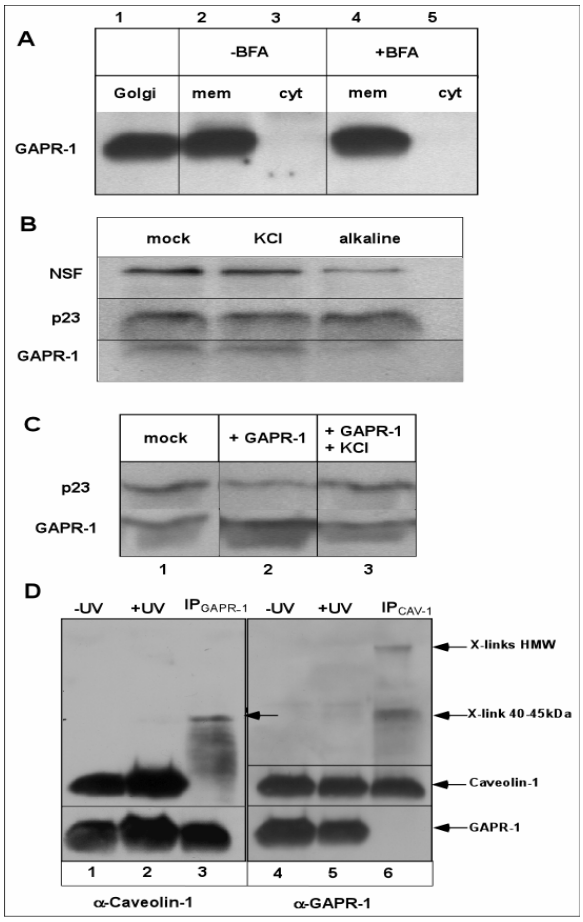

Figure 7. **Interaction of GAPR-1 with Golgi membranes.** The incubations were analyzed by SDS-PAGE and western blotting for the presence of the indicated proteins. (A) CHO cells were incubated for 30 minutes in the absence (lane 2 and 3) or presence of 5 µM Brefeldin A (lane 4 and 5). After homogenization, the homogenate was centrifuged for 1 hour at 100,000 g to yield a total membrane (lanes 2 and 4) and a cytosolic fraction (lanes 3 and 5). GAPR-1 was immunoprecipitated from the membrane fraction (2mg) or from the cytosolic fraction (2mg). As a control, GAPR-1 was immunoprecipitated from isolated CHO Golgi membranes (50µg) (lane 1). (B) 50µg of CHO Golgi membranes (lanes1-3) were incubated for 30 minutes on ice in the absence (lane 1) or presence of 1 M KCl (lane 2) or with 0.1 M Na_2CO_3, pH 11 (lane 3). After centrifugation through a 15% (w/v) sucrose cushion, equal amounts of membranes (29 nmol phospholipid) were analyzed. (C) CHO Golgi membranes (25 µg) were incubated for 30 minutes at 4°C in the absence (lane 1) or presence (lanes 2 and 3) of 3µl of bacterial expressed and purified, non-myristoylated GAPR-1 (5.3 mg/ml) in 25 mM Hepes/KOH, pH 7.2, 20 mM KCl, 2.5 mM magnesium acetate, 0.1 M sucrose, 1 mg/ml ovalbumine and 10 mM DTT. Subsequently, KCl (1 M final concentration) was added to one incubation (lane 3) and incubated further for 30 min at 4°C. Golgi membranes were re-isolated by centrifugation through a 15% (w/v) sucrose cushion. (D) CHO Golgi membranes (50µg) were incubated with N-Hydroxylsulfosuccinimidyl-4-azidobenzoate (5mM) in PBS for 30 minutes at RT and left on ice (lane1, and 4) or irradiated for 10 minutes at 254 nm (lane 2 and 5) and analyzed for crosslinked products. For immunoprecipitation (lane 3, and 6), 500 µg of Golgi membranes each were used for immunoprecipitation of GAPR-1 or Caveolin-1. After western blotting, the PVDF membrane (left, immunoprecipitation using α-GAPR-1) was incubated first with α-Caveolin-1, followed by α-GAPR-1, or the PVDF membrane (right, immunoprecipitation using α-Caveolin-1) was incubated first with α-GAPR-1, followed by α-Caveolin-1

1.5 Phosphorylation of GAPR-1 *in vivo*.

The partitioning of myristoylated proteins to cellular membranes can be sensitive to additional factors that affect the binding of these proteins to membranes. These factors can control the reversible translocation of myristoylated proteins onto membranes. The primary structure of GAPR-1 shows several predicted phosphorylation sites (NETPHOS 2.0 http://www.cbs.dtu.dk/services/NetPhos/) (Table 2). This program calculates a score based on the confidence of the prediction and similarity to known phosphorylation sites. To investigate whether GAPR-1 can be phosphorylated *in vivo*, CHO cells were incubated 4 hrs with radiolabeled inorganic phosphate (^{32}Pi). Cells were lysed, and cytosol and total membranes were isolated by centrifugation. The membrane fraction was solubilized in 1% SDS, quenched to 0.1% SDS with PEN buffer containing 1% Triton X-100, and subjected to immunoprecipitation with an antibody against GAPR-1 (α-1852). Fig. 8 (lane 2) shows that the immunoprecipitated protein GAPR-1 (western blot) is radioactively labeled due to incorporation of ^{32}P in the protein. These data indicate that GAPR-1 is phosphorylated *in vivo*. The extent of GAPR-1 phosphorylation seems not to be affected by treatment with phosphatase inhibitors (lane 2 and 3).

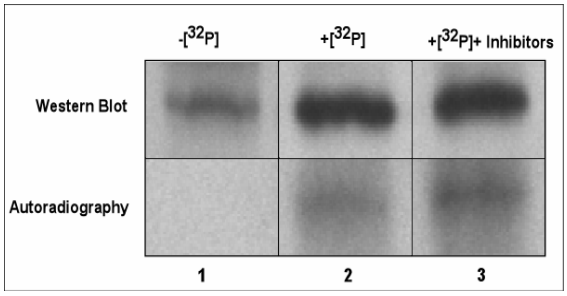

***Figure 8. In vivo* phosphorylation of GAPR-1.** Confluent CHO wt cells were incubated for 4 hrs in DMEM medium (phosphate and serum free) at 37°C in the absence (lane 1) or presence (lanes 2 and 3) of [^{32}P] 0.25mCi/ml. Cells were incubated in the absence (lanes 1 and 2) or the presence (lane 3) of phosphatase inhibitors. Phophatase inhibitors were added during homogenization and IP. Cells were washed, harvested and lysed. The homogenate was centrifuged 1hr at 100,000 x*g* to isolate a total membrane fraction (*pellet*). The total membrane fraction was dissolved in 1% SDS and incubated 5 min at 95°C. After incubation, the fraction was quenched to 0.1% SDS by 10-fold dilution in PEN buffer containing 1% Triton X-100. GAPR-1 was immunoprecipitated using α-GAPR-1 (α-1852) antibody. Immunoprecipitated proteins were separated by SDS-PAGE and analyzed by western-blotting (upper panel) and autoradiography by exposure of the western blot to X-ray film (lower panel).

Sequence	Position	Score*	Prediction
ILKHSPESS	55	0.998	*S*
HSPESSSRGQ	58	0.995	*S*
VGKASASDG	121	0.994	*S*
SYDQTGKEV	75	0.985	*T*
VWKNTKKMG	112	0.809	*T*

Table 2. Predicted phosphorylation sites present on GAPR-1. The program NETPHOS (2.0) was used to predict phosphorylation of amino acids in GAPR-1. Phosphorylation sites are sorted by their score. *Score indicates the likeliness of phosphorylation. Threshold score: 0.500.

1.6 Effect of phosphorylation on the partitioning of GAPR-1 to lipid-enriched microdomains.

Triton X-100 treatment of Golgi membranes or plasma membranes in the cold allows isolation of a detergent-insoluble fraction. The partitioning of proteins to the detergent-resistant fraction can depend on post-translational modifications (Moffet, S. B. *et al*. 2000). Phosphorylation therefore may have an effect on the partitioning of GAPR-1 into Golgi-derived microdomain complexes (GICs) as well. To analyze this possibility, total cell membranes, obtained from ^{32}P-treated CHO cells, were resuspended in cold PEN buffer containing 1% Triton X-100 and detergent-soluble and insoluble fractions were analyzed for the presence of phosphorylated GAPR-1. A major pool of GAPR-1 is insoluble in Triton X-100 (Fig. 9A, lane 1, *upper* panel), and this fraction is highly phosphorylated (Fig. 9A, lane 1, *bottom* panel); a minor pool of GAPR-1 is soluble in Triton X-100 (Fig. 9A, lane2, *upper* panel). This soluble fraction shows a low level of phosphorylation (Fig. 9A, lane 2, *bottom* panel). Interestingly, CHO cytosol of treated cells shows a barely detectable fraction of GARP-1 by western blot analysis (Fig. 9A, lane 3, *upper* panel), but a relatively high level of phosphorylation (radioactivity/amount of protein) is observed in this sample (Fig. 9, lane 3, *bottom* panel). The radioactive signals were

quantified using the program Quantity One® (BioRad™). Fig. 9B shows that approximately 32.5% (calculated as percentage of total radioactive signal) of the incorporated Phosphate in GAPR-1 has a cytosolic localization. The soluble fraction in Triton X-100 represents approximately 11.6%. These data suggest that GAPR-1 can be phosphorylated *in vivo* and that phosphorylation of GAPR-1 can play a role on the dynamics of GAPR-1 association with Golgi membranes.

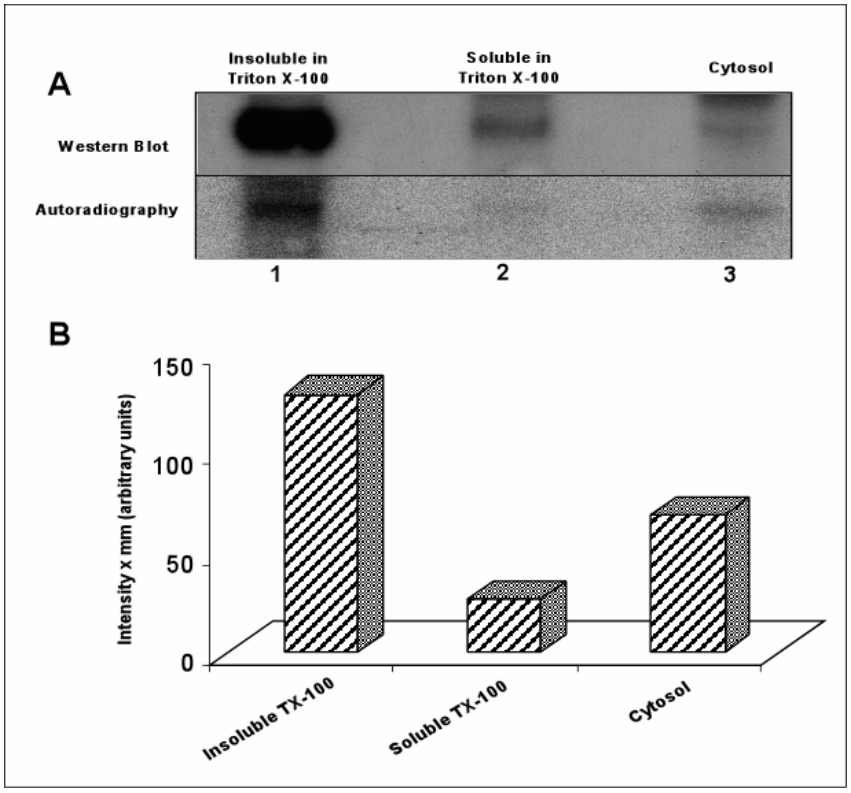

Figure 9. **Phosphorylation of GAPR-1 and partitioning into lipid rafts.** A) Confluent CHO wt cells were incubated for 4 hrs in DMEM medium (phosphate and serum free) at 37°C in the presence of [^{32}P] 0,25mCi/ml. Cells were washed, harvested and lysed. The homogenate was centrifuged 1hr at 100,000 xg to isolate a total membrane fraction (*pellet*) and a cytosol fraction (*supernatant*). The total membrane fraction was dissolved in 1% TX-100/PEN buffer and incubated for 30 min in the cold. After incubation, the fraction was centrifuged 1 hr at 100,000 xg to yield soluble (lane 2) and insoluble (lane 1) fractions. GAPR-1 was immunoprecipitated from both fractions as well as from cytosol of lysated cells (lane 3). Proteins in the immunoprecipitates were separated by SDS-PAGE and analyzed for the presence of GAPR-1 by western-blotting (upper panel) and for phosphorylation of GAPR-1 by autoradiography (lower panel). B) Quantification of the radioactive signals by Quantity One® (Biorad).

2 Structural Characteristics of GAPR-1

2.1 Large Scale Purification of GAPR-1

Structure determination of proteins is important in several ways. The function of a protein is linked to its three dimensional structure, and highly resolved structures can lead to a clear understanding of the possible function of a protein. Structures can also discriminate between evolutionary changes in the primary structure of related or non-related species. To obtain a crystal structure of GAPR-1, it was necessary to obtain protein crystals of suitable size and diffraction quality for X-ray analysis. GAPR-1 has several biochemical characteristics that can be used to obtain a highly purified protein fraction: an isoelectric point (pI) of 9.4, and a molecular weight of 17,2 KDa, useful in ion exchange and gel filtration chromatography, respectively.

The cDNA encoding GAPR-1 was cloned in the vector pQE60, and after transformation, GAPR-1 was overexpressed in M15/REP4 bacteria. Recombinant wtGAPR-1 was purified from overexpression in 12 liters of LB-medium (Fig. 10). Diluted lysates were applied on to a DEAE-sepharose (anion exchange support) to remove most of the bacterial proteins in the lysate, followed by a High S-support column (cation exchange). GAPR-1 has a high pI (9.4), and the overexpressed protein was bound to the High S-support (Fig. 10A, lane 5). After washing, proteins were eluted from the cation exchange column by a salt gradient. The chromatogram and corresponding gels (Fig. 10B (left part), panel A and B) indicate that GAPR-1 eluted at a salt concentration of 250-300mM, corresponding to fractions 18 to 22. These fractions were pooled and loaded onto a Superdex 200 gel filtration column. Separation of proteins by gel filtration produced several fractions (46-53) (Fig. 10B (right part), panel B) with GAPR-1, purified to apparent homogeneity. These fractions were used for further studies, including the generation of GAPR-1 crystals by Dr. Matthew Groves.

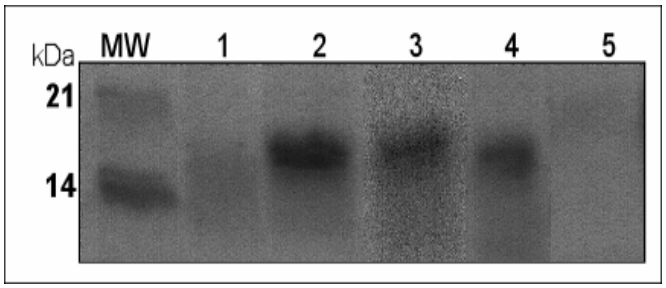

***Figure 10A*. Overexpression of GAPR-1 in bacteria (M15/REP4).** Figure shows distinct steps during induction of GAPR-1 expression. Cells collected prior to induction (lane 1) by 1mM IPTG, and after 3 hrs of induction (lane 2). Cells were collected and lysed by French press. The homogenate (lane 3) was cleared after 100000 x*g* centrifugation, and diluted 1:6 with buffer Tris-HCl 50mM; pH 7.5; 50mM. 1.2 L of Lysate was loaded onto a DEAE column at a flow rate of 0.5 ml/min and the flow through (lane 4) was applied to a cation exchange column (High S-support), and washed Tris-HCl 50mM pH7.5; 50mM NaCl (lane 5, flow through). Proteins were eluted from the column with a NaCl gradient (50mM to 1000mM).

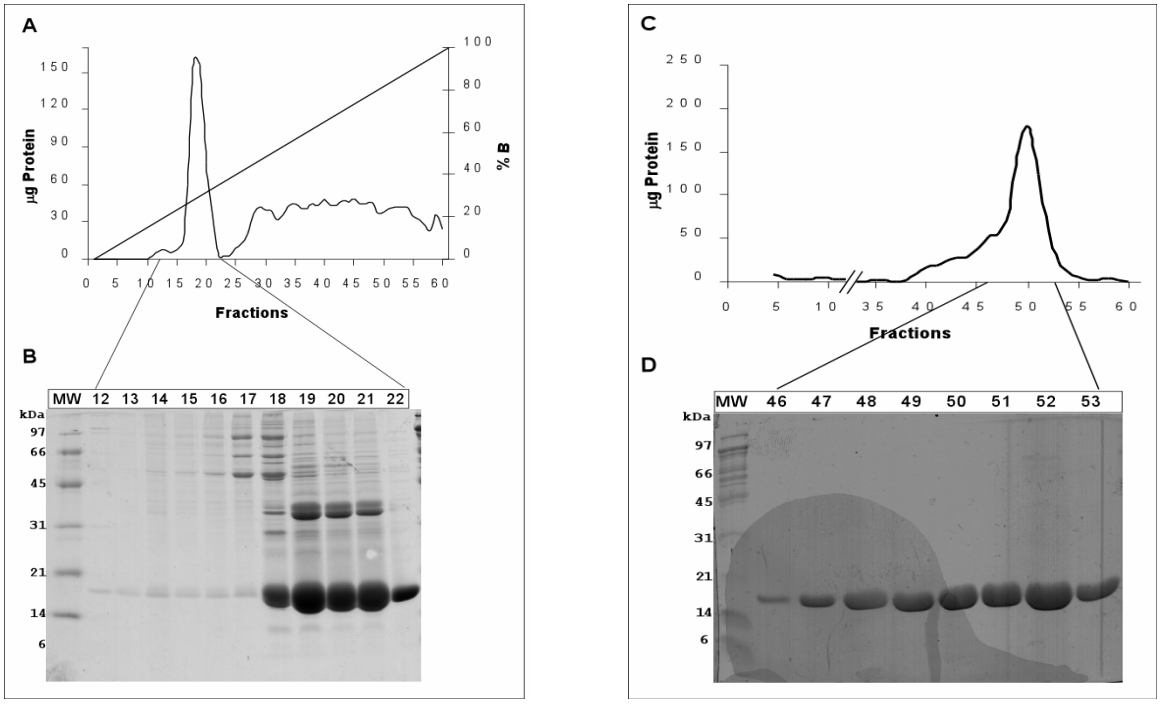

***Figure 10B*. Large scale purification of GAPR-1. Left panel: Cation exchange chromatography (High S-support cation exchange column).** Panel A shows the chromatogram profile (amount of protein and conductivity versus fractions) obtained during elution of proteins from the High S column by a sodium chloride (NaCl) gradient (in 50 mM to 1M in Tris 50 mM, pH 7.5). Proteins eluted between 250 to 300mM NaCl were analyzed by SDS-PAGE (14%), and coomassie blue staining. **Right panel: Gel filtration (Superdex 200).** Upper panel (C) shows the chromatogram profile (µg protein vs fractions) of eluting proteins (Tris 50 mM, pH 7.5, 50 mM NaCl), and the bottom panel (D) shows the analysis of selected fractions by SDS-PAGE (14%) and coomassie blue staining.

2.2 Crystal structure of GAPR-1

Two conditions from the initial screen produced micro crystals from which further screens were designed. Lens-shape crystals large enough for X-ray analysis were obtained in 20% (v/v) PEG 8K, 100mM Bis-Tris-HCl pH 7.0, 200mM magnesium acetate. These crystals appeared after 3-4 days and were suitable for analysis after 6-7 days (0.4 x 0.2 x 0.2mm). Diffraction from these crystals was measured in-house to 3.0Å. Hexagonal crystals were obtained in 30% PEG 4K, 100mM Tris-HCl ph 8.0, 140mM magnesium chloride. These crystals appeared after 7-8 days and were suitable for analysis after 10-12 days (0.4 x 0.4 x 0.4mm). The hexagonal crystals had similar cell parameters to the lens-shaped crystals and shared the same point group, but diffracted in-house to 2.1Å. A complete data set to 1.5Å was collected on a MarCCD detector at beamline ID14 EH-2 at the ESRF (Table 3). A low resolution pass was made using a crystal-to-detector distance of 200mm and an oscillation range of 100^{o} in 1^{o} steps. A high resolution pass was made at a crystal-to-detector distance of 110mm and an oscillation range of 130^{o} in 0.5^{o} steps. Auto-indexing yielded unit-cell parameters of a=b=73.5, c=63.2Å, $\alpha=\beta=90^{o}\gamma=120^{o}$ in the trigonal point group P32l. The 00l axial reflections are markedly stronger for l=3n (n integer) indicating that the space group is either $P3_121$ or $P3_221$. Data completeness and I/σ(I) were 97.2% and 3.6, respectively, overall and 90.4% and 2.8, respectively, for the 1.56-1.49Å highest resolution shell. Using a molecular weight of 17kDa for the monomer, the predicted Matthews coefficient (V_M) for a single molecule in the asymmetric unit is 2.81, within the usual range for a protein crystal, whereas the Matthews coefficient for two molecules in the asymmetric unit is 1.3. Similarly, the predicted solvent content for a single molecule in the asymmetric unit is 56% and for two molecules the predicted solvent content is 11%. Crystal structure solved by single isomorphous replacement (SIR). All crystal structure data were obtained and analyzed by Dr. Matthew Groves at the European Molecular Biology Laboratory (EMBL)/ Biochemistry Center Heidelberg (BZH).

Table 3. X-Ray diffraction data.

Data Collection		
Space group	$P3_121$	
Unit cell parameters (Å, °)	$a=b=73.5$, $c=63.2$; $\alpha=\beta=90$, $\gamma=120$	
No. of observed reflections	235802	(23839)
No. of unique reflections	30262	(3937)
Resolution range (Å)	44.1-1.49	
I/s (I)	3.6	(2.8)
Completeness (%)	97.2	(90.4)
Rmerge (%)	9.9	(25.1)

Values in parentheses refer to the highest resolution shell (1.56-1.49Å)

Our data indicate that GAPR-1 is a Golgi localized peripheral membrane protein, with a cytosolic orientation (Eberle, H. B. *et al.* 2002). To investigate further the implications for its orientation, a working model was proposed for the topological positioning of GAPR-1 at the Golgi membrane. GAPR-1 has a positive cluster at the N-terminus (Fig. 11), and C-terminus, both of which are proposed to interact to the membrane cytosolic leaflet. The interaction proposed is via positive residues (Lys-Arg), and a myristic acid. Fig. 11 depicts these positive elements, and suggests a geometric representation of the interaction. However, it is possible to separate GAPR-1 in several structural features or regions, and representing each one of them in the model. Region I can be assigned from amino acid 2 (Gly) to 21, which includes the *N*-myristoylation and five positive residues. Region II assigned to the amino acids 25 to 55, representing a “hepta repeat”. This structure has been suggested as protein-protein interacting motif. Region III assigned to the putative caveolin-binding motif and the C-terminus. The folding of the “caveolin binding motif” in region III seems to result in a highly strained conformation for each amino acid residue in the structure that is exposed on the surface (Fig. 11). The cleft region is formed between region II and III. A Similar conformation has shown to be present in p14a, and suggested to be a conserved active site (Szyperski, T. *et al.* 1998). The shape of the cleft is like a left-hand hollow in which region I form the palm, region II the fingers and domain III casts the thumb. The cleft runs across the protein, and opens up towards the cytosol and has a α-β-α sandwich core

structure- (Fig. 11). Four amino acids that locate to the cleft (His 54, Glu65, Glu86 and His 103) are conserved throughout the family members of plant-pathogenesis-related proteins (group1) and could represent an active site.

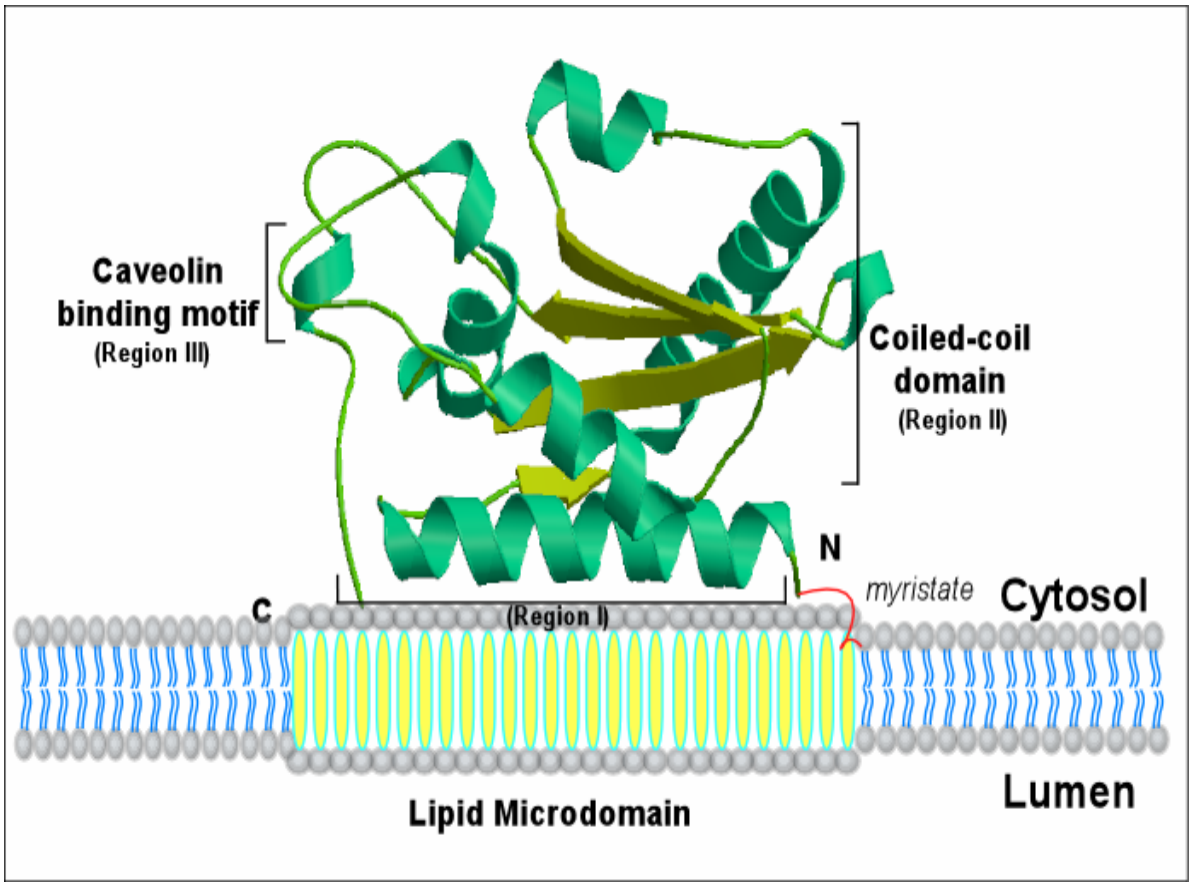

Figure 11. **Representation of GAPR-1 attachment to the membrane.** Overall structure of GAPR-1 showing distinct regions. Region I, positive stretch of amino acids within the C- and N-terminus, and myristate. Region II, assigned to the coiled-coil structure. Region III, represents the Caveolin-binding motif. Between Region II and III runs a cleft through the protein, and possibly represents an active center in GAPR-1. Ribbon representation of GAPR-1 obtained by Dr. Matthew Goves using Raster3D® (Bacon, D. Anderson, W. 1988); and MolScript® (Kraulis, P. 1991)

2.3 Role of conserved amino-acids in GAPR-1

To evaluate the possibility that the potential active site (His54, Glu65, Glu86, and His103) has any implication in the function of GAPR-1, a mutant of GAPR-1 was produced in which His54, His103, Glu65, and Glu86 were replaced with alanines (Fig. 12).

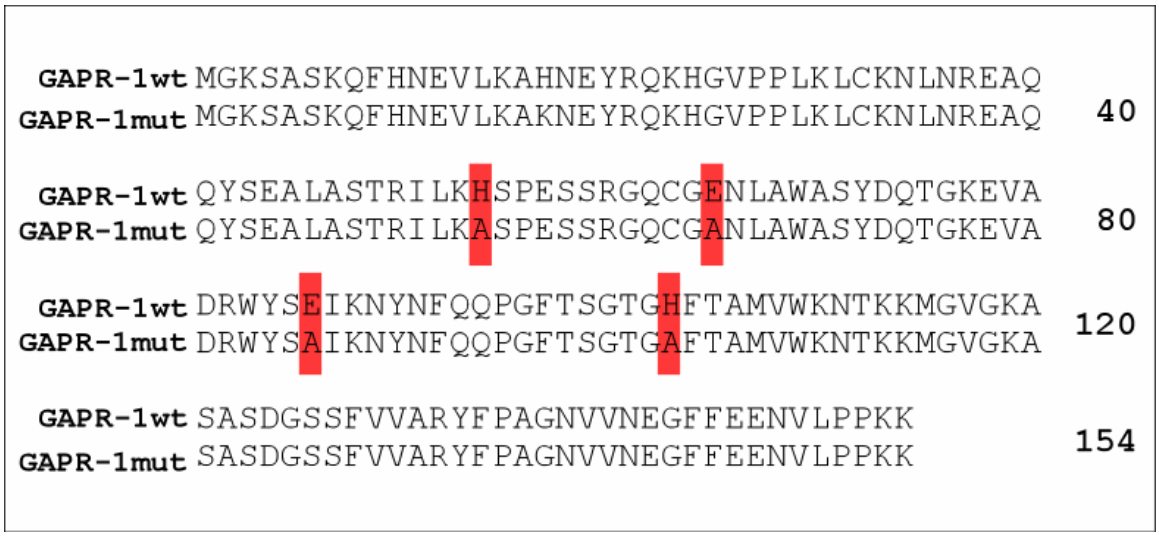

Figure 12. **Site-directed mutagenesis of GAPR-1.** Primary sequence of GAPR-1 wild type showing the amino acid changed during site-directed mutagenesis. His54, Glu65, Glu86 and His103 were replaced by alanine in the same position to yield a mutant protein (GAPR-1 mut), bearing Ala54, Ala65, Ala86 and Ala103. The changes in GAPR-1 wild type were confirmed by DNA sequencing. Site-directed mutagenesis was performed as described by QIAGEN site-directed mutagenesis kit.

The protein lacking the “conserved cluster” (GAPR-1mut) was overexpressed and purified using similar procedures as described for the wt protein (see above). To determine possible interacting partners of GAPR-1, both GAPR-1wt and GAPR-1mut (as a negative control) were covalently linked to CNBr-Sepharose 4B for affinity chromatography. To analyze whether this mutation has an impact on the possible interaction of GAPR-1 to unknown cytosolic components, the affinity columns both GAPR-1wt and GAPR-1mut were loaded with equal amounts of CHO cytosol. After washing the columns, bound proteins were eluted from the column by use of a salt gradient. Fig. 13 shows the chromatographic profiles and corresponding analyses by SDS-PAGE of fractions collected during the elution.

SDS-PAGE analysis of proteins interacting with GAPR-1wt shows a complex protein mixture binding to the column, which eluted at 330 mM NaCl approximately (Fig. 13A, *upper* panel, peak at fraction 14). For GAPR-1mut, a somewhat broader peak eluted from the column (Fig. 13B, *upper* panel, peak ranging from 200 mM to 740 mM NaCl), and the amount of protein was approximately two fold less as compared to the GAPR-1wt chromatographic profile at 280nm. The protein profiles eluted from GAPR-1wt and GAPR-1mut column show a similar protein pattern, indicating that the same proteins bind, with different degrees of affinity (Fig. 13A and B, *bottom* panels).

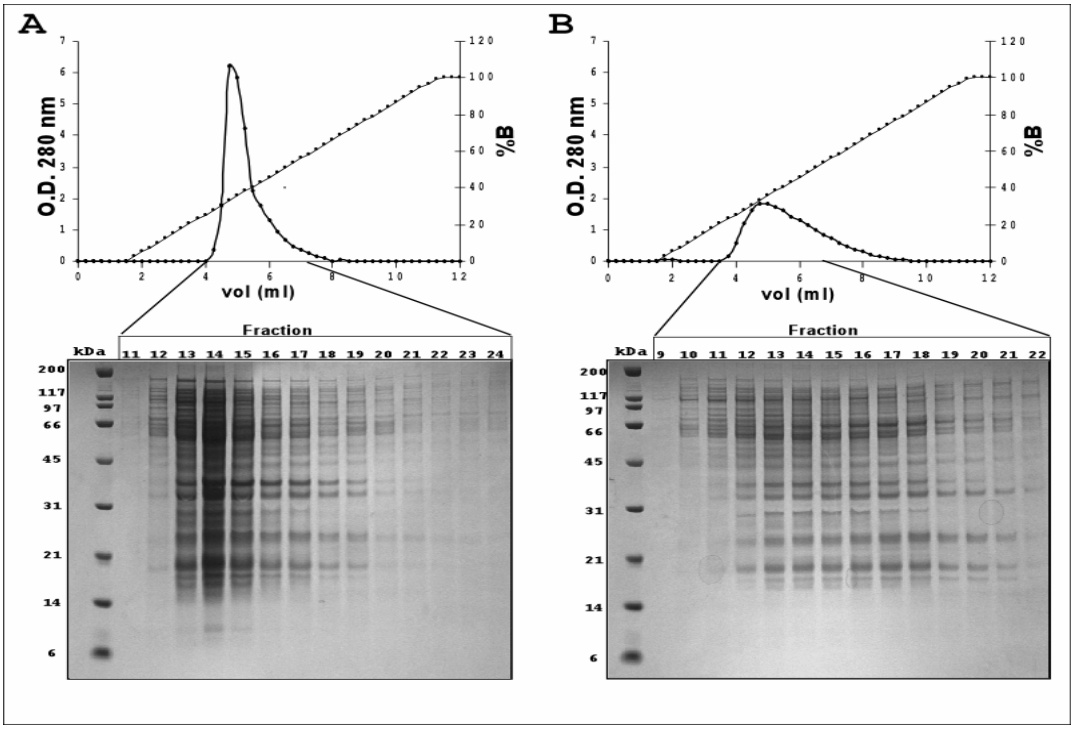

***Figure 13*. Affinity chromatography of CHO cytosolic proteins to Sepharose-bound GAPR-1.** (**A**) 5 mg of GAPR-1 wt were bound to 1ml of swelled-gel CnBr-Sepharose 4B fast flow. CHO cytosol was prepared according to the protocol described in Materials and Methods. 200 ml of cytosol (1mg/ml) was applied onto the GAPR-1 wt column at a flow rate of 0,5ml/min, washed with 100 volumes of buffer Tris-HCl 50mM, NaCl 50mM, pH7.4, until an optical density of 0,01 (or lower) at 280 nm was reached. After washing, a NaCl gradient (50mM to 1M) in buffer (50mM Tris-HCl, pH7.4) was applied at a flow rate of 50µl//min, and fractions were collected. Fractions 11 to 24, corresponding to the peak fractions observed on the protein profile were analyzed by SDS-PAGE and coomassie blue staining. (**B**) 5 mg of GAPR-1 mut were bound to 1ml to CnBr-Sepharose 4B fast flow. Determination of proteins from cytosol that interact with GAPR-1mut was exactly as described for GAPR-1wt. Note: The coupling efficiency was determined by BCA protein quantification and indicated that the coupling efficiency was similar for both GAPR-1wt and for GAPR-1mut (98% coupling efficiency of protein binding to beads).

2.4 Identification of proteins that bind to the GAPR-1 affinity column

2.4.1 Identification of proteins in CHO cytosol that bind GAPR-1

To pursue the identification of the interacting partners of GAPR-1, a mass spectrometric (MALDI-TOF) analysis was performed on the major protein bands, eluting from the GAPR-1wt affinity column (Fig. 14). Eluted proteins were resolved on two different types of gels: a 4-12% SDS-PAGE gel for identification of proteins above 31kDa (Fig. 14, panel A), and a 12% SDS-PAGE for proteins below 31kDa (Fig. 14, panel B). By peptide mass fingerprinting, 17 proteins were identified in 20 selected bands (Table 4). When these proteins were analyzed for functional motifs, the most interesting common feature was the presence of an RNA binding motif in 9 of the 17 proteins identified (Burd, C. G., Dreyfuss, G 1994). The identified RNA-binding proteins fall into three major functional groups: 1) t-RNA synthetases such as Tyrosyl and Threonyl -tRNA synthetases and bifunctional aminoacyl-tRNA synthetase (Weiner, A. M. Maizels, N. 1999) (Wakasugi, K. Schimmel, P. 1999); 2) proteins involved in RNA modificiation or stabilization, such as hnRNPs; and 3) regulators of cell cycle and apoptosis such as Nucleolin, NS1-associated protein 1 (Hresko, R. C. Mueckler, M. 2002; Mizutani, A. *et al.* 2000). Mass spec analysis (by fingerprinting) of the bound CHO proteins was limited due to the fact that not the entire genome of this species is known. Most of the proteins identified are not exact matches but have homologs in *Homo sapiens*. Only for two bands a *Cricetulus griseus* protein was found: Nucleolin (Bugler, B. *et al*. 1982), and thioredoxin peroxidase (Hofmann, B. *et al.* 2002).

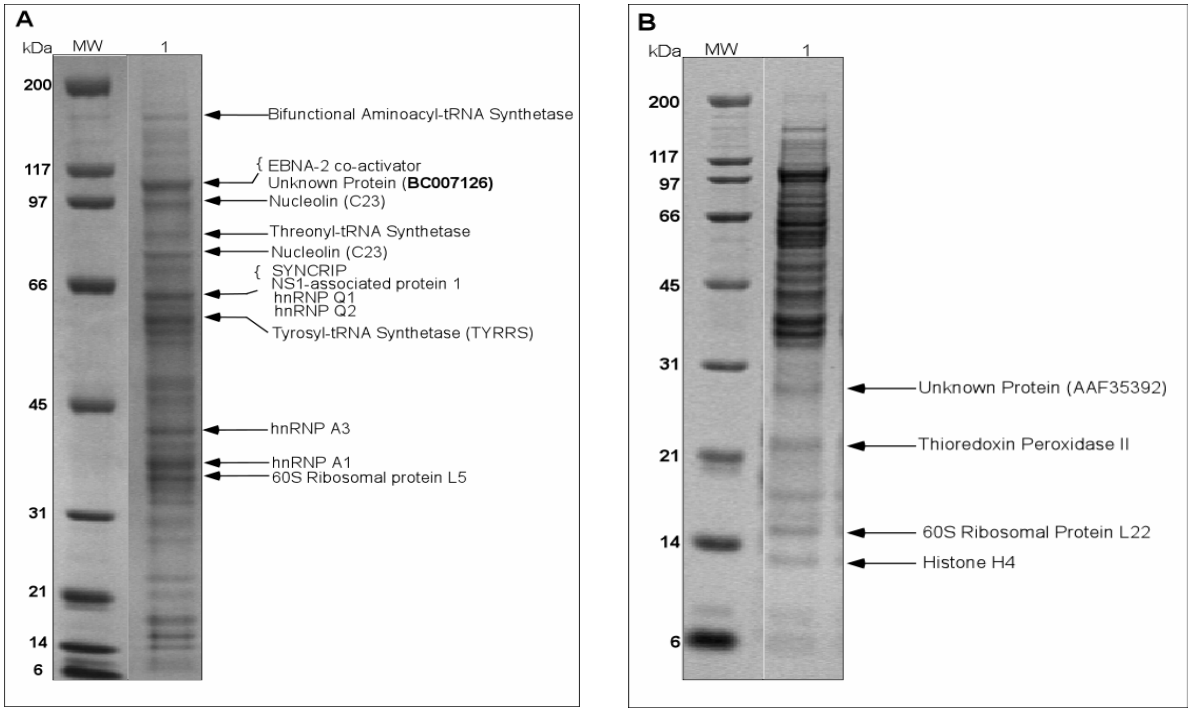

Figure 14. **Identification of CHO cytosolic proteins binding to GAPR-1wt.** Panel A shows peptide mass fingerprinting of major protein bands above 31kDa, separated by SDS PAGE (4-12%) and stained by coomassie blue. Panel B shows peptide mass fingerprinting of major protein bands below 31kDa, separated by SDS-PAGE (12%) and stained by coomassie blue.

2.4.2 Identification of proteins present in complex pull down by GAPR-1 affinity column in HeLa cells

Due to the lack of a comprehensive database for Chinese Hamster (*Cricetulus griseus*), the experiments were repeated with cytosol from HeLa cells (*Homo sapiens* derived) cytosol as a source for the identification of interacting partners. In fact, GAPR-1, employed in these experiments, was cloned from a human fetal brain library (Eberle, H. B. *et al.* 2002). Fig. 15 shows the components in HeLa cell cytosol that bound to the GAPR-1wt column and which were identified by MALDI-TOF. Of the 42 proteins identified, 7 are ribosomal proteins: 3 are part of the large ribosomal subunit, and 4 are part of the small ribosomal subunit. Among the non-

Table 4. CHO proteins identified to bind GAPR-1wt. Protein identification was performed by a combination of in-gel digestion, MALDI-TOF and database searching (http://129.206.154.159/mascot/).

Protein	Mr[a]	pI(Theoretical)[b]	Accession #	amino acids	Similar
Bifunctional aminoacyl-tRNA synthetase	171739	7,75	XM_129647	1512	Mus musculus
EBNA-2 co-activator	103037	6,88	XM_011618	914	Homo sapiens
Histone H4	11445	11,48	S03427	103	Mus musculus
hnRNP A1	34158	9,27	NM_010447	320	Mus musculus
hnRNP A3	33809	8,40	XM_143653	301	Mus musculus
hnRNP Q1	62789	7,18	AY034483	561	Homo sapiens
hnRNP Q2	65900	8,69	AAK59704	588	Homo sapiens
NS1-associated protein 1	62861	5,7	XM_135019	468	Mus musculus
Nucleolin (C23)	73302	4,69	M15825	679	Cricetulus griseus
Ribosomal protein L5	34607	9,78	XM_132197	297	Mus musculus
60S Ribosomal Protein L22	14676	9,21	JC2119	128	Mus musculus
SYNCRIP	62733	7,18	AB035725	561	Mus musculus
Thioredoxin Peroxidase II	22534	8,99	AAF32369	199	Cricetulus griseus
Threonyl-tRNA synthetase Cytoplasmic	84294	6,23	XM_004009	723	Mus musculus
Tyrosyl-tRNA Synthetase	59448	6,61	NM_003680	528	Homo sapiens
Unknown protein	102709	7,08	BC007126	910	Mus musculus
U2 snRNP A'	28325	8,73	AAF35392	254	Mus musculus

A summary of proteins identified after separation by 4-12% and 12% SDS-PAGE. **a**. Represents the theoretical molecular weight. MS analysis of all proteins listed were found to be in good agreement with the theoretical molecular weight. **b**. Isoelectric point (pI) determined by ProParamTool (*http://www.expasy.org/tools/protparam.html*), a web based software for computation of various physical and chemical properties of a given protein.

ribosomal proteins identified are: Alternative Splicing Factor 1, 2 and 3; Casein kinase 2, aminoacyl-tRNA synthetases (Asparagine, Histidine, Isoleucine, Tyrosine), Template activating factor 1 (α,β), DNA helicase 2, and RNA helicase A (Table 5). GAPR-1 bound proteins from Hela cell cytosol can be grouped by functional features as well: several proteins are involved in: 1) ribosome biogenesis (Ginisty, H. *et al.* 1999), RNA binding, and processing; and 2) cell cycle, proliferation and apoptosis (Burd, C. G., Dreyfuss, G 1994; Yanagida, M. *et al.* 2001) Zhu, D. *et al*. 2002; (Wakasugi, K. Schimmel, P. 1999). This classification overlaps significantly with that for proteins from CHO cytosol and several of these cytosolic HeLa cell proteins interacting to GAPR-1 have been identified in CHO cytosol as well such as bifunctional aminoacyl-tRNA synthetase, 60S ribosomal protein L22, U2 sn- RNP protein A, ribosomal protein L5, and nucleolin (table 4 and 5).

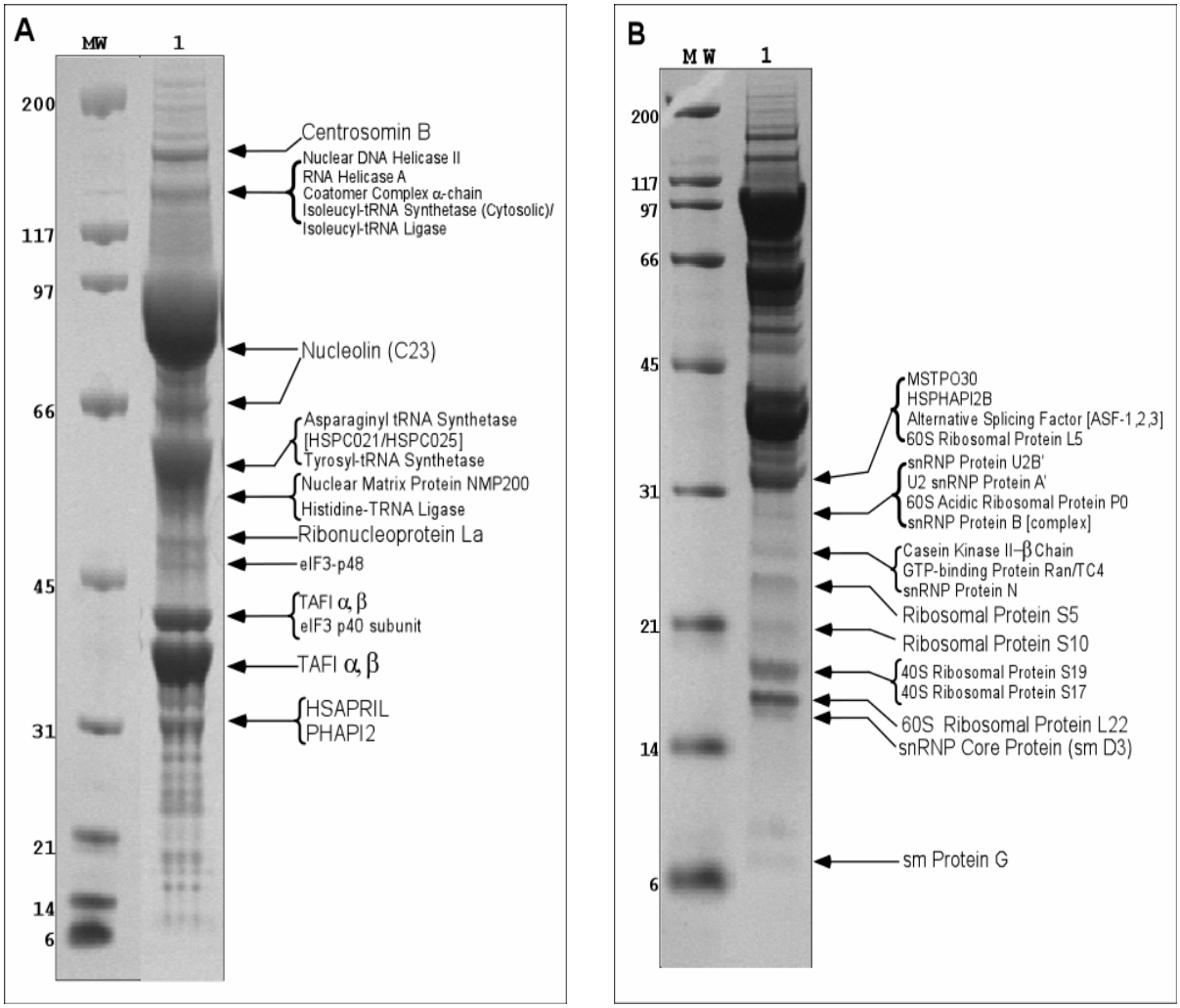

Figure 15. **Identification of Hela cell cytosolic proteins binding to GAPR-1wt.** Panel A shows peptide mass fingerprinting of major protein bands above 31kDa, separated by SDS PAGE (4-12%) and stained by coomassie blue. Panel B shows peptide mass fingerprinting of major protein bands below 31kDa, separated by SDS-PAGE (12%) and stained by coomassie blue.

Table 5. Hela cell proteins identified to bind GAPR-1wt. Protein identification was performed by a combination of in-gel digestion, MALDI-TOF and database searching (http://129.206.154.159/mascot/).

Table X. Proteins that are identified binding to the GAPR-1 affinity column by the combination of in-gel digestion, MALDI-TOF and database searching

Protein	Mr	pI(Theoretical)	Accession #	amino acids
Alternative Splicing Factor				
1	27482	10,37	A40040	248
2	22560	5,61	B40040	292
3	32321	7,73	C40040	201
Asparaginyl t-RNA Synthetase	63758	5,9	BAA34600	548
Casein Kinase 2 b-chain	25268	5,33	A39459	215
Centrosomin B	166868	6,38	BAA09488	1382
Coatomer Complex a Chain Homolog	139784	7,70	ERHUAH	1224
eIF3-p48	52587	5,71	AAC51760	445
eIF3-p40	40075	6,09	AAD03465	352
GARP-1(endogenous)	17332	9,4	Q9H4G4	154
GTP-Binding Protein Ran/TC4	24579	7,01	TVHUC3	216
Histidine t-RNA ligase	57945	5,72	SYHUHT	509
HSPHAPI2B	22434	4,19	CAA68856	195
HSAPRIL	28695	3,95	CAA69265	249
PHAPI2 protein	28941	3,94	Q92688	241
HSPC025/21	66913	5,94	Q9Y262	564
Isoleucyl t-RNA Synthetase (cytosolic)	146818	5,86	Q9H588	1266
Isoleucyl t-RNA Ligase	146178	5,8	I59314	1266
MSTP030	34569	9,73	AAG39281	297
Nucleolin	76224	4,59	A35804	707
Nuclear DNA Helicase II	142100	5,99	CAA71668	1215
Nuclear Matrix Protein NMP200	55603	6,14	CAB51857	504
Ribonucleoprotein La	46979	6,68	A31888	408
RNA helicase A	143410	6,35	A47363	1279
Ribosomal Protein S5 (cytosolic)	22934	9,59	S55916	204
Ribosomal Protein S10 (cytosolic)	18886	10,15	S55918	165
40S Ribosomal Protein S17	15466	9,85	R4HU17	135
40S Ribosomal Protein S19	16051	10,31	I52692	145
60S Ribosomal Protein L22	14704	9,21	P35268	128
60S Ribosomal Protein L5 (cytosolic)	34654	9,76	S55912	297
60S Ribosomal Protein P0 (acidic)	27602	5,72	P05388	234
SnRNP core protein (sm D3)	14021	10,33	AAA57034	126
sm Protein G	8547	8,98	S55054	76
snRNP protein N	24769	11,20	A33270	240
snRNP protein B'	24765	11,20	S09377	240
snRNP protein U2B'	25470	9,72	A25910	225
Tyrosyl t-RNA Synthetase/ Tyrosyl t-RNA Ligase	59448	6,61	P54577	528
Tyrosyl t-RNA Synthetase	44048	8,73	AAB39406	388
Template Activating Factor I	33469	4,23	I59377	290
α,β	32115	4,12	A45018	277
U2 snRNP protein A'	28540	8,73	S03616	255

A summary of proteins identified after separated by 4-12% and 12% SDS-PAGE. [a] Represents the theoretical molecular weight. MS analysis of all proteins listed were found to be in good agreement with the theoretical molecular weight. [b] Isoelectric point (pI) determined by ProParamTool (*http://www.expasy.org/tools/protparam.html*), a web based software for computation of various physical and chemical properties of a given protein.

2.4.3 Identification of a potential GAPR- High Molecular Weight complex that binds GAPR-1

It seemed unlikely that so many different proteins could all bind directly to GAPR-1. Rather, we explored the possibility that several of these proteins belong to a large complex that binds the column due to an interaction of one (or more) of its protein components with GAPR-1. To analyze this possibility, 10ml of CHO cytosol (20mg/ml) were separated into two pools by gel filtration. By use of a pre-calibrated Superdex 200 column (26mm x 70cm), a pool containing proteins with a molecular mass higher than 100kDa (HMW), and another pool with proteins lower than 100kDa (LMW) were obtained (Fig 16, panel A). These two pools were loaded separately onto a GAPR-1wt affinity column, and after extensive washing, a sodium chloride gradient was applied. SDS-PAGE analysis of the eluted proteins (Fig. 16, panel (B)) showed that several proteins in the HMW fraction bound to the column. In contrast, only a very weak band is observed to bind from the LMW fraction.

These results indicate that proteins binding to GAPR-1 affinity column are at least partially present in a large complex in the cytosol. In addition, this result shows a protein pattern similar to that observed for total cytosol (Fig. 13), suggesting that the same complex binds in both cases. Of note, the intensity of the bands eluted from the column loaded with HMW cytosol is lower as compared to the intensity of bands eluted after loading with whole cytosol (Fig. 13). This is probably due to dilution of the cytosolic components in the gel filtration.

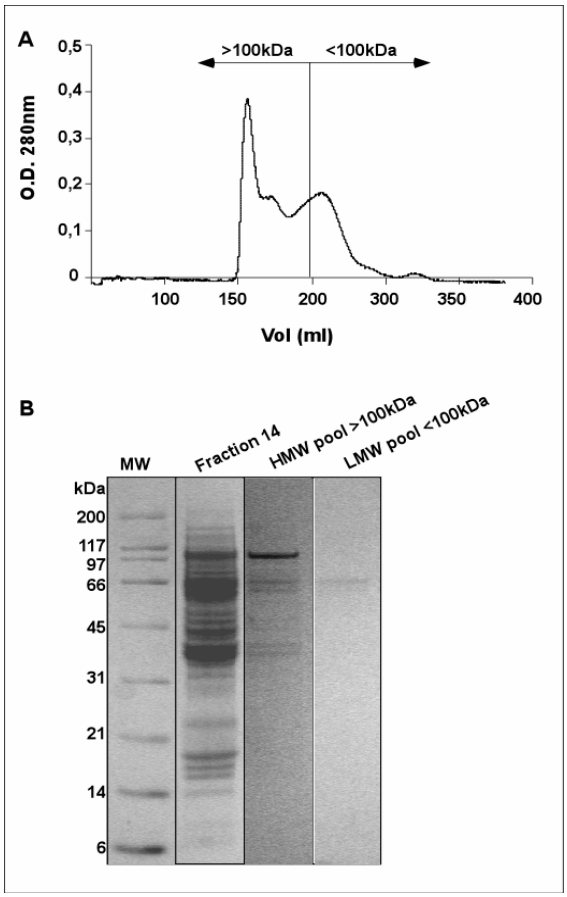

Figure 16. **GAPR-1 association to a cytosolic complex.** Panel (A) shows separation of 10 ml CHO cytosol (20 mg/ml) in buffer (50 mM Tris-HCl, pH 7.5; 50 mM NaCl) on a pre-calibrated Superdex 200 gel filtration column (see Material and Methods). Collected fractions were combined in two different pools: a pool containing proteins above 100kDa (HMW pool), and a pool containing proteins below 100kDa (LMW pool). Panel (B) shows a SDS-PAGE analysis of peak fractions eluting from GAPR-1wt affinity column, after loading with different cytosolic pools: Lane 2, Fraction 14 (peak fraction Fig. 10, panel A); Lane 3, Peak fraction eluting from GAPR-1wt affinity column loaded with HMW pool; Lane 4, Peak fraction eluting from GAPR-1wt affinity column loaded with LMW pool.

2.4.4 GAPR-1 interacting partner *in vitro*

The above described results suggest that GAPR-1 interacts with a protein complex present in the cytosol. To investigate which protein(s) in the complex interact directly with GAPR-1, HeLa cytosol was incubated at 95^{o}C in buffer (50 mM Tris-HCl, 50 mM NaCl, pH 7,5) containing 1% SDS, followed by quenching with 1%Triton X-100 to decrease the sodium dodecyl-sulphate concentration to 0,1%. The solution was loaded onto a GAPR-1wt affinity column at a flow rate of 0,5ml/min, washed and bound proteins were eluted by a sodium chloride gradient. As a result of this treatment, the protein complex dissociated, and only 3 major components eluted from the column (fig. 17, *lane* 1). The 3 proteins were identified by MALDI-TOF as Nucleolin (NCL), Template Activating factor I (TAFI) and HSPAHPI2B. Nucleolin seems to be the major component present in the preparation, and its identity was confirmed by western blot analysis (Fig. 14, *lane*

3). A similar preparation was loaded onto the GAPR-1mut column, and only a faint band was observed at 115kDa in the peak fraction eluting from the column (Fig. 17, *lane* 2). This minor component was identified by western blot as NCL as well (data not shown). This result suggests that NCL, TAF1 and HSPAHP12B are potentially interacting partners of GAPR-1, and that the amino acids mutated in GAPR-1mut are essential for the interaction. Nucleolin runs around 97 to 110 on a 12% SDS-PAGE (Gilchrist, J. S. *et al.* 2002), even though Nucleolin is a 76,5 kDa protein (Lischwe, M. A. *et al.* 1985). This behavior has been explained by phosphorylation at the N-terminus region of the protein, which might function as a post-translational modification mechanism for the regulation of protein function (Rao, S. V. *et al.* 1982; Peter, M. *et al.* 1990). Fig. 17 (Lane 1) shows a similar behavior for Nucleolin, both in SDS-PAGE and western blot analysis (Lane 3).

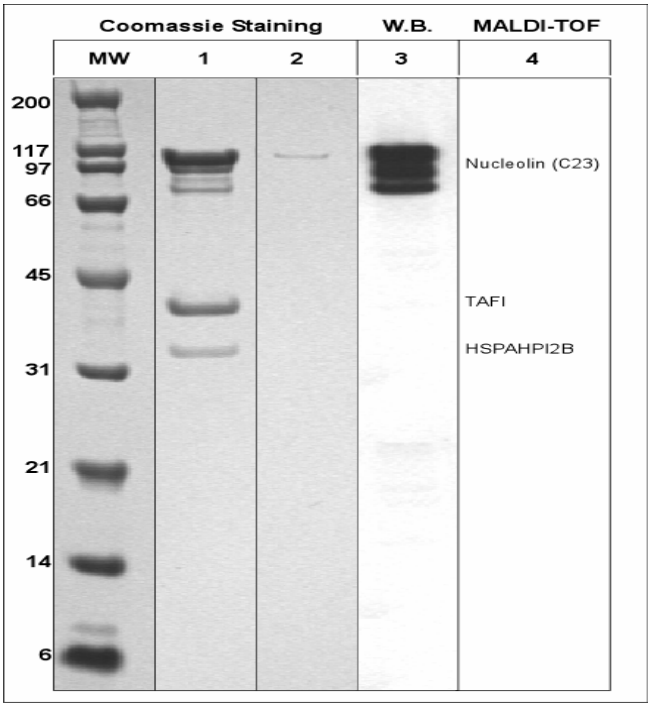

***Figure 17*. Identification of primary interacting partners of GAPR-1**. 200 ml of HELA cytosol (1mg/ml) were incubated at 95°C for 15 min in buffer (50 mM Tris-HCl; 50 mM NaCl) containing 1%SDS, followed by quenching with 1,8L of buffer (50 mM Tris-HCl; 50 mM NaCl) containing 1% Triton X-100. The sample (2L) was loaded onto GAPR-1wt affinity column. A similar preparation was loaded onto GAPR-1mut affinity column. *Lane* 1 shows the peak fraction after elution by a sodium chloride gradient. Lane 3 represents a western blot analysis performed on the peak fraction after elution, using a Nucleolin antibody. Lane 2 shows the peak fraction after elution by sodium chloride gradient on a GAPR-1mut affinity column. Lane 4 shows the identity of the proteins, determined by MALDI-TOF.

3 Structural Characterization of GAPR-1

3.1 Characterization of Recombinant GAPR-1wt and GAPR-1 mut

The mutations in GAPR-1 could have an effect on the overall structure of the protein. To analyze this, GAPR-1wt and GAPRmut were compared by different methods. Both forms of GAPR-1 (wild type and mutant) were purified to homogeneity. The two proteins behaved similar on cation exchange chromatography, and both proteins showed the same reactivity to the GAPR-1 C-terminal antibody (α-1852). The molecular masses of the folded wt and mutant proteins were analyzed by size exclusion chromatography light scattering (SEC-LS) using a pre-calibrated Superdex 200 gel filtration column. GAPR-1 has a slight tendency to form dimmers in solution (Fig. 18): the major peak eluting between 17.9 and 18.2ml represents the monomeric form of GAPR-1. A small peak eluting between 16.8 and 17.2ml contains the homodimer form of GAPR-1wt. GAPR-1mut behaves different in solution and the majority of this protein elutes between 16.2 and 16.7ml, indicative of a predominantly homodimeric form of GAPR-1mut (Fig. 18, *Inset*). The second and smaller peak observed in the profile for GAPR-1mut represents the monomeric form of the protein. These data suggest that the equilibrium between monomeric and dimeric forms of the protein in solution has been altered by the mutation, creating conditions for GAPR-1mut to be present mostly as a homodimer in solution. This might explain that the conditions used so far for crystal formation of GAPR-1wt were not suitable for GAPR-1mut and that dimerization of the protein may effect crystal formation of GAPR-1mut.

3.2 GAPR-1/GAPR-1 interaction in vivo

To determine whether GAPR-1 can form dimers on Golgi membranes, isolated CHO Golgi membranes were crosslinked with N-Hydroxylsulfonsuccinumydyl-4-azidobemzoate, similar as described in section 1.4. Upon immunoprecipitation of lysates using antibodies against GAPR-1, an irradiation-dependent cross-link product appears at 34kD when the immunoprecipitates were analyzed for the presence of GAPR-1 (Fig. 19). These data suggest that GAPR-1 is present as a

dimer on the Golgi membrane (Fig. 19). However, it does not exclude the possibility GAPR-1 interacts with an unknown protein of similar molecular mass.

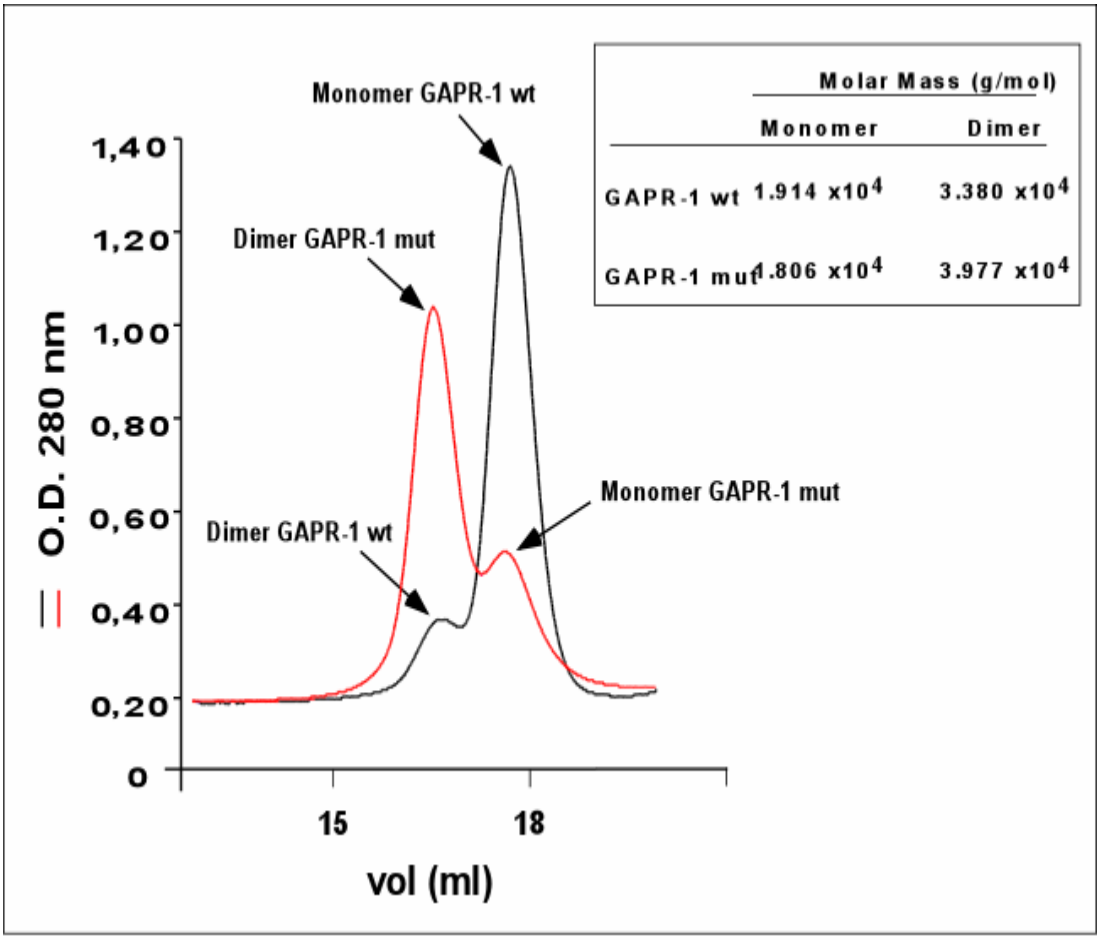

Figure 18. **Size-exclusion chromatography (SEC-LS) of GAPR-1wt and GAPR-1mut.** 200µl samples of pure GAPR-1wt or GAPR-1mut (100µg/ml) were subjected to size-exclusion chromatography at 8°C in a buffer containing 50mM Tris-HCl, pH 8.0 and 300mM NaCl. The concentration of GAPR-1wt and GAPR-1mut in sample loaded on the column was 0.3mM. Elution profile of GAPR-1wt (black line): the peak of absorbance at 280 nm eluted between 17.9 and 18.2ml for GAPR-1wt (monomer). The peak eluted between 16.8 and 17.2ml represents a homodimer form of GAPR-1wt. Elution profile of GAPR-1mut (red line): The peak of absorbance at 280 nm eluted between 16.2 and 16.7ml for GAPR-1mut (homodimer), and the peak eluted between 17.3 and 17.6ml for the monomer form of GAPR-1mut. Inset shows the calculated molar masses of the proteins eluting from the pre-calibrated Superdex200.

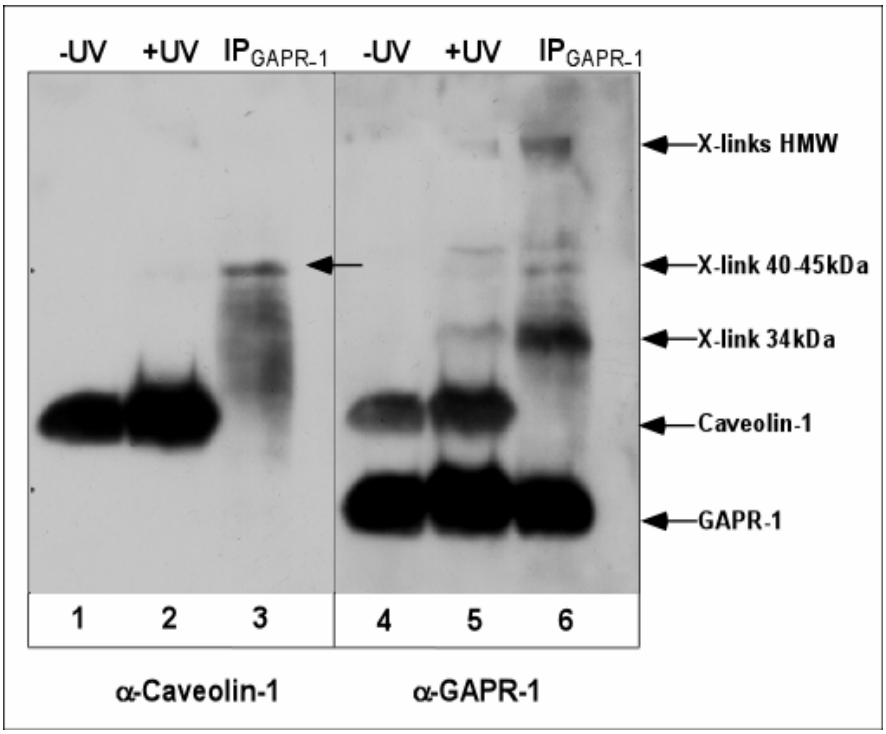

Figure 19. **GAPR-1 dimerization on Golgi membranes.** CHO Golgi membranes (50µg) were incubated with N-Hydroxylsulfosuccinimidyl-4-azidobenzoate (5mM) in PBS for 30 minutes at RT and left on ice (lane1, and 4) or irradiated for 10 minutes at 254 nm (lane 2 and 5) and analyzed for crosslinked products. For immunoprecipitation (lane 3, and 6), 500 µg of Golgi membranes were used, and GAPR-1 was immunoprecipitated using an α-GAPR-1 (α1852) antibody). After western blotting, the PVDF membrane was incubated first with α-Caveolin-1, and subsequently blotted with α-GAPR-1.

3.3 Circular Dichroism analysis of GAPR-1

Circular dichroism (CD) spectroscopy is an important method, complementary to crystallography in studies of protein structure, stability and folding (Kelly, S. M. Price, N. C. 2000). CD spectra of proteins are usually quite complex, as they represent the sum of positive and negative sign contributions of backbone peptide groups in different conformations and aromatic side chains. Circular dichroism provides a possibility for defining the contribution of those residues of GAPR-1wt, and of replaced residues in GAPR-1mut.

Fig. 20A shows far-UV (190-250nm) CD spectra of GAPR-1wt and GAPR-1mut in solution. Far-UV CD spectra analyses secondary structures in proteins and the CD spectrum of GAPR-1wt shows a negative trough in the 202-240nm region,

whereas GAPR-1mut shows a negative depression in the 200-240nm. Both curves show a similar behavior in term of secondary structural elements (α-helix, β-sheet): GAPR-1wt has a minimum intensity absorption in the far-UV at 208nm, and GAPR-1mut has a minimum at 207-208nm, whereas a positive signal is observed for both proteins in the range from 190-200nm. The weak negative signals for GAPR-1wt at 211 and 218-219nm are indicative of β-sheet forms. The negative signals at 208 and 224 can be assigned to α-helix structures (Kelly, S. M. Price, N. C. 2000). The spectrum of the GAPR-1mut, as compared to GAPR-1wt, evidences differences in the relative amplitude of the 208nm and 224nm minima, probably related to slight changes in the β-sheet content. Nevertheless, there appears to be no major differences between GAPR-1wt and GAPR-1mut in α-helix, and β-sheet content.

Changes in the tertiary structure can be highlighted by examining the near CD spectra. Fig. 20B shows near-UV CD spectra of wild-type and mutant GAPR-1. Differences in shape and intensity of the near-UV signals correlate with the different contents of aromatic amino acid residues. Analysis of amino acid sequence revealed that GAPR-1 contains five tyrosine (Tyr-20, Tyr-42, Tyr-72, Tyr-84, Tyr-90), three tryptophan (Trp-69, Trp-83, Trp-109), eight phenylalanine (Phe-9, Phe-92, Phe-97, Phe-104, Phe-128; Phe-134, Phe-144, Phe-145), and five histidine residues (His-10, His-17, His-24, His-54, His-103). Signals in the region from 250-270nm are attributable to phenylalanine residues, and they seem to be the major determinants of the near-UV spectra. It appears that their positioning is altered due to the mutation in GAPR-1 (Fig. 20B). Based on the crystal structure, Phe-134 and Phe-144 seem to be most exposed to solvent, and have the fewest inter-residue contacts of all aromatic amino acids in GAPR-1. The presence of significant near-UV signals is a good indication that the protein is folded into a well-defined structure (Kelly, S. M. Price, N. C. 2000). Changes in the near-UV spectrum of GAPR-1mut (Fig. 20B) could be explained by the formation of GAPR-1mut homodimers in solution, which represents the major component as shown by SEC-LS. Therefore it is reasonable to assume that the

tertiary structure is retained. The differences of intensity in the near-UV spectra between 270 -290nm (Fig. 20B) suggest the presence of a Tyr residue in the monomer that has been perturbed by dimer formation. The major changes in intensity of near-UV spectrum for GAPR-1mut (between 270-290 nm) suggest that the tyrosine environment at the interface in the homodimer has been altered (Fig. 20B).

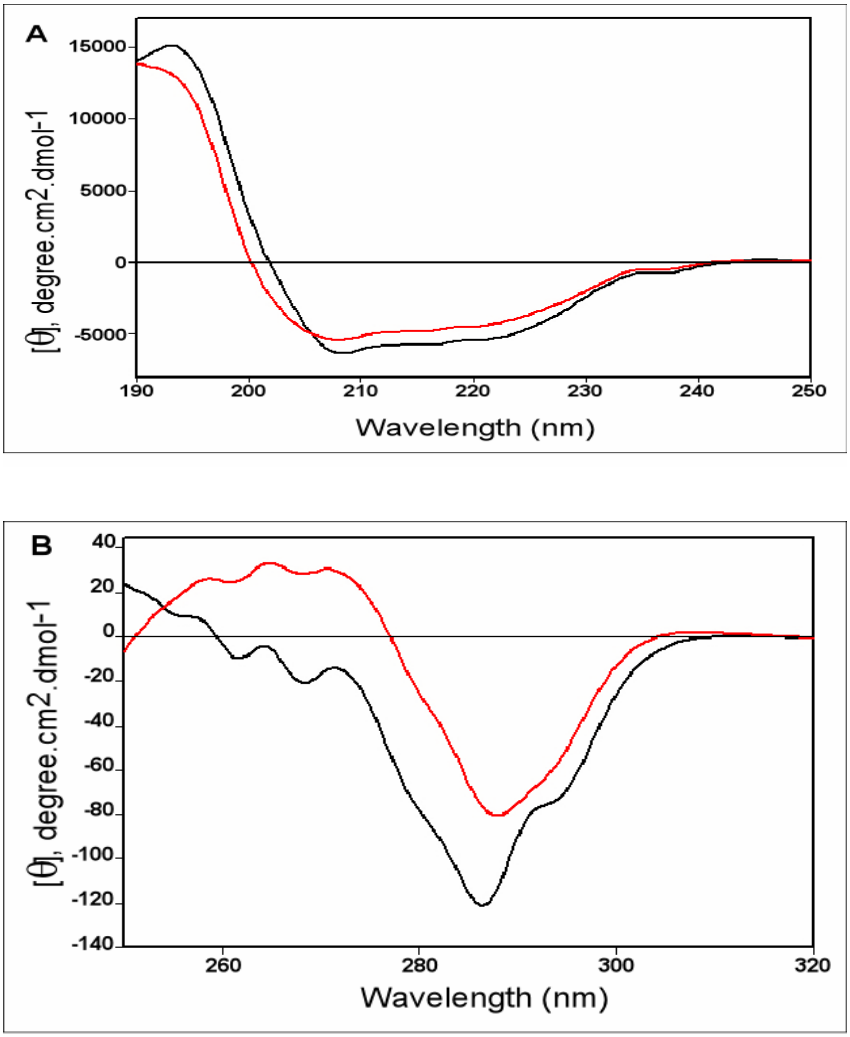

Figure 20. **Circular dichroism spectra for GAPR-1wt and GAPR-1mut.** Far UV-spectra (CD) of GAPR-1wt in 5mM Phosphate buffer, pH 8.0 (black line), and GAPR-1mut in the same buffer (red line) in the far-UV (**A**) and the near-UV (**B**). Graphs obtained by Dr. Valerie Paneels using Sigma Plot®.

4 Interaction Trap or two hybrid system

4.1 Nucleolin- GAPR-1 interaction.

To extend the results of the *in vitro* interaction assays, studies were carried out using the yeast two-hybrid system to determine whether Nucleolin and GAPR-1 can interact under *in vivo* conditions and also to confirm the interaction by an independent method. For this purpose, Nucleolin was fused to the *Escherichia coli* B42 activation domain of the prey plasmid pJG4.5 to produce pJGNCL. GAPR-1 (wild-type or mutant) was fused to the *lexA* DNA-binding domain sequence of the bait plasmid pEG202 to produce pEGGAPR-1wt and pEGGAPR-1mut. *Vice versa,* Nucleolin and GAPR-1 were also cloned in pEG202 and pJG4.5, respectively to yield pEGNCL, and pJGGAPR-1wt -or pJGGAPR-1mut. In the pJG4.5 construct, expression of the B42 fusion construct is repressed by glucose and induced by galactose. The two plasmids were introduced into *Saccharomyces cerevisiae* strain EGY48 containing the reporter plasmid pSH18-34. Thus, the plasmid expressing the *LexA*-fused bait protein activates a reporter system responsive to transcriptional activation through the *LexA* operator (Fig. 21). Transformants were tested for the production of β-galactosidase as a phenotype indicative of interaction between the two fusion proteins. Strains harboring both plasmids grew on medium lacking leucine, uracil, and triptophane (Fig. 21B). Discrimination based on color is achieved when yeast is grown on medium containing X-gal (Fig. 21A). Expression of either fusion protein in combination with empty complementing plasmid resulted in a non-interactive phenotype (data not shown). GAPR-1wt strongly induced transcription of the β-galactosidase reporter gene when tested against Nucleolin (Fig 22A, panel 1 and 2). GAPR-1mut (mutations in His54, Ala; Glu65, Ala; Glu86, Ala; His103) showed a decreased level of interaction (Fig. 22A, panel 3 and 4), implying these amino acid residues contribute to the interaction of GAPR-1 and Nucleolin. The reverse combination, Nucleolin (*LexA*) induced transcription of the reporter gene was somewhat less efficient when tested against GAPR-1 (B42) (Fig. 22A, panel 1 versus 2 respectively), and a similar effect is observed for GAPR-1mut (Fig. 22A, panel 3 versus 4, respectively). In agreement with the

tendency of GAPR-1 to form dimers, GAPR-1wt activated the β-galactosidase reporter gene when tested against GAPR-1wt or GAPR-1mut. Any combination of GAPR-1 (wild type or mutant) in the prey and bait plasmid showed an interaction in the two hybrid system (Fig. 22A, panels 5-8). These results suggest that the mutation does not have a significant effect on GAPR-1/GAPR-1 interaction, consistent with the results observed by size exclusion chromatography.

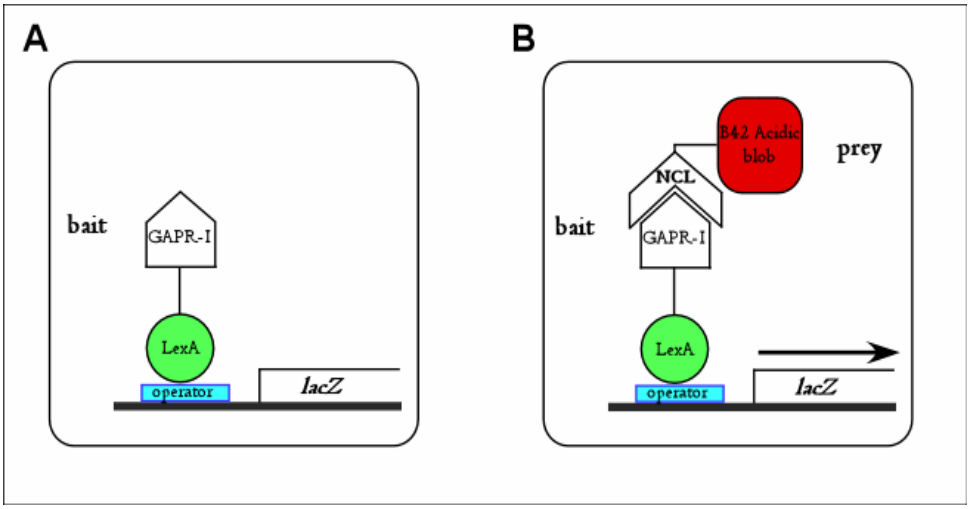

Figure 21. Schematic representation of the two hybrid system assay. (A) An EGY48 yeast cell containing the *LexA* operator-responsive reporter, and the plasmid bearing the *GAL1* promoter-*lacZ* fusion gene (causing yeast to turn blue on medium containing Xgal). (B) A positive interaction is shown between GAPR-1 and Nucleolin, fused to the B42 acid blob (domain) in pJG4.5, resulting in the activation of the operator by the reporter *LexA* fused to GAPR-1, thus causing a blue color on medium containing X-gal. Symbols: blue rectangle, LexA operator sequence; green circle, LexA protein; open pentagon, GAPR-1; open bent rectangle, Nucleolin; red box, activator protein B42 (acid blob).

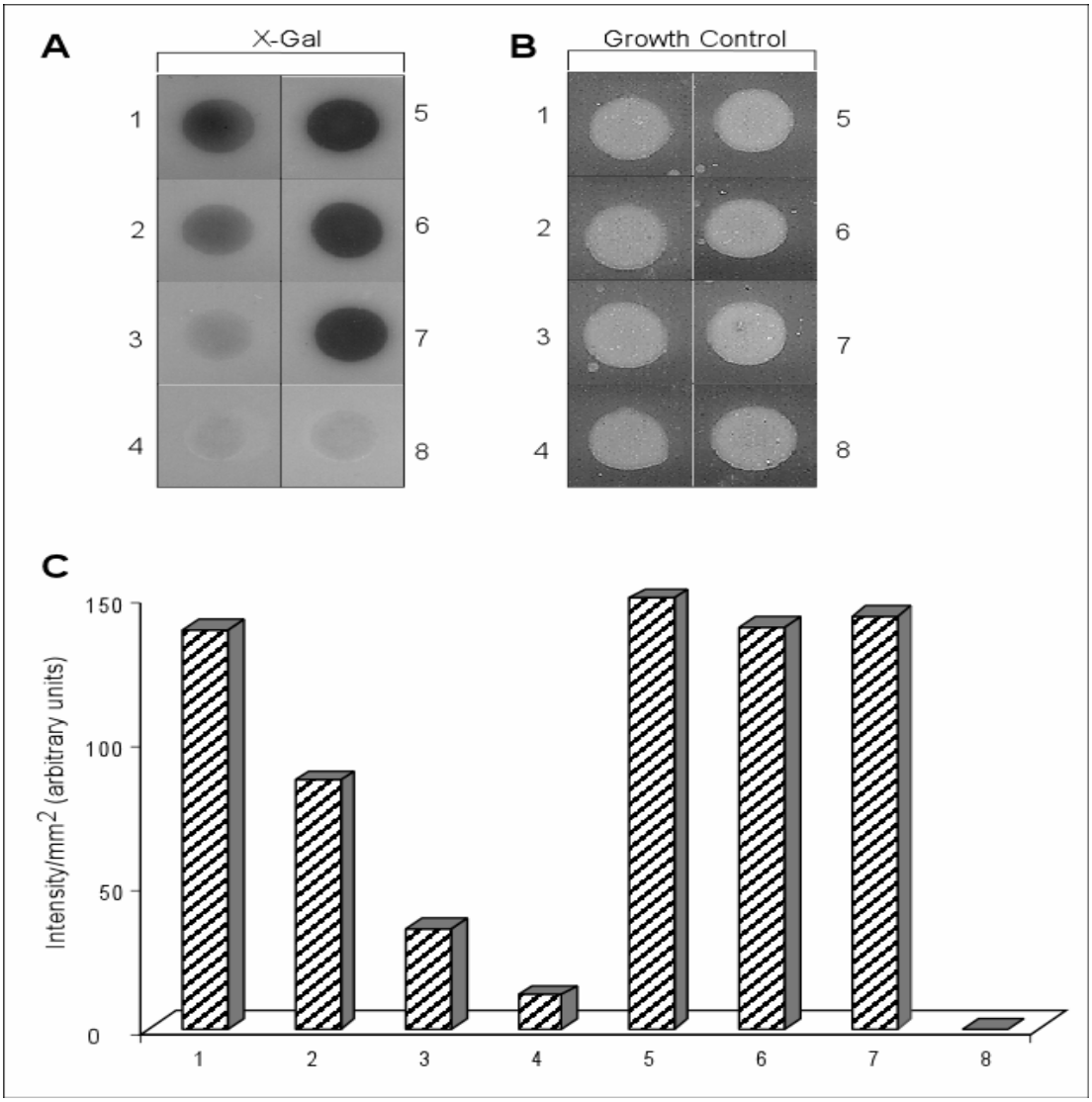

Figure 22. **Interactions between GAPR-1 (wild-type and mutant) and Nucleolin.** Strains of *Saccharomyces cerevisiae* EGY48 harboring interaction constructs of the bait plasmid pEG202 and the prey plasmid pJG4-5, containing GAPR-1wt, GAPR-1mut or Nucleolin as indicated, were tested for growth (panel B) on medium containing: glucose, without leucine, tryptophan and uracil, and X-gal (panel A). Positions represent the growth patterns of strains expressing: 1) GAPR-1wt (pGEGAPR-1wt) + Nucleolin (pJGNCL); 2) GAPR-1wt (pJGGAPR-1wt + Nucleolin (pEGNCL); 3) GAPR-1mut (pEGGAPR-1mut) + Nucleolin (pJGNCL); 4) GAPR-1mut (pJGGAPR-1mut) + Nucleolin (pEGNCL); 5) GAPR-1wt (pGEGAPR-1wt) + GAPR-1wt (pJGGAPR-1wt); 6) GAPR-1mut (pEGGAPR-1mut) + GAPR-1wt (pJGGAPR-1wt); 7) GAPR-1mut (pEGGAPR-1mut) + GAPR-1mut (pJGGAPR-1mut); 8) Nucleolin (pEGNCL) + Nucleolin (pJGNCL). ***C.*** Quantitation of Nucleolin / GAPR-1 interactions and GAPR-1/GAPR-1 in EGY48 bearing plasmids as indicated in panel a,b. Relative intensities were determine (intensity/mm^2 arbitrary units) for each colony on X-gal versus controls bearing empty plasmids.

5 Regulation of GAPR-1 expression

5.1 Effect of serum starvation on GAPR-1 expression in CHO cells

GAPR-1 is not expressed in cells tissues terminally differentiated in G_0 (e.g. brain and skeletal muscle) (Eberle, H. B. *et al.* 2002), and highly expressed in tissues with higher turnover rate. It is known that serum starvation also induces cells to arrest in the G_0/G_1 phase of the cell cycle in cell cultures (Cooper, S. 2003). To investigate a possible effect of serum starvation on GAPR-1 expression, CHO cells at 70-80% confluence were transferred to serum free medium and grown for various periods of time (0, 3, 9 and 48 hrs). After each incubation period, the cells were lysed and a total membrane fraction was obtained. Western Blot analysis (Fig. 23 *upper* panel A) shows the effect of serum starvation on GAPR-1 expression and indicates that the protein is completely down-regulated after 48hrs when cells have entered the G_0/G_1 phase. This observation suggests that expression of GAPR-1 may be induced at a specific stage of the cell cycle and that the down regulation of GAPR-1 could be associated with the entry of cells into G_0. A different type of regulation occurs for Caveolin-1 (Fig. 23 panel A). It is known that caveolin is up-regulated in G_0/G_1 (Volonte, D. *et al.* 2002) (Galbiati, F. *et al*. 2001), and as expected, increased expression of this protein was observed after 48 hrs under serum deprivation conditions.

5.2 Localization of Nucleolin to Golgi membranes

Nucleolin has been reported as a nucleolar protein in eukaryotic cells (Ginisty, H. *et al.* 1999), but is has also been found in the cytoplasm (Srivastava, M. Pollard, H. B. 1999) and at the cell surface (Hovanessian, A. G. *et al.* 2000). In order to investigate whether Nucleolin can localize to the Golgi apparatus, sub-cellular fractionation of HeLa cells and rat liver was performed to obtain Golgi membranes and a cytosolic fraction. The presence of Nucleolin was determined by immunoblotting using a commercially available antibody against Nucleolin (Fig. 24). This antibody cross-reacts with human and rat Nucleolin. Interestingly, this Nucleolin antibody is able to recognize a band at 110kDa, which represents

Nucleolin in the HeLa Golgi (Fig. 24, lane 2), as well as in the cytosol (Fig. 24, lane1). In rat liver Golgi, Nucleolin could not be detected (Fig. 24, lane 4), although Nucleolin is present in rat liver cytosol (Fig. 24, lane 3). These blots were analyzed for GAPR-1 to confirm its localization to the same compartments. As shown in Fig. 24 (lane 2 and 4), GAPR-1 is present in the Hela Golgi (Fig. 24, lane 2), but absent from rat liver Golgi (Fig. 24 lane 4). This result confirms previous findings (Eberle, H. B. *et al.* 2002) (Eisenberg, I. *et al.* 2002), where GAPR-1 could not be detected in liver membranes, both by immunoblotting and by mRNA detection (Eisenberg, I. *et al.* 2002). Unfortunately, it was not possible to use CHO Golgi membranes in these experiments, since the Nucleolin antibody does not react with the hamster version of the protein.

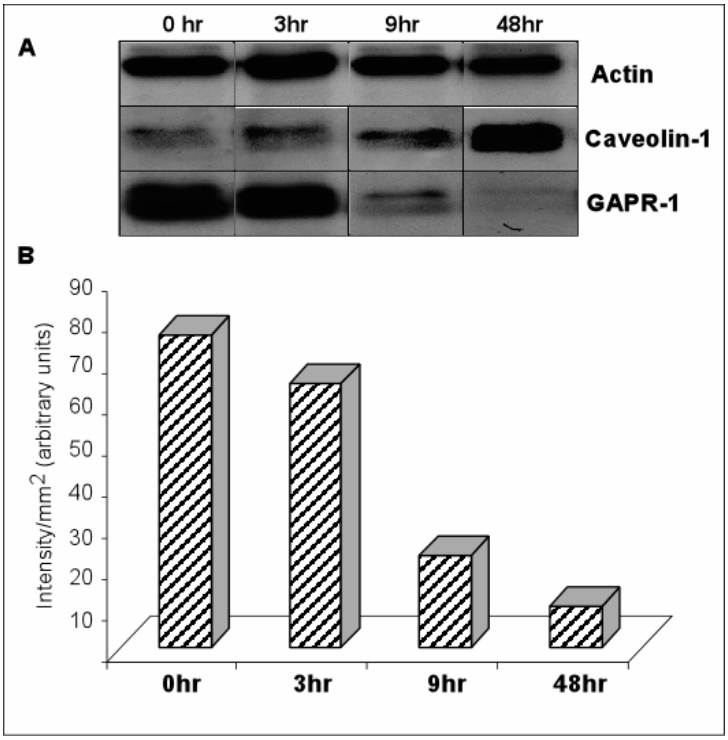

***Figure 23*. Effect of serum starvation on GAPR-1 expression in CHO cells. A**. CHO cells at 70-80% confluence were incubated in serum-free α-DMEM for different time periods (0, 3, 9 and 48 hrs). Cells were harvested and lysed in Tris-HCl pH 7.5; 200mM Sucrose (as described in Materials and Methods). Total membranes were obtained from the post nuclear supernatant by centrifugation at 100,000 x*g*, 1hr. 25µg of total protein were separated by SDS-PAGE (14%), and analyzed by western blotting. PVDF membranes were first incubated with α-GAPR-1 (α-1852), followed by α-Actin, and α-Caveolin-1. **B**. Relative intensities of GAPR-1 expression were determined (intensity/mm^2 arbitrary units) for each band using the software Quantity One® (Biorad) and plotted versus incubation times.

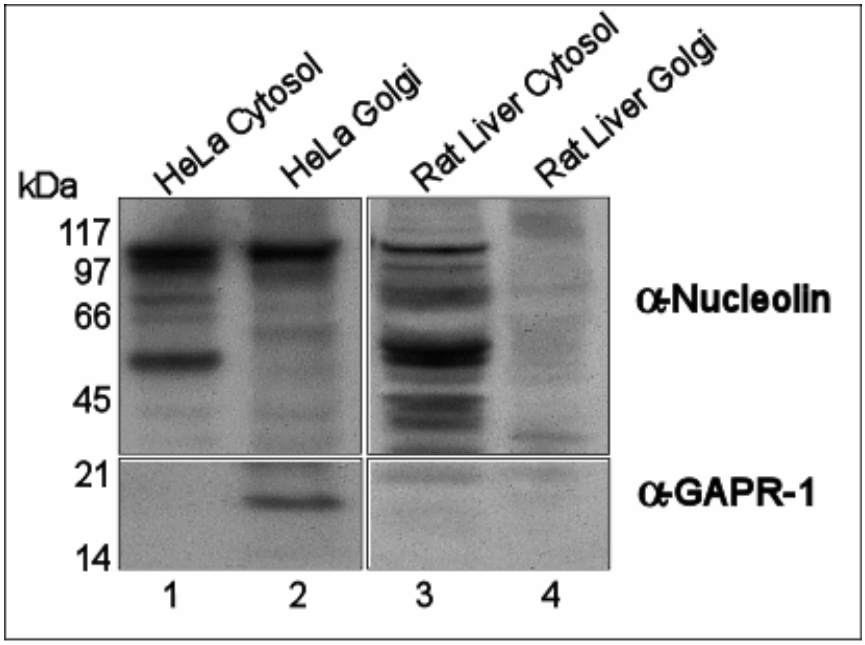

***Figure 24*. Nucleolin localization on Golgi membranes.** Golgi membranes and cytosol were obtained from HeLa cells as indicated in Materials and Methods. 20µg of total Golgi membranes or 20µg cytosolic proteins were separated by SDS-PAGE, and analyzed by western blot for the presence of Nucleolin and GAPR-1 using specific antibodies against these proteins (C23 (Nucleolin) and α-1852, respectively).

Discussion

GAPR-1 is a novel human protein that belongs to Group 1 of the plant pathogenesis-related proteins, a superfamily of proteins sharing structural similarities (Murphy, E. V. *et al.* 1995; Yamakawa, T. *et al.* 1998). Although an antifungal activity has been described for plant members of the superfamily (Antoniw, J *et al*., 1980), little is known about their function. Recent evidence suggests, however, a more general role in signaling during host-pathogen interactions in plants. This may suggest a role in the (innate) immune system for mammalian family members, which is reminiscent of the plant immune system.

1 Binding of GAPR-1 to Golgi membranes

GAPR-1 was originally identified in a low-density detergent-insoluble fraction (GICs) from a Golgi-enriched fraction (Gkantiragas, I. *et al*. 2001). The presence of GAPR-1 in these lipid-enriched microdomains implies a strong membrane association of the protein, and several lines of evidence suggest that GAPR-1 is tightly bound to membranes (Fig. 7) (Eberle, H. B. *et al*. 2002). Here, several characteristics of GAPR-1 were investigated, which may be involved in the membrane binding of GAPR-1.

1.1 GAPR-1 binding to membranes

GAPR-1 contains the consensus sequence for N-myristoylation, which is the substrate for N-myristoyl- transferase, as has been shown *in vitro* (*E. coli*) (Fig. 5). Native GAPR-1 was found to be myristoylated by mass spectroscopic analysis (Fig. 6). For many proteins, the myristate chain is required for membrane binding, which in turn is required for proper cellular function (Zheng, J. *et al*. 1993). It has been suggested that fatty acylation – myristoylation and/or palmitoylation- may represent a common mechanism for targeting cytoplasmic molecules to caveolae or other membrane domains (Lisanti, M. P. *et al.* 1994). However, it is unlikely that N-myristoylation is the only motif for membrane binding in GAPR-1, since the binding energy of myristate to membranes is not sufficient to stably anchor a protein to a membrane (Peitzsch, R. M. McLaughlin, S. 1993). In support of this, several

myristoylated proteins do not show exclusive membrane localization (McCabe, J. B. Berthiaume, L. G. 2001). Therefore, a second interaction is required for efficient membrane-binding of myristoylated proteins (reviewed in Resh, M. 1999). The two-signal model for membrane binding of N-myristoylated proteins -defined as either a polybasic cluster of amino acids or a palmitate moiety- (Resh, M. D. 1999) (Fig. 25) could explain the binding of GAPR-1 to membranes. As GAPR-1 is expected to be highly charged at physiological pH (pI=9.4), electrostatic interactions could provide an additional anchoring signal as it has been shown for MARCKS proteins (McLaughlin, S. Aderem, A. 1995). GAPR-1 has positive clusters of amino acids both at the N- and C-terminus which could be involved in binding to Golgi membranes. Thus, the interaction of GAPR-1 with membranes is proposed to occur *via* positive residues (Lys-Arg) (Kim, J. *et al.* 1991), and a myristate group. Non-myristoylated recombinant GAPR-1 is able to interact with many types of membranes such as liver Golgi membranes and peroxisomes that do not contain endogenous GAPR-1 (data not shown); these interactions are likely due to electrostatic interactions properties of the protein with membranes.

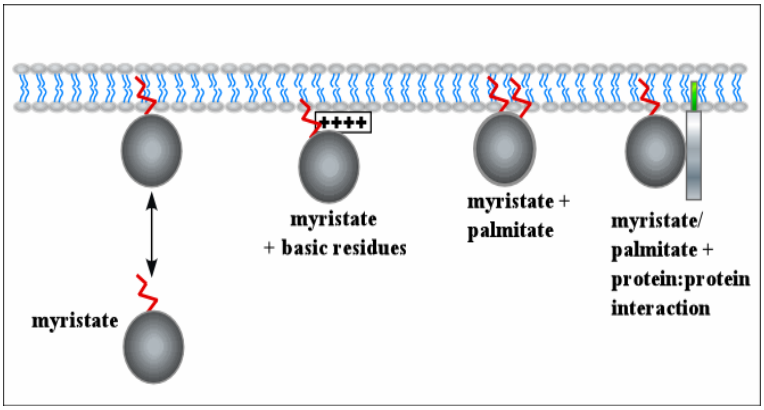

***Figure 25*. The two-signal model for membrane binding of myristoylated proteins**. Myristoylated proteins require a second membrane binding signal. A cluster of basic residues can provide electrostatic interactions with acidic phospholipid head groups at the inner leaflet of the bilayer (myristate + basic). One or two palmitate moieties can provide additional hydrophobic interactions with the bilayer (myristate + palmitate). Alternatively, membrane interaction of singly acylated proteins can be enhanced by protein-protein interactions with other membrane-bound proteins (Resh, M. D. 1999).

According to the two-signal model for membrane-binding, protein-protein interactions could be involved in membrane-binding of GAPR-1 as well. Proteins belonging to the GICs such as B subunit of the vATPase, flotillin-1, caveolin and GAPR-1 interact with each other after disruption of the microdomain scaffold (Gkantiragas, I. *et al.* 2001). These results suggest that the lipid scaffold may not be absolutely necessary for membrane-binding of GAPR-1. In this work it is reported that GAPR-1 interacts directly with caveolin-1 (Fig. 7, and Eberle, H. B. *et al*. 2002). This interaction is possibly mediated *via* a potential caveolin-binding motif (Okamoto, T. *et al.* 1998), although this remains to be addressed. However, the interaction of GAPR-1 with Caveolin does not clarify the lipid raft localization of GAPR-1: in contrast to caveolin-1, GAPR-1 has not been detected at the plasma membrane, which is the major site of caveolin localization. Nonetheless, Caveolin-1 does exist at the trans-Golgi network and earlier compartments (Gkantiragas, I. *et al.* 2001; Fielding, C. J. Fielding, P. E. 2003).

Alternative to the two-signal model it is possible that an N-myristoyl group plays a structural role to stabilize a protein conformation on the membrane (Zheng, J. *et al.* 1993), In this case, GAPR-1 binds the membrane by its electrostatic and protein-protein characteristics, and the myristate-group would determine its conformation on the membrane. It is also possible that GAPR-1 is subject to a “myristoyl switch”, triggered by electrostatic and protein-protein interactions, which can affect the membrane binding (reviewed in Resh, M. D. 1999). The myristoyl-switch can be activated by ligand binding (ADP-ribosylation factor), by electrostatic interactions (MARKCS) (McLaughlin, S. Aderem, A. 1995) or by proteolysis (Zhou, W. *et al.* 1994).

1.2 A possible role of phosphorylation in membrane partitioning of GAPR-1?

Dynamic partitioning of selected proteins to lipid microdomain appears necessary to provide rapid, efficient, and specific propagation of stimuli to targets (Oh, P. Schnitzer, J. E. 2001) (Prior, I. A. Hancock, J. F. 2001). Phosphorylation of proteins can *e.g*. control their interaction to other proteins,

their location in the cell, and their propensity for degradation by proteases. Sawai, T. et al., (1993) have shown that phosphorylation of MARCKS – an *N*-myristoylated protein- moves it reversibly off the membranes, implying a mechanism to control the reversible binding of myristoylated proteins to membranes. For MARCKS the mechanism is understood to some extent, since phosphorylation occurs to the calmodulin-binding domain of MARKCS, a basic cluster that also binds to acidic lipids in membranes. GAPR-1 does not have the same positive cluster arrangement as MARCKS, but phosphorylation of GAPR-1 may change its partitioning to membranes (Fig. 26). Phosphorylation experiments show that highly phosphorylated GAPR-1 is present in cytosol. Phosphorylation of GAPR-1 is, however, not restricted to the cytosolic pool and the largest pool of phosphorylated GAPR-1 is found in lipid microdomains. Given the high amounts of GAPR-1 molecules in microdomains, the degree of phosphorylation per molecule of GAPR-1 seems however, lower. Since the level of phosphorylation seems dissimilar between different pools, phosphorylation might allow GAPR-1 to distribute between different compartments within the cell i.e. the raft fraction, the non-raft fraction, and cytosol. Phosphorylation of GAPR-1 could effect the electrostatic interactions with membranes, similar as for the MARCKS proteins (McLaughlin, S. Aderem, A. 1995; Resh, M. D. 1999). Phosphorylation could also affect the conformation of GAPR-1, thus affecting its partitioning to different pools. A conformation-dependent microdomain localization has been described for H-ras (Prior, I. A. *et al.* 2001). GTP loading shifts this equilibrium to the fluid phase membrane. The exact mechanism is unknown, but it is believed that GTP loading causes a conformational change, which is transmitted through to the membrane anchor to reduce lipid microdomain affinity.

1.3 Alternative roles of phosphorylation of GAPR-1

Many proteins are degraded upon phosphorylation (Johnson, G. L. Lapadat, R. 2002). Serum starvation conditions -used to treat CHO cells for different periods of time (3, 6, 9, 24 and 48 hrs) - cause a proliferative arrest in G_0/G_1 (Cooper, S. 1998; Cooper, S. 2003) (Fig. 23). During this process, GAPR-1 is

down-regulated. This is in agreement with the differential expression of GAPR-1 in various tissues. GAPR-1 is absent in tissues terminally differentiated (brain and skeletal muscle) (Eberle, H. B. *et al.* 2002). In other types of cells, including some lymphocytes, GAPR-1 is highly expressed. The experimental conditions used for phosphorylation induces arrest in G_0/G_1. It has been proposed that cells are able to enter the G_0 phase at the instant of starvation (Zetterberg, A. Larsson, O. 1985). Thus, GAPR-1 phosphorylation may result in release from the membrane and subsequent degradation.

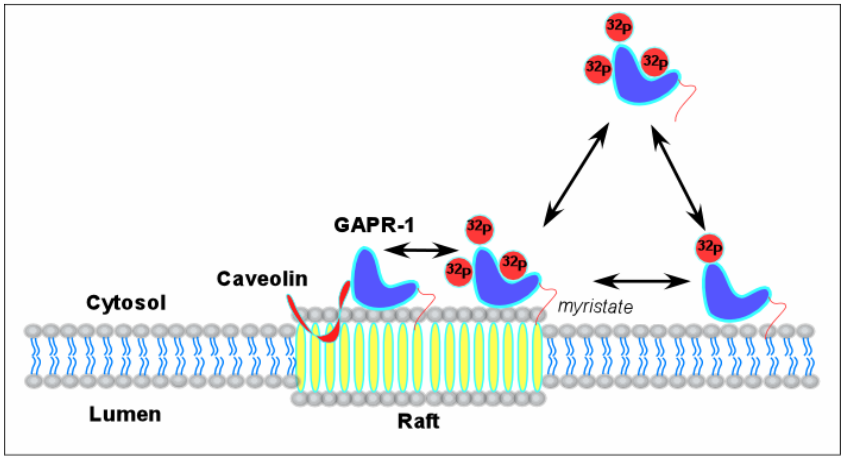

Figure 26. **Schematic view of the GAPR-1 partitioning to Golgi membranes and phosphorylation.** GAPR-1, located to Golgi microdomains, may distribute differentially upon phosphorylation. Highly phosphorylated GAPR-1 localizes to the lipid rafts and cytosol, whereas a low phosphorylated fraction seems to be membrane bound but non-raft associated. The scheme also depicts GAPR-1 interaction with Caveolin-1. Symbols: red hairpin shape, Caveolin-1; blue nudge shape, GAPR-1; red circles, phosphate-groups (phosphorylation).

Phosphorylation could also regulate GAPR-1 interaction with Caveolin-1. This might affect GAPR-1 activity, as has been proposed for other caveolin interacting proteins (Smart, E. J. *et al.* 1999): Caveolin-1 can suppress GTPase activity of heterotrimeric G proteins and it inhibits kinase activity of Src family tyrosine kinases. Inhibition occurs via the caveolin-binding domain, which is also present in GAPR-1. In all cases, the caveolin-binding motif is located within the enzymatically active catalytic domain of a given signaling molecule (Smart, E. J. *et al.* 1999). In GAPR-1 the caveolin-binding domain is

not located within the cleft suggested to be a potential active center, but rather exposed to the exterior of the molecule (Fig. 11). This implies a distinct mechanism of regulation.

Preliminary studies show an inverse correlation between the expression of GAPR-1 and Caveolin-1 in CHO cells. As shown before, GAPR-1 expression is up-regulated in cell lines and tissues with a high turnover (Eberle, H. B. *et al.* 2002). On the other hand, Caveolin-1 expression is down regulated in human tumors, in cell lines derived from human tumors, and in cell lines transformed by oncogenes (reviewed in Volonte, D. *et al.* 2002). It is been suggested that Caveolin represents a candidate protein in mediating cellular senescence, and it is known that overexpression of Caveolin-1 in mouse embryonic fibroblast is sufficient to lock these cells in the G_0/G_1 phase of the cell cycle (Galbiati, F. *et al.* 2001). This implies that Caveolin-1 mediates cell cycle arrest. The cell cycle arrest has a differential impact on the expression of both proteins: GAPR-1 is down-regulated, whereas Caveolin-1 is up-regulated (Fig. 23). If GAPR-1 is a signaling molecule, then Caveolin may function as a negative regulator to inhibit its activity, as has been suggested for other signaling molecules with Caveolin-binding motif (Okamoto, T. *et al.* 1998).

2 Structure function-relationship of GAPR-1

2.1 GAPR-1and the superfamily of the plant pathogenesis-related proteins

Sequence alignment of GAPR-1 (Fig. 27) shows significant homology and identity with members of the plant pathogenesis-related proteins (group 1). These proteins share typical characteristics present in most family members: among them are the absolutely conserved histidines (His54 and His103 in GAPR-1) and glutamates (Glu65 and Glu86), and the highly conserved motifs GENL(A) and gHyTQvVW (amino acids 64-68 and 102-109 respectively, in GAPR-1) (Eberle, H. B. *et al.* 2002). For plant pathogenesis-related protein (PR-1) many hypotheses have been proposed to understand the role of the conserved amino acid residues in family members (Fernandez, C. *et al.* 1997;

Szyperski, T. *et al.* 1998; Henriksen, A. *et al.* 2001). Szypersky, T *et a*l. (1998) show that His-69 and His-127 are “solvent exposed and strictly conserved” in p14a (a plant PR-1 protein), and suggested that these residues are candidates for a role in the active site. Moreover, they stated that the two histidines are in close spatial proximity to the conserved glutamates 88 and 113 concluding that these amino acids seem not to have a structural role in both P14a and/or GliPR. The same authors calculated that the pocket containing the “conserved active site” residues is the largest cleft on both protein surfaces (Szyperski, T. *et al.* 1998), suggesting that GliPR and P14a proteins might function as enzymes. GAPR-1 contains similar conserved residues (His54, His103, Glu65, and Glu86) in its structure and shows similar features for the cleft region together with the two other member proteins of this superfamily that have been studied in terms of their structures (P14a and Ves-v 5) (Szyperski, T. *et al.* 1998; Henriksen, A. *et al.* 2001) (Fig. 28). In GAPR-1 (Fig. 29), the cleft contains highly (blue) and absolutely (red) conserved residues found throughout the PR-1 family of proteins, which suggests that this region is of extreme importance for the role of this group of proteins.

What is known about possible functions of family members? In plants, PR-1 proteins are synthesized upon interaction with pathogens. Mammalian family members are present in e.g. snake venom (Morrissette, J. *et al.* 1995; Yamazaki, Y. *et al.* 2002) or produced in reproductive organs and cells (Kasahara, M. *et al.* 1989). The only indication for a biological function of the mammalian family members has been i) the weak trypsin-inhibiting effect of GliPR, ii and iii) the blocking by the toxin helothermine of the ryanodine receptors and of the high K+-induced contraction of the artery. So far GAPR-1 is the only intracellular member of the PR-1 family with a tight membrane association. It lacks the signal sequence present in other PR-1 family members, resulting in an intracellular localization of the protein (Eberle, H. B. *et al.* 2002). The plant pathogenesis-related proteins have been implicated in a mechanism of defense against pathogen attacks of plants (Heil, M. Bostock, R. M. 2002) (Van Loon, L; Van Strien, E. 1999). Interestingly, GAPR-1 not

only localizes to the Golgi, but also to other membrane structures within the cell, such as phagosomes that are also involved host-pathogen interactions (Dora Kaloyanova unpublished data).

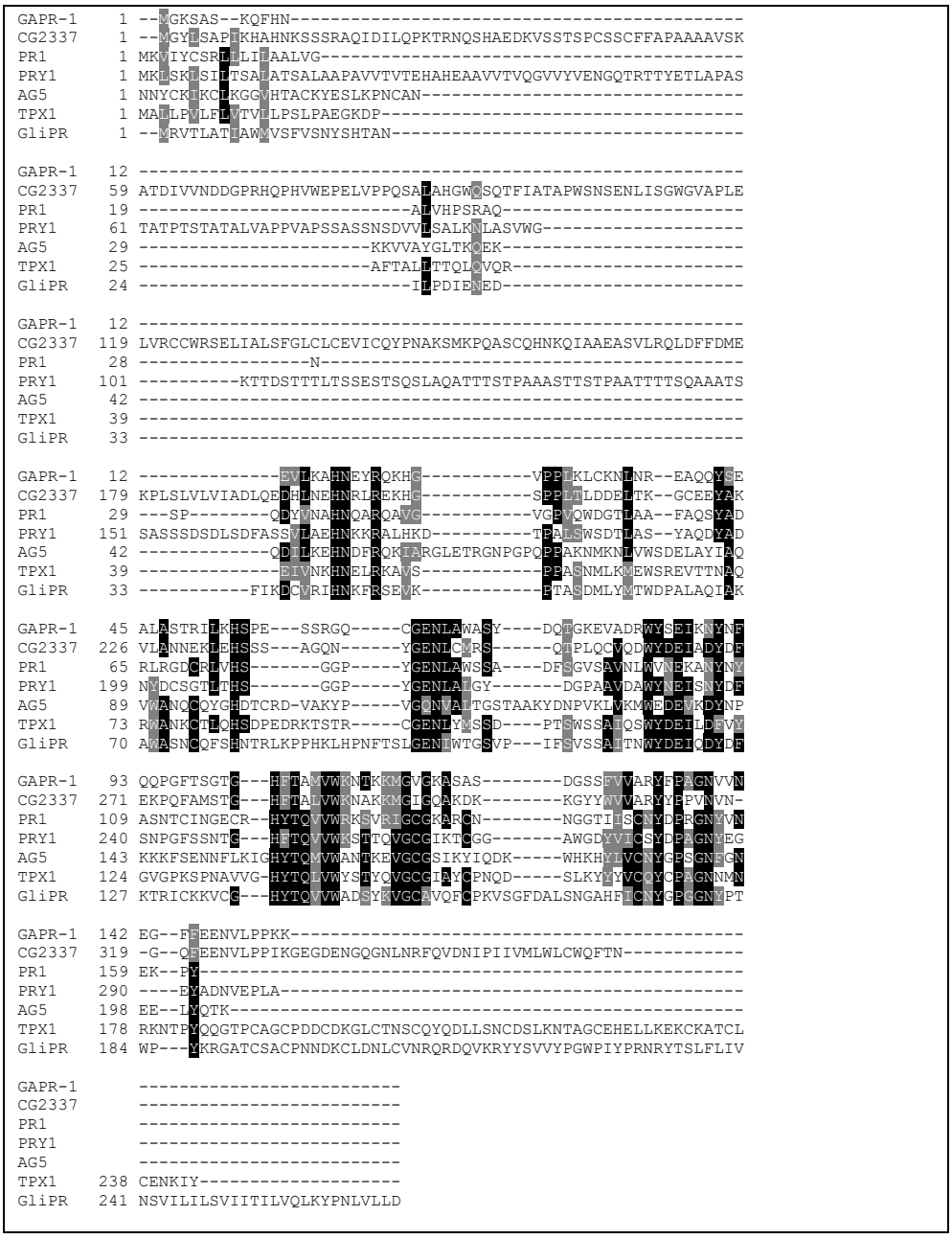

Figure 27. **Amino acid sequence alignment of GAPR-1 with relatives of the superfamily of plant pathogenesis-related proteins (PR-1).** For each of the subfamilies, including human GliPR, CRISPs, plant PR-1 proteins, allergens of insect venom and snake or lizard venoms, the protein sequence of the member with the highest homology to GAPR-1 is aligned to GAPR-1. Identical amino acid residues in family members are highlighted in black. Conservative amino acid exchanges are highlighted in grey.

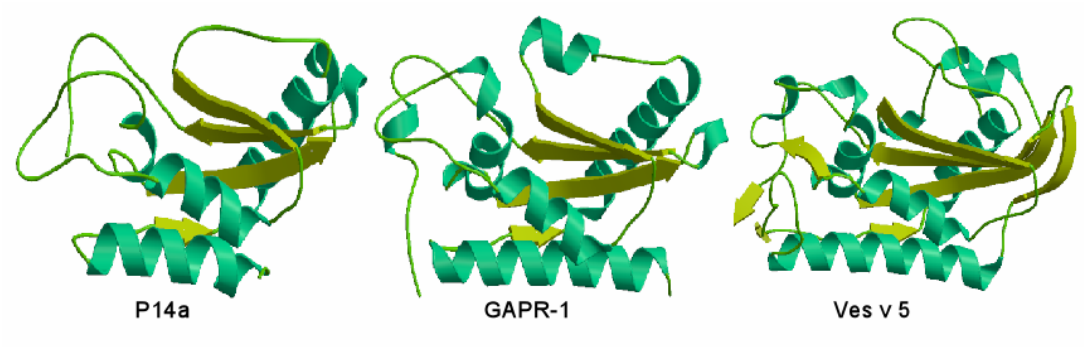

Figure 28. **Comparison of the three-dimensional structure of GAPR-1, p14a (PDB entry 1CFE) and Ves v 5 (PDB entry 1QNXA), members of the plant pathogenesis-related group 1 (PR-1).** **a**, The overall structure of P14a tomato (left) is closely related to the structure of GAPR-1 (center) and Ves V 5 (right). Figures prepared by Dr. Matthew Groves, using MolScript® software (Kraulis, P. 1991).

In plants, interaction with viruses, bacteria or fungi will elicit a set of localized responses in and around the infected host cells. These responses include an oxidative burst (Heil, M. Bostock, R. M. 2002) that leads to a hypersensitive response (HR), and a concomitant increase in the synthesis of PR proteins (Klessig, D. F. *et al.* 2000). The oxidative response is another line of defense in the innate immunity, where the production of reactive oxygen intermediates (ROI) and reactive nitrogen intermediates (RNI) can lead to cell death (Kombrink, E., Schmelzer, E. 2001). High output production of reactive oxygen intermediaries (ROI) is the specialty of mammalian phagocytes. Phagocytes assemble an NAPDH oxidase complex on phagosomal membranes that catalyzes the production of a series of highly toxic oxygen derived compounds, i.e. (O_2^-) or nitric oxide (NO). Production of NO induces cell cycle arrest and cytostasis in mammalian cells (Pervin, S. *et al.* 2001), In plants, the NO and ROS production correlates with the up-regulation of the expression of PR proteins (Klessig, D. F. *et al.* 2000). This raises the question whether similar mechanisms may apply to GAPR-1 during the production of ROS and NO in mammalian cells.

2.2 Effect of mutations on GAPR-1 structure

To study the role of the most conserved amino acids present in GAPR-1, site-directed mutagenesis was carried out to study their effect on protein interactions to potential cytosolic partners, as well as on the structure of

GAPR-1. The mutation on GAPR-1 did not significantly affect its behavior during purification, including GAPR-1mut purification by cation exchange chromatography, suggesting that the electrostatic properties were not changed. However, GAPR-1mut crystals did not grow when the same screening methods for crystallization were used.

The Far-UV spectra obtained by circular dichroism revealed no major differences between GAPR-1wt and GAPR-1mut in their content of α-helixes and β-sheets. The minor changes observed in the CD spectrum (Far-UV) of GAPR-1mut protein (Fig. 20A) may originate from an altered content in amino acids residues rather than from alterations in the conformation of the polypeptide backbone. In Near-UV (Fig. 20B), the complex spectrum reflects the sum of proportion and position of the combined aromatic residues in the protein. As mentioned before (see Results), GAPR-1 contains several aromatic residues that contribute to the near-UV spectrum. It is possible that changes in the 250-290nm region of the spectrum are due to phenylalanines exposed to solvent and to tyrosines (Tyr20, Tyr72, Tyr84, and Tyr90) at the contact interface (Fig. 29 and 30). The distribution or positioning of these amino acids may have been altered by the formation of dimers. This would be in agreement with the CD spectra, showing equal amounts of α-helixes, and β-sheets. In addition, these spectra for GAPR-1 (wt and mut) reflect the behavior observed in size-exclusion chromatography. The tendency of GAPR-1 to form dimers was confirmed by independent experiments. Crosslink experiments revealed a crosslink product at 34kDa, strongly suggesting that GAPR-1 is present as a dimer at the membrane. The existence of a dimer may have implications for GAPR-1 function. It was not possible to determine whether Caveolin-1 interacts with the dimer or monomer form of GAPR-1, due to experimental limitations of the chemical crosslinking method.

The crystal structure predicts the area of interaction between the two GAPR-1 molecules in the homo-dimer. This area (Fig. 29, *right* view, in blue and light-grey) overlaps partially with the area where the highly conserved amino acid residues are located (Fig. 29, *left* view). Therefore, mutations in the highly

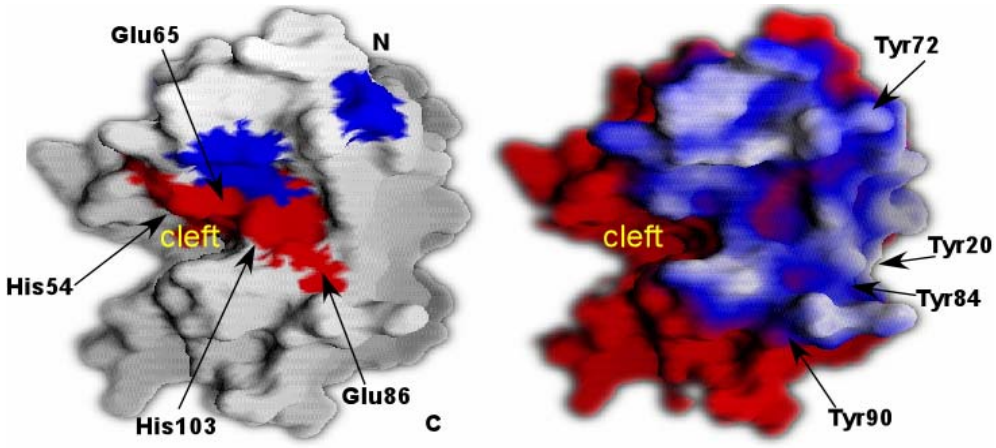

Figure 29. **Structure of the GAPR-1 monomer**. ***Left view***: molecular surface representation of a GAPR-1 monomer with highly (blue) and absolutely (red) conserved amino acids. His54, His103, Glu64 and Glu86 are located in the absolutely conserved area (red); ***Right view***: region of GAPR-1 potentially responsible for the interaction during dimer formation or contact interface (blue). Dark blue depicts region of contact during dimer formation; light blue-white represents regions of closer contact; red represent regions in GAPR-1 distant from the contact interface. The aromatic residues (Tyr20, Tyr20, Tyr84 and Tyr90) located in the contact interface in dimer are pointed out. Contact region in GAPR-1 includes the highly and absolutely conserved amino acids. Similar amino acid residues have been pointed out in P14a and Ves v 5 to be conserved and involved in the potential function of these proteins. Space-filling representations of GAPR-1 were prepared by Dr. Matthew Groves using Grasp® (Nicholls, A. *et al*. 1993).

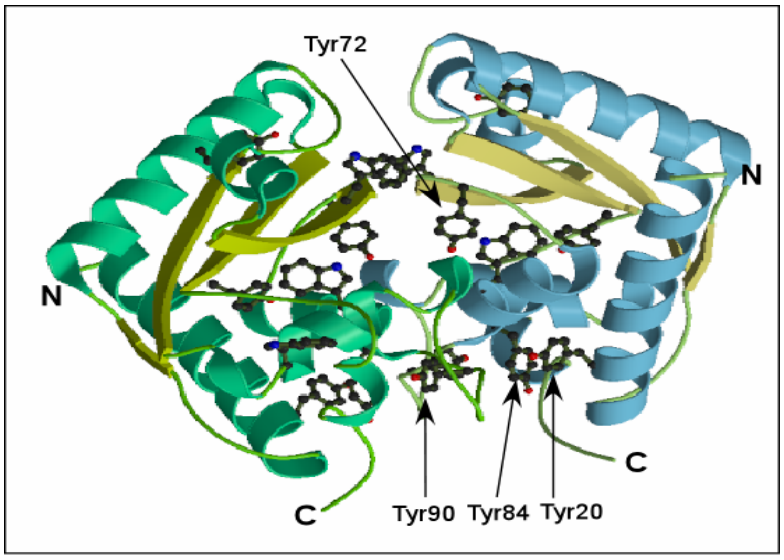

Figure 30. **GAPR-1 dimer structure.** GAPR-1dimer, showing the aromatic amino acids at the interface between the two molecules. Emphasis has been put on Tyrosine residues, whose contribution in circular dichroism (near-UV spectrum) may have changed in GAPR-1mut (see Results, Fig. 17, panel B). Figure depicts Tyr20, Tyr72, Tyr84 and Tyr90, and their position in the dimer structure. Ribbon structure representation of GAPR-1 dimmer obtained by Dr. Matthew Groves using MolScript® (Kraulis, P. 1991), Raster3D® (Bacon, D. Anderson, W. 1988).

conserved amino acids may affect the binding forces in the contact area. Thus, the conserved amino acids may not only play a role in the function of the protein, but also in GAPR-1/GAPR-1 interactions and therefore its interaction with other proteins.

The crystal structure of GAPR-1 shows that the active center is buried between the two molecules forming the dimer, since this area forms part of the contact interface of the protein (Fig. 30). Thus, in the dimmer the active center of GAPR-1 is not accessible for interaction. It is tempting to speculate that there is a dynamic equilibrium on the membrane between the monomer and dimer, where the monomer represents an “active state” (Fig. 11), and the dimer represents an “inactive state”.

3 Interaction of GAPR-1 with cytosolic proteins

The GAPR-1 mutant was a useful tool for identification and determination of potential interacting partners. The affinity chromatography elution profile of CHO cytosol –from both the GAPR-1 wild type and mutant columns- shows similar patterns in terms of proteins eluted from the columns. To increase the specificity of binding to the column, elutions were also performed in presence of 1% Triton X-100. The protein pattern obtained in those conditions was, however, similar to elutions without detergent treatment (data not shown). More protein, however bound to the wild type column and the amount seems to correlate with the ratio of dimer and monomer in GAPR-1wt and GAPR-1mut (as observed by size exclusion chromatography). Since a fraction of GAPR-1 exists as dimer on Golgi membranes, protein-protein interactions occurring in the column (GAPR-1mut) could resemble the protein-protein interactions in vivo, where dimerization may imply a mechanism of negative regulation for protein interactions with GAPR-1 on the Golgi membrane. Peptide mass fingerprinting of proteins eluted from GAPR-1wt affinity column revealed an interaction with a cytosolic complex. The protein pattern appears similar when CHO and HELA cytosols were applied to the column (see Results, Table 4 and 5). Independent of the source of cytosol or pre-treatment

of cytosol with SDS, the major component eluting from the column is NCL (Fig.17).

Nucleolin is a ubiquitous, nonhistone nuclear phospho-protein of exponentially growing eukaryotic cells, which runs between 100 to 115kDa (calculated molecular mass of 76 kD) on a 12% gel (SDS-PAGE) (Lischwe, M. A. et al. 1985; Ginisty, H. et al. 1999). It has been implicated in many cellular processes, including transcription, packing and transport of ribosomal RNA, replication and recombination of DNA, cell cycle progression, and apoptosis.(Yang, T. H. et al. 1994; Thiede, B. et al. 2001; Mi, Y. et al. 2003). Although generally considered a predominantly nucleolar protein, Nucleolin is also found in the nucleoplasm, cytoplasm, and at the cell surface (Dumler, I. *et al.* 1999; Daniely, Y. Borowiec, J. A. 2000; Wang, Y. *et al.* 2001). Yanagida and colleagues (Yanigida, M. *et al*. 2001) isolated and characterized the major NCL binding proteins in a ribonucleoprotein complex. NCL in known to interact to 7 ribosomal proteins that were also found in the HeLa preparation eluted from GAPR-1 column, and is also known to bind to the identified nonribosomal proteins like casein kinase 2, eIF, DNA and RNA helicases, and NS-1 associated protein (Yanagida, M. *et al.* 2001). NCL can interact with about half of ribosomal proteins present in the large and small subunits (Yanagida, M. *et al*. 2001). The complex identified to bind GAPR-1 resembles that reported by Yanagida, M. (2001), except for a reduced amount of ribosomal proteins. Because NCL was reported not to bind the mature ribosomal particles found in the cytoplasm (Ghisolfi-Nieto, L. *et al.* 1996), the ribosomal proteins found to bind GAPR-1 are unlike to belong to mature cytoplasmic ribosomes and polysomes.

The *in vitro* interaction between GAPR-1 and NCL was also observed in the yeast two hybrid system (Fig. 22). In addition, it was possible to determine that the conserved amino acids residues in the cleft of GAPR-1 play an important role in the interaction, since GAPR-1mut showed less activity in the yeast two hybrid system (Fig. 22). Nucleolin consists of three functional domains, *i.e.* an amino (*N*)-terminal domain, and RNA binding domain (RBD),

and a carboxyl-terminal domain (RGG) (Ginisty, H. *et al.* 1999). At this point it is unknown to which domain GAPR-1 interacts with (see also below), but the two hybrid system would be a suitable method to determine which Nucleolin domain interacts with GAPR-1.

Ribonuclease activity has been suggested for P14a due to the arrangement of the two histidines in the putative active center (Szyperski, T. *et al.* 1998) and such an activity for GAPR-1 could make sense in the context of a large ribonucleoprotein complex . Preliminary experiments, however, did not show any evidence for such activity (data not shown). Could GAPR-1 have a RNA binding activity? Sequence alignment of GAPR-1 with known RNA binding motif (Burd, C. G., Dreyfuss, G 1994) does not show any specific similarity or identity.

Nucleolin (NCL) expression is regulated during the cell cycle (Belenguer, P. *et al.* 1989)Derenzini, M. *et al*. 1995; Srivastava, M. Pollard, H. 1999). During G_0/G_1 NCL is down-regulated and localizes entirely to the nucleus. Concomitantly -but not necessarily related- GAPR-1 shows down-regulation at G_0 of the cell cycle; thus, the interaction could take place when both proteins are simultaneously expressed. So far, NCL has not been shown to be present at the Golgi. Preliminary experiments show Nucleolin localization to an isolated, Golgi-enriched fraction (Fig. 24).This Nucleolin localization could be due to the presence of GAPR-1 on the same membranes, as indicated in the same experiment, where both Nucleolin and GAPR-1 are not present on the rat liver Golgi. This result opens the possibility that GAPR-1 and Nucleolin interact at the Golgi. Alternatively, the cytosolic pool of GAPR-1 could interact with cytosolic or even nuclear Nucleolin, but these experiments must be conducted.

In addition to NCL, Template-Activating Factor I α (TAFI α) (accession n^o I59377), and an unknown protein, designated HSPHAPIB or HSAPRIL (accession n^o CAA69265) were found in the GAPR-1 affinity column after dissociation of cytosolic protein complex. TAFI has been identified as a chromatin remodeling factor in HeLa cells (Kawase, H. *et al.* 1996), and levels

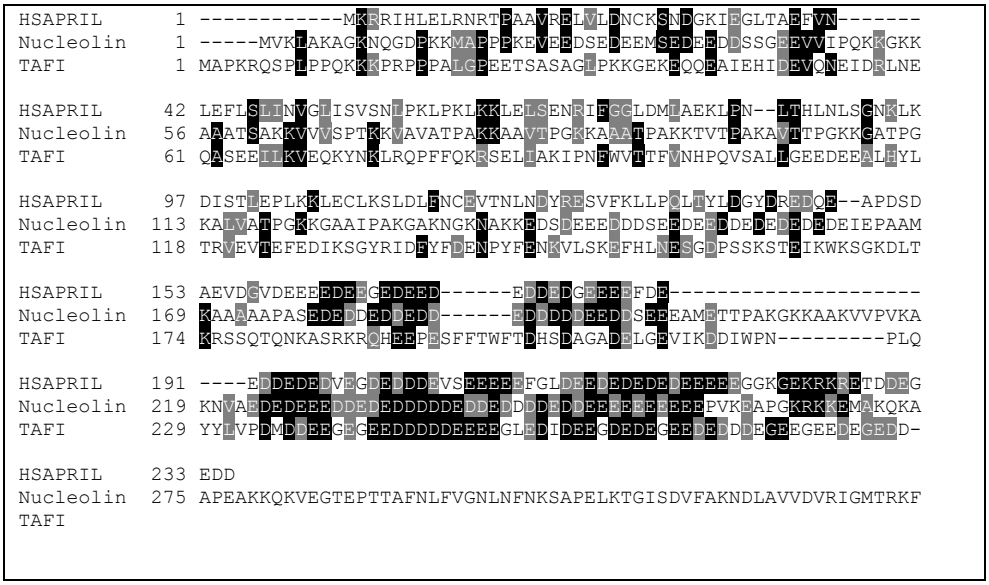

Figure 31. **Sequence alignment of the potential interacting partners of GAPR-1 from HeLa cell cytosol.** Nucleolin (accession n° A35804, alignment from amino acid 1 to 345), Template activating factor I α (TAFI α) (accession n° I59377) and HSAPRIL (accession n° CAA69265) were identified by MALDI-TOF after elution from GAPR-1 affinity columns. Cytosolic complexes were dissociated by 1% SDS prior to loading on the columns (see Results 2.4.4). The C-terminus region of TAFI α and HSAPRIL shows the highest homology to the Nucleolin N-terminal domain (Yanagida, M. *et al.* 2001).

of TAF-I protein are regulated through the cell cycle in which the chromatin structure is dynamically changed (reviewed in (Nagata, K. *et al.* 1998; Okuwaki, M. Nagata, K. 1998). TAFI α and β proteins differ by only a short amino terminal regions, but in both proteins a long acidic tail in the carboxyl-terminal region is present (Nagata, K. *et al.* 1995). The acidic region is critical for TAF-1 activity, and the level of TAF-I activity is dependent on the length of the acidic region. This C-terminal region in TAFIα shares homology with N-terminus of Nucleolin and is also present in HSPHAPIB/HSAPRIL (Fig. 31) The N-terminal domain in Nucleolin and C-terminal domain in TAFI have been implied as nuclear localization signals (Schmidt-Zachmann, M. S. Nigg, E. A. 1993; Nagata, K. *et al.* 1998), and these regions contain multiple phosphorylation sites, which are regulated during the cell cycle. Little is known about HSAPRIL function, although it is potentially involved in Leukemia (Mencinger, M. *et al.* 1998), as it has been pointed out for TAFI (Seo, S. B. *et al.* 2001). Mouse TAFI β is ubiquitously expressed in contrast to TAFIα (i.e. Jurkat), which is not present in the mouse liver or brain, but is expressed in

spleen and lung, resembling to some extent the differential expression of GAPR-1 (Eberle, H. B. *et al.* 2002). TAFI α and TAFI β show a nuclear and cytoplasmic localization in HeLa cells. The function of TAFI α seem to be less clear as for TAFI β ((Seo, S. B. *et al.* 2001; Cervoni, N. *et al.* 2002), but there are some similarities with functions reported for Nucleolin.

4 Perspectives of GAPR-1 function: Rafts and Nucleolin

The function of GAPR-1 remains to be determined. Its potential regulation during the cell cycle, its interaction with other proteins such as Caveolin-1 and Nucleolin, as well as its presence on other membranes within the cell (i.e. phagosomes) can help to understand its role.

The presence of GAPR-1 in phagosomes supports the premise of its potential involvement in the innate immunity, since phagocytosis is one of the initial lines of defense in animals. GAPR-1 is associated with lipid microdomains at the phagosomes (Dora Koloyanova unpublished data), and these microdomains may act as a platform to concert a specific response during bacterial infection. Interestingly, many other proteins found in GICs (Gkantiragas, I. *et al.* 2001) seem to be associated with phagosomes (Dermine, J. F. *et al.* 2001) as well, suggesting a possible pathway between the Golgi and other membrane structures within the cell. Microdomains at phagosomal membranes may have a role in phagosome maturation (Vieira, O. V. *et al.* 2002).

There have been reports of a variety of signaling pathways associated with lipid rafts at the plasma membrane and other organelles (Brown, D., London, E. 1998). These include several signaling proteins, such as heterotrimeric G proteins, Ras, Src, endothelial nitric oxide synthase (eNOS), and protein kinase C. Many of these proteins have been reported to interact with the caveolin-1 scaffolding domain (Okamoto, T. *et al.* 1998), although it is still matter of debate whether this scaffolding domain in Caveolin-1 has functional significance. GAPR-1 is present in microdomains at the Golgi apparatus, along with some proteins described to interact with Caveolin-1, such as the

heterotrimeric G proteins (Gα subunits) (Gkantiragas, I. *et al.* 2001). Additionally, Caveolin-1 is down-regulated in transformed cells (Volonte, D. *et al.* 1999), whereas GAPR-1 seems to be up-regulated (i.e. in NRK and AT3 cells, data not shown). If any negative effect on GAPR-1 activity results from an interaction with Caveolin-1, then this may be modulated by the expression levels of both proteins in the cell. In phagosomes, Caveolin-1 is absent (Dermine, J. *et al*. 2001; Dora Koloyanova unpublished data), whereas GAPR-1 is present on the phagosomes and associated with lipid microdomains. In conclusion, a specific combination of proteins in protein complexes likely determines the final outcome of signaling pathways. Specific combinations of proteins in protein complexes can be regulated in several ways, for example by the expression levels of proteins, by containment is similar or different sub-cellular membranes, or even within a membrane by containment with lipid rafts. Based on these considerations, GAPR-1 could have a different function at the Golgi complex as compared to phagosomes.

A GAPR-1 interaction with Nucleolin has been identified during these studies, but what are the implications of this interaction? Nucleolin has been suggested to play a role in innate immunity in mammals (Garcia, R. *et al* 2000). This suggestion comes from the observation that phosphorylation of Nucleolin in macrophages-like cells upon infection with *Mycobacterium avium*. These studies imply that infection impaired phosphorylation of Nucleolin, and showed that only cytosolic Nucleolin seems to be affected. The authors suggested that these phosphorylation events are related to cellular apoptosis, and prevention of programmed cell death could result in the possibility of a prolonged intracellular survival of mycobacteria. It is known that the N-terminus of Nucleolin is highly phosphorylated during the cell cycle, and phosphorylation affects the distribution of the Nucleolin within the cell (Ginisty, H. *et al.* 1999). If GAPR-1 interacts with the N-terminal domain in Nucleolin, this could imply a way to regulate phosphorylation during pathogen attack. The interaction between Nucleolin and GAPR-1 could occur at Golgi membranes (Fig. 24) and this interaction may regulate the amount of cytosolic Nucleolin available for phosphorylation. Nucleolin has been shown to

associate to lipid raft components at the cell surface (Nisole, S. *et al.* 2002; Said, E. A. *et al.* 2002) and was implicated in a mechanism of early events in the HIV entry process. Interestingly, Nucleolin localization to lipid microdomains seems to be dependent on infection, since Nucleolin in uninfected cells is not detergent-insoluble associated (Nisole, S. *et al.* 2002). The interaction between GAPR-1 and Nucleolin may represent a new mechanism of regulation of innate immunity in mammalian cells.

Materials and Methods

Materials

1 Chemicals

All commonly used chemicals were purchased from either Merck (Darmstadt), Sigma (Deisenhofen), Roth (Karlsruhe), Fluka (Taufkirchen), Qiagen (Hilden), Amersham-Biotech (Freiburg), BioRad (München) or Boehringer (Mannheim). The reagents were ordered directly at the company or via the chemical centre Heidelberg (Theoretikum der Universität Hiedelberg).

1.1 Detergents

Triton X-100, Tween-20 and NP-40 were obtained from Merck, Sigma and Calbiochem, respectively.

1.2 Inhibitors

Brefeldin A was purchased from Sigma, stored in aliquots of 7.5 mM in methanol. The working concentration of Brefeldin A was 5 µM. Mixtures of protease inhibitors were obtained from Roche as tablets. Each tablet was sufficient for a 50 ml solution.

1.3 Buffers

A List of most commonly used buffers during this experimental work is shown below. All buffers were prepared as aqueous solutions.

PBS buffer

10X PBS: 1.36 M NaCl, 357 mM Na2HPO4, 143 mM KH2PO4 and 30 mM KCl. PBST was obtained by mixing PBS buffer supplemented with Tween-20 to 0.05% final concentration. PBS was adjusted to pH 7.4.

PEN buffer

PEN buffer was prepared as a 5X stock solution, containing 125 mM PIPES, 10 mM EDTA and 1.5 M NaCl, and adjusted to pH 6.5 with NaOH.

TAE buffer

50X TAE contained 242 g Tris base, 57.1 ml of glacial acetic acid and 18.61 g of EDTA, and adjusted to 1 L solution with MiliQ H_2O.

Running buffer for electrophoresis

10X SDS-PAGE running buffer contained 30.2 g Tris base, 188 g of glycine and 10 g of SDS, and adjusted to 1 L solution with MiliQ H_2O.

Blotting buffers for semi-dry transfer

Anode I: 300 mM Tris and 20% (v/v) methanol.

Anode II: 25 mM Tris and 20% methanol.

Cathode buffer: 25 mM Tris, 40 mM aminocaproic acid and 20% methanol.

Sample cocktail buffers

Sample buffer for DNA: 6X stock solution contained 0.25% bromophenol blue, 40% sucrose, 60 mM Tris-HCl, pH7.4 and 6 mM EDTA.

Sample cocktail I (SCI): 50 mM Tris-HCl pH 6.8 and 4% SDS

Sample cocktail II (SCII): A 3X stock solution contained 187.5 mM Tris-HCl pH6.8, 15% β-mercatoethanol, 6% SDS, 30% glycerol and 0.0675% bromophenol blue.

Staining Solution for SDS-PAGE

Staining buffer: 40% ethanol, 10% glacial acetic acid and 0.25% coomassie blue R-250.

Destaining buffer: 20% ethanol and 5% acetic acid.

Ponseau S solution: prepared by adding 0.8g of the dye dissolved in 4% (w/v) TCA.

1.4 Media

Mammalian cells culture media

α-MEM and DMEM were purchased from Gibco BRL (Invitrogen), reconstituted into water, sterilized by passing through 0.2μM filters and supplemented with 10% of fetal calf serum and 10 mg/ml of penicillin and

streptomycin. L-Glutamine was added to both media. Non-essential amino acids were added to DMEM only.

Bacteria and yeast culture media

Luria-Bertani broth (LB) was prepared according to guidelines of Molecular Cloning (3rd Edition). 1 L of medium contained 10 g of sodium chloride, 10 g of Bacto-Trypton and 5 g of yeast extract. pH was adjusted to 7.4. For plates, 15 g/L agar was added to the preparation.

YPD medium was prepared as follows: 10 g of BactoYeast extract, 20 g of BactoPeptone and Dextrose were dissolved in 1 L of MilliQ water and autoclaved.

SDC-URA plates

For preparation of plates, 3,375 g of yeast nitrogen base were added to 500 ml of MilliQ, complemented with 1 g of glucose and 0.275 g of complete supplement mixture (CSM) without Leucine, Triptophan, Histidine and Uracil, and 5 g of agar. The medium was autoclaved and poured into the plates.

Xgal plates for Two Hybrid Assay

These plates were used with the yeast strain EGY48 bearing the plasmids pSH18-34, pJG4.5 and pEG202. In 800 ml of MilliQ water 6.7 g of Yeast nitrogen base (without amino acids), 0.54 g CMS-all, and 20 g of agar were added. The mix was autoclaved. Before preparing the plates, the mix was adjusted with a solution containing: 10 ml of 10 g/L leucine, 100 ml of 20% Galactose, and 10% Rafinose (preheated at 50^{o}C), 100 ml 10X BU salts (preheated at 50^{o}C), and 4 ml of 20 mg/ml X-Gal dissolved in Dimethylformamide.

BU salts 10X (1 L): 261 mM $Na_2HPO_4.2H_2O$; 250 mM $NaH_2PO_4.H_2O$.

The pH was adjusted to 7.0 with NaOH. pH must be controlled carefully, since some interactions in the two hybrid system can be affected by variations of 0.2 pH units of the plate.

2 Antibodies

2.1 Primary Antibodies

For the immunochemical studies the following antibodies were used:

- Caveolin-1 antibody (N-20) (rabbit). Santa Cruz Biotechnology Inc. (USA);
- GAPR-1 antibody (α-1852) (rabbit). (Eberle, H. PhD Thesis);
- Nucleolin antibody (mouse). Santa Cruz Biotechnology Inc. (USA);
- Actin antibody (rabbit). Sigma Co. Saint Louis, MO. (USA);
- p23 antibody against luminal domain of p23 (KAI2/3) (Sohn, K. *et al.* 1996).

2.2 Secondary Antibodies

HRP-conjugated goat anti-rabbit IgG(H+L) and HRP-conjugated goat anti-mouse IgG(H+L) were obtained from BioRad. HRP-conjugated Protein G Sepharose Beads was purchase from BioRad.

3 Plasmids

The following plasmids were used during this work various purposes as indicated below:

pQE60 (Qiagen). GAPR-1 overexpression

pbb131 (Duronio, R. J. *et al.* 1990). Expression of N-myristoyl transferase in *E. Coli* to acylate GAPR-1.

pCDNA3.1(-/+) (Invitrogen). GAPR-1 expression in mammalian cells.

pEG202 (Kindly provided by Dr. Maribel Geli) Two Hybrid System. Fusion of GAPR-1 or Nucleolin to *lexA* (Bait plasmid)

pJG4.5 (Kindly provided by Dr. Maribel Geli). Two Hybrid System. Fusion of GAPR-1 or Nucleolin to B42 (Prey plasmid)

pEGFP-N1 (Invitrogen). GAPR-1 fusion with Green fluorescence Protein (GFP) or Nucleolin fused to GFP (Dr. J. A. Borowiec, NYU, School of medicine, New York, USA)

pIRES2-EGFP (BD Biosciences). Bicistronic plasmid for simultaneous expression of GAPR-1 and GFP.

pKG-NUC (Kindly provided by Dr. Ahamed Saleem and Dr. Eric Rubin (Haluska, P. *et al*. 1998) containing full length Nucleolin fused to GST.

4 Oligonucleotides

The oligonucleotides used in this thesis were synthesized by NAPS (Goettingen) (HPLC grade). All oligonucleotides were solubilized in sterilized water to a final concentration of 100µM. All sequences are presented in table 6.

Designation	Sequence (5'-3')	Purpose
p17-2-hy1	AAACCAGAATTC***ATG***GGCAAGTCAGCTTCCA	Two Hybrid system (THS)
p17-2-hy2	AAACCACTCGAG***TTA***CTTCTTCGGCGGCAG	
NCL-2-hy1	AAACCAGAATTC***ATG***GTGAAGCTCGCGAAG	
NCL-2-hy2	CCACCGCTCGAG***CTA***TTCAAACTTCGTCTTCTTTCCTT	
PEG1	CGTCAGCAGAGCTTCACCATTG	Sequencing of THS constructs
PJG1	CTGAGTGGAGATGCCTCC	
MUT1	AAGCACAGCCCGGAGTCCAGCCGTGGCCAGTGTGGG***GCT***AAC	Mutation: substitution GLU65 to ALA65
MUT2	GTT***AGC***CCCACACTGGCCACGGCTGGACTCCGGGCTGTGCTT	
MUT3	ACGAGGATCCTCAAG***GCT***AGCCCGGAGTCCAGCCGTGGC	Mutation: substitution HIS54 to ALA54
MUT4	GCCACGGCTGGACTCCGGGCT***AGC***CTTGAGGATCCTCGT	
MUT5	GAGGTGGCTGATAGATGGTACAGT***GCT***ATCAAGAACTATACCTTCCAG	Mutation: Substitution GLU86 to ALA86
MUT6	CTGGAAGTTATAGTTCTTGAT***AGC***ACTGTACCATCTATCAGCCACCTC	
MUT7	GGCTTCACCTCGGGGACTGGA***GCT***TTCACGGCGATGGTATGG	Mutation: Substitution HIS103 to ALA103
MUT8	CCATACCATCGCCGTGAA***AGC***TCCAGTCCCCGAGGTGAAGCC	
52169N(1)	GGGCTTCTTCGAAGAAAACGTCCTG***CCG***AAGAAGTAAAGATCTC	cutting site for SacII at GAPR-1 C-terminus
52170N(2)	GAGATCTTTACTTCTT***CCG***CGGGACGTTTTCTTCGAAGAAGCCC	

Table 6. Oligonucleotides used to prepared constructs for the two hybrid system, site-directed mutagenesis of GAPR-1, and for GAPR-1 fusion to GFP.

5 Equipments

PCR cycler was from ThermoHybaid, ultra-centrifuges were from either Beckman or Kontron Instruments (Watford, UK). Other centrifuges were from either Eppendorf or Heraeus. All rotors, including SW28, SW41, SW50, SW60, JA12.500, and TLA45 were from Beckman. Electrophoresis system, including plates, spacers and combs, and blot systems, including semi-dry trans-blot and wet blot were from Bio-Rad (Munich, Germany) or Invitrogen (Karlsruhe). Cell incubators were from Heraeus.

Methods

6 Methods in Cell Biology and Immunology

6.1 Cell culture

Chinese Hamster Ovary Cell (CHO) wild type, either adherent (monolayer) or in suspension, were grown in α-MEM medium supplemented with 10% Fetus Bovine Serum, L-glutamine and 10 mg/ml of penicillin and streptomycin and maintained at 37°C, 95% relative humidity in a 5% CO_2 incubator (Heraeus). Rat Kidney fibroblast (NRK) as well as cervical carcinoma (HeLa) cells were maintained in DMEM medium, supplemented as indicated above for α-MEM. To check for viability in the spinner culture, the cells were counted using a Neubauer chamber, after treatment with a solution of Trypan blue to a final concentration of 0.3%.

6.1.1 Passing of cells

Cells growing as a monolayer (CHO, NRK, and HeLa) were split after reaching confluency. 10 ml of media were used to resuspend cells from a 10 cm plate (around 5 x10^7 cells), and 1 ml of cells were transferred into a new 10 cm plate containing 9 ml of fresh growth media. Cells were incubated at 37°C in an incubator, as described above.

6.1.2 Culture of CHO and HeLa cell in suspension

Four plates (10 cm) of confluent CHO or HeLa cells were washed once with PBS, followed by trypzination. The cells were resuspended in medium and transferred to a 1.5 L Spinner bottle containing 500 ml of α-MEM (CHO) or DMEM (HeLa). The bottles were placed into the incubator, and the medium was continuously swirled until cells reached 5-6 $x10^5$ cells/ml. Additional medium was added to dilute the cells 3 to 4 times and the cultures were incubated until they reached confluency. Cells were centrifuged at 500 *xg* using a preparative centrifuge (Heraeus).

6.1.3 Transfection of cells

Transfection procedures were conducted according to manufacturer's guide (Invitrogen) with minor modifications. In each transfection, 1.5 µl of Lipofectamine™ 2000 and 1 µg of plasmid DNA were used for one well of a 6-well plate (5 µl and 5 µg for a 5 cm dish, respectively). One day before transfection, cells were plated in normal growth media so that they were 60% confluent at the time of transfection. For transfection, in different tubes the appropriate amount of plasmid and Lipofectamine™ 2000 were diluted in 100 µl of Opti-MEM® reduced medium. After incubation at room temperature for 5 min, the two diluates were combined (200 µl in total) and mixed gently by pipetting or shaking. The mix was incubated for 30 min at room temperature, followed by the addition of 0.8 ml of Opti-MEM® I reduced medium and gentle mixing. All mixtures were applied to cells pre-washed first with PBS, and Opti-MEM® I reduced medium respectively. The solution was spread evenly over the plate by gently shaking or by rocking back and forth. The plates were incubated at 37°C in a CO2 incubator for 3 – 5 hrs. After incubation, 2 volumes of normal growth media were added and cells were placed in the incubator. Cells were analyzed by immunoflourescence.

6.1.4 Isolation of Primary Hepatocytes

The isolated liver was preperfused in a non-recirculating manner with about 250-300 ml of a Ca^{2+} -free Krebs-Henseleit bicarbonate medium (NaCl 119 mM; KCl 4.7 mM; $MgSO_4$ 1.2 mM; KH_2PO_4 1.2 mM; $NaHCO_3$ 25 mM, pH 7.4

at 37° C when equilibrated with 95% O_2 : 5% CO_2 and glucose 11 mM. The buffer was equilibrated with 95% O_2:5%CO_2 before adding $NaHCO_3$), and then perfused by recirculating 100 ml of the medium to which 2.5 mM $CaCl_2$ and 0.05% collagenase were added. Preperfusion and collagenase recirculation both lasted for about 10 min after which time tissue dissociation was normally completed. The softened tissue was resuspended in 50 ml of recirculation medium, cut into about 10 pieces and incubated in a 250 ml siliconized round bottom flask for 10 min at 37°C in a shaking water bath. The cells were successively sieved through three layers of Nylon of 250, 100, and 60 µm pore size and were washed and isolated by centrifugation at 20 *xg* for 3 min in a refrigerated centrifuge (Heraeus). The cell preparation was finished normally within 1 h. As tested by their ability to exclude trypan blue (0.3% final concentration) the viability of the hepatocytes obtained by this technique was 95%. After 2 days, the cells were transfected with appropriated plasmid.

6.2 Synchronization of mammalian cells

6.2.1 Synchronization of mammalian cells by serum starvation

CHO cells were grown in α-MEM supplemented with fetal bovine serum until they reached 80-90% confluency in 10 cm plates. At this point, the medium was removed, and plates were washed 2 times with sterile PBS. The medium was replaced by serum free α-MEM, and the cells were incubated for 3 hrs, 6 hrs, 9 hrs, 24 hrs or 48 hrs in a CO_2 incubator at 37°C. After incubation, the cells were harvested after homogenized (as indicated in part 6.4 of Material and Methods) to obtain total membranes. A protein determination (Lowry) was carried out for all the samples, and 25 µg of protein were loaded on a 14% gel. After separation of proteins by SDS-PAGE, and transfer to a PDVF membrane by western blot, the blots were analyzed for the presence of Caveolin-1, GAPR-1 and Actin by use of α-Caveolin-1 (Santa Cruz Biotechnology Inc.), GAPR-1 (α-1852) and α-Actin (Sigma Co.) antibodies, respectively. The signal on X-ray films of detected proteins were determined by Quantity One® software (BioRad).

6.2.2 Synchronization of mammalian cells by drugs

CHO cells grown on 10cm plates with 80-90% of confluency were incubated in serum-free α-MEM medium for 48hrs to enrich the culture in cells predominantly in the G_1 phase of the cell cycle. Alternatively, cells in G_1 were enriched after treatment with 50 μM Lovastatin (Sigma Co.) for 24 hrs or 48 hrs. CHO cells were enriched in the S phase by incubation with serum-free α-MEM medium for 24 hrs, followed by addition of aphidicolin (Sigma Co.) (2 μg/ml). After incubation for 20 hrs in the presence of aphidicolin, cells were incubated for 3 hrs in complete medium in the absence of aphidicolin. CHO cells were arrested in G_2/M phase of the cell cycle by incubation in complete α-MEM medium containing 0.8μg/ml of nocodazole (Sigma Co.) for 16-20 hrs.

6.2.2.1 Propidium Iodide Staining and Flow Cytometry

Propidium iodide (PI) staining together with flow cytometry was used to determine the degree of cell synchronization in CHO cells. Treated cells (at a density of $1x10^6$ cells) were washed with 2 ml of PBS and then digested with 1ml of trypsin solution at 37^oC for 5min. Cells were harvested by spinning down at 1200 rpm for 5min, followed by washing twice with 1ml of cold PBS (1ml). The pellet cells were resuspended in 1 ml fridge-cold 70% ethanol while vortexing the cell pellet gently, and then kept on ice for 30 min. Once in ethanol, samples could be kept for up to two weeks. Fixed cells were spun down at 2000 rpm for 5 min to remove ethanol and washed twice with 1ml PBS. The pellet was resuspended in 1ml PBS containing RNAse (100 μg/ml), and incubated for 5 min at room temperature. 400μl of propidium iodide (50 μg/ml in PBS) were added to the cell suspension. Cells were stored in the dark for 30 min at room temperature and analyzed by flow cytometry.

6.3 Immunofluorescence microscopy

Indirect immunofluorescence was carried out according to standard procedures. Cells on cover-slips were washed twice in cold PBS and fixed with methanol at -20°C for 30 seconds. Cells were subsequently blocked in PBS containing 2% bovine serum albumin for 1 hr at room temperature or

overnight at 4°C. Permeabilization was achieved during the methanol fixation. For double labeling, cells were incubated with rabbit antibodies against GAPR-1 (1:2000) and mouse antibodies against GM130 (1:500). Primary antibody labeling was then visualized by incubation with Alexa Fluor® 488 anti-rabbit IgG (1:1, 000) and/or Alexa Fluor® 568 anti-mouse IgG antibodies (1:1000). A Zeiss LSM510 flourescence microscope with appropriate filters was used. Images were collected and processed with LSM510 software.

6.4 Phosphorylation of GAPR-1 in vivo

CHO cells were cultured in 10 cm plates until they reached 80-90% confluency. After washing using HEPES buffer 50 mM pH7.5, the culture medium was replaced by 4 ml of phosphate free α-MEM or DMEM (Sigma Co.), containing HEPES at a final concentration of 20 mM (This allowed the cells to be incubated outside a CO_2 incubator).1 mCi final concentration of H_3PO_4 (ortho-phosphate ^{32}P) was added to the plates, and incubated for 4 hrs at 37^oC. The medium was carefully removed from the plates, and the cells were washed twice by using cold PBS, and then harvested by using a rubber policeman (Cell Scraper). The cells were collected by centrifugation at 500 *xg* for 10 min. Lysis of cells was carried out by passing them through a 27G needle. 90% or more of the cells were broken as determined by trypan blue staining. The lysate was centrifuged at 500 *xg* for 10min, and the post-nuclear supernatant (PNS) was collected. PNS, containing cytosol and total membranes, was centrifuged 1hr at 100000 *xg*. The sample was separated in pellet (total membranes) and supernatant (cytosol). The pellet (total membranes) was resuspended in 0.1 ml of 1% SDS, Tris-HCl 50 mM, pH 6.8, and heated to 95^oC for 5 min. SDS was quenched by diluting with 0.9 ml of immunoprecipitation (IP) buffer (PEN buffer, containing 1% Triton X-100). The solubilized total membranes and cytosol were used for subsequent immunoprecipitation. Immunoprecipitation was carried out using a α-GAPR-1 antibody (α-1852 R2), coupled to Sepharose 4B beads (see below). The antibody-beads were incubated with either the solubilized membranes or cytosol overnight at 4^oC. After incubation, the beads were washed twice with PEN buffer containing 1% TX-100, and 4 times wash with PEN buffer,

respectively. The washed beads were resuspended in 15 µl of SCI and 15 µl SCII, incubated for 2 min at 95^{o} C, and centrifuged at 14000 rpm for 30 seconds. The supernatant was loaded onto a 14% gel, and proteins were analyzed by SDS-PAGE and western blotting. To analyze for the presence of GAPR-1 in the immunoprecipitate, the membranes were incubated with α-GAPR-1 as primary antibody (same used for IP) and HRP-Protein G conjugated as a secondary antibody. After analysis, the membrane was washed several times in PBS-T buffer. To analyze the presence of phosphorylated GARP-1, the dried membrane was exposed to an X-ray film for autoradiography.

6.5 Immunoprecipitation

10µl of polyclonal serum against the C-terminus of GAPR-1 (α-1852) or 10 µl of Caveolin-1 antibody (Santa Cruz Biotechnology Inc. USA) were incubated with 50 µl of protein A Sepharose (Fast Flow, Amersham Pharmacia Biotech, Freiburg, Germany) and 50µl of PBS containing 0.5% milk for 90 minutes at RT. The beads were washed twice with PBS and twice with IP buffer (PEN buffer containing 1% TX-100) before use. Golgi membranes (500 mg) were centrifuged (100,000 *g* for 30 minutes at 4°C), and the pellet was resuspended in 100 µl 1%SDS and incubated for 5 minutes at 95°C. The sample containing denatured proteins was diluted with 900 µl of PEN containing 1% TX-100 and used for immunoprecipitation of GAPR-1 or Caveolin-1 by incubation overnight at 4°C with the protein-A beads. Subsequently the beads were washed twice in PEN buffer containing 1% TX-100 and four times in PEN before analysis. For western blot analysis, a HRP-protein G conjugate (BioRad) was used that does not recognize the denatured IgGs on the blot that were eluted from the beads used in immunoprecipitation.

7 Methods in Molecular Biology

7.1 Polymerase Chain Reaction (PCR)

7.1.1 Polymerase chain reaction (PCR) for site-directed mutagenesis

All reactions were carried out according to the manufacturer's guidelines. The reaction volumes were 50 µl, using the *PfuTurbo* polymerase (Stratagene). The reaction mix contains the following components: 5 µl of 10 X reaction buffer (Stratagene), 2 µl (10ng) of pQE60 plasmid carrying GAPR-1, 1.25 µl of each oligonucleotide (100 ng/µl), 1 µl of dNTPs (0.2mM), 1 µl of *PfuTurbo* (2.5 U/µl), and MilliQ water to adjust the total volume to 50 µl. The PCR reaction was initiated with 1 cycle at 95°C for 30 sec, followed by 18 cycles starting at 95^{o}C for 30 sec, 55^{o}C for 1 min, and 68^{o}C for 11 min.

7.1.2 Polymerase chain reaction (PCR) for Two Hybrid System

Similar as mentioned above, the reaction volumes were 50 µl, using the polymerase *PfuTurbo* (Stratagene). The PCR reaction was initiated from denaturation at 95°C for 2 min, followed by denaturation at 94°C for 30 – 60 sec. The annealing reaction was performed at appropriate temperatures (based on different primer pairs designed for the two hybrid assay (Table 6, section 4), in principle 10 - 15°C lower than the Tm of 55^{o}C for 30 – 60 sec. Elongation was performed at 68°C for 3 min for Nucleolin (Nucleolin fragment is 2.1 kB) and for 1 min for GAPR-1 (GAPR-1 fragment is 0.5kb) (*PfuTurbo* amplified at 2 min/kb) and stopped at 68^{o}C for 10 min for both Nucleolin and GAPR-1. In all cases, the reactions were performed for 30 cycles in the conditions indicated above. 5µl of PCR products were analyzed by agarose gel electrophoresis to ensure efficient amplification. Then, the PCR amplified fragments were purified from agarose gel slices with the use of Nucleobond extract kit (QIAGEN). Doubly digested plasmid vectors were also purified with this kit. Purified PCR products were either directly used for cloning into pJG4.5 or pEG202 after digestion with restriction enzymes (double enzyme digestion) or treated with DpnI in the case of site-directed mutagenesis products (in oder to digest the methylated, nonmutated parental DNA template). If the two used enzymes could not work in the same buffer, the

digestion mixtures were purified from gel, and the digestion repeated for the second enzyme.

7.1.3 Subcloning

All ligation reactions were carried out in 10 µl at either 4°C. The reaction mix contains 1 X ligation buffer (MBI Fermentas), 50 ng of DNA fragment, 25 ng of vector pJG4.5 or PEG202, and 2U of T4 DNA ligase (MBI). 5 µl of ligation mixtures were used to transform competent cells, either XL-1 Blue (Stratagene) for site-directed mutagenesis, or SURE super-competent cells (Stratagene) for the Two Hybrid assay, by heat-shock. Briefly, 50 µl of competent cells were mixed gently with 5 µl of ligation mixtures and incubate on ice for 30 min. The cells were heat-shocked at 42°C (XL-1 Blue and SURE super-competent cells) for 30 sec, followed by incubation on ice again for 2 min. 1ml of pre-warmed medium was added to the transformation mixtures and incubated at 37°C for 1 hr with shaking. Cells were plated on LB agar plate containing appropriate antibiotics and incubated at 37°C overnight.
Several colonies were randomly picked and inoculated into 4 ml of LB media supplemented with appropriate antibiotics. The cultures were incubated at 37°C for 16-18 hrs. Plasmid DNA extraction was done using QIAgen miniprep kit or Machery-Nigel nucleospin kit. The protocol of these two kits is basically the same (modified alkaline lysis). Briefly, cells were pelleted by centrifugation at 4000 rpm 4°C for 10 min, and resuspended in 0.2 ml of solution I containing RNase. Cells were lysed by adding 250 µl of solution II, followed by mixing carefully the solution (upside-down movement for several times. The lysates were neutralized by the addition of 300 µl of solution III. The solution was cleared by centrifugation, and supernatants were loaded onto the binding column and spun down. The flow-through was discarded, and the columns washed with buffer PB and PE as indicated by the manufacturer. In the last wash, centrifugation was performed for 2 min to remove traces of ethanol. The plasmids were eluted with 50 µl MilliQ water sterile. All recombinant plasmids were identified by digestion with appropriated enzymes and confirmed by commercial DNA sequencing (Medigenomix GmbH).

7.1.4 Lithium acetate transformation of EGY48-pSH18-34

To carry out the two hybrid assay, it was necessary to transform the yeast strain EGY48-pSG18-34, containing the galactosidase reporter, with the bait plasmid pEG202 and the prey plasmid pJG4.5. The yeast was grown in 100 ml SDC-URA medium to an optical density (OD) at 600nm of 0.4 - 0.8 units, equivalent to 1-2 x10^7 cells/ml, followed by harvesting the cells in a 50 ml tube. The cells were washed twice, by centrifugation at 4000 rpm for 10 min, with 15 ml of Li-TE buffer containing 10 mM Tris-HCl pH7.5, 1 mM EDTA, and 100 mM lithium acetate (Li) adjusted to pH7.5 with acetic acid. The pellet was resuspended in 0.5 ml of Li-TE, and left at room temperature while preparing the DNA. For each transformation, 3-5 µl of carrier DNA 10 mg/ml (Herring Sperm DNA, Clontech) were mixed with 1 to 2 µg of plasmid DNA, 50 µl of cells and 150 µl of a 50% (w/v) polyethyleneglycol (PEG) solution (50g of PEG3500 dissolved in 100ml of TE buffer). The mix was vortexed by 5 pulses at full speed. The suspension was incubated for 30 min at room temperature, followed by incubation at 42^{o}C for 15 min, and then 200 µl of TE were added to the incubation. The samples were plated on the appropriate minimal media.

Table 7. List of transformations carried out in EGY48-pSH18-34 to determine a GAPR-1 interaction with Nucleolin or GAPR-1

GAPR-1wt-pEG202 (pEGGAPR-1wt)	Nucleolin-pJG4.5 (pJGNCL)	Possible interactions analyzed by the two hybrid system assay.
GAPR-1wt-pJG4.5 (pJGGAPR-1wt)	Nucleolin-pEG202(pEGNCL)	
GAPR-1mut-pJG4.5(pJGGAPR-1mut)	Nucleolin-pEG202(pEGNCL)	
GAPR-1mut-pEG202 (pEGGAPR-1mut)	Nucleolin-pJG4.5 (pJGNCL)	
GAPR-1wt-pEG202 (pEGGAPR-1wt)	Nucleolin-pEG202(pEGNCL)	
GAPR-1wt-pJG4.5 (pJGGAPR-1wt)	Nucleolin-pJG4.5 (pJGNCL)	
GAPR-1mut-pEG202 (pEGGAPR-1mut)	Nucleolin-pEG202(pEGNCL)	
GAPR-1mut-pJG4.5(pJGGAPR-1mut)	Nucleolin-pJG4.5 (pJGNCL)	
GAPR-1wt-pEG202 (pEGGAPR-1wt)	GAPR-1wt-pJG4.5 (pJGGAPR-1wt)	
GAPR-1wt-pEG202 (pEGGAPR-1wt)	GAPR-1mut-pJG4.5(pJGGAPR-1mut)	
GAPR-1mut-pEG202 (pEGGAPR-1mut)	GAPR-1mut-pJG4.5(pJGGAPR-1mut)	
GAPR-1wt-pJG4.5 (pJGGAPR-1wt	GAPR-1mut-pEG202 (pEGGAPR-1mut)	
GAPR-1wt-pJG4.5 (pJGGAPR-1wt)	GAPR-1wt-pJG4.5 (pJGGAPR-1wt)	

GAPR-1wt-pEG202 (pEGGAPR-1wt)	GAPR-1wt-pEG202 (pEGGAPR-1wt)	Controls designed for the two hybrid system assay.
Nucleolin-pEG202(pEGNCL)	Nucleolin-pJG4.5 (pJGNCL)	
Nucleolin-pJG4.5 (pJGNCL)	Nucleolin-pJG4.5 (pJGNCL)	
Nucleolin-pEG202(pEGNCL)	Nucleolin-pEG202(pEGNCL)	
GAPR-1wt-pEG202 (pEGGAPR-1wt)	empty vector pJG4.5	
empty vector pEG202	GAPR-1wt-pJG4.5 (pJGGAPR-1wt)	
GAPR-1mut-pEG202 (pEGGAPR-1mut)	empty vector pJG4.5	
GAPR-1mut-pJG4.5(pJGGAPR-1mut)	empty vector pEG202	
empty vector pEG202	empty vector pJG4.5	

8 Methods in Biochemistry

8.1 Isolation of Golgi membranes

8.1.1 Golgi membranes from CHO cells

Solutions:

EDTA stock solution	100 mM	EDTA/KOH pH7.1
Homogenization buffer	250 mM	Sucrose
	10 mM	Tris-HCl pH7.4
Sucrose Solutions	29%(w/w)	Sucrose in 10 mM Tris-HCL pH7.4
	35%(w/w)	Sucrose in 10 mM Tris-HCL pH7.4
	62%(w/w)	Sucrose in 10 mM Tris-HCl pH7.4

Golgi membranes were prepared as described previously (Balch, W. *et al*. 1984; Malhotra, V. *et al*. 1989; Serafini, T. *et al*. 1991). One preparation of Golgi membranes from CHO requires 10 L of cultured cell with a density of $7x10^5$cells/ml approximately. CHO cells were harvested at 500 *xg* and washed twice in cold PBS. The pellet was further washed with cold homogenization buffer. The wash steps were conducted at 1,500 *xg* for 10 min. The pellet was resuspended in 5 volumes of cold homogenization buffer, followed by breaking of the cells with the Balch homogenizer. 50-60 strokes were needed to disrupt more than 90% of the cells. To 12 ml of homogenate, 11 ml of 62% (w/w) sucrose solution was added and 250 µl of 100 mM EDTA (pH7.1). The sucrose concentration was determined by refractometer. If the sucrose was out of the range of 36.5-37.5% (w/w), it was adjusted by adding either 10 mM

Tris-HCL buffer (pH7.4) or sucrose solution. This adjustment was achieved by using the following formula:

If more sucrose was needed, the volume of 2 M sucrose solution in 10 mM Tris-HCl pH7.4 necessary was calculated:

$$\frac{V_{original} \times (C_{wanted} - C_{original})}{(C_{stock\ solution} - C_{wanted})} = V_{to\ add}$$

If less sucrose was needed, the volume of 10 mM Tris-HCl pH7.4 was calculated:

$$\frac{V_{original} \times (C_{wanted} - C_{original})}{(C_{wanted})} = V_{to\ add}$$

$V_{original}$ = Volume of homogenate solution after adding 62% (w/w) sucrose;

$V_{to\ add}$ = Volume to add of either 2M sucrose solution or 10 mM Tris-HCL buffer.

$C_{original}$ = Sucrose concentration of homogenate solution after adding 62% (w/w) sucrose.

C_{wanted} = Desire concentration of sucrose (i.e. 37% (w/w))

$C_{stock\ solution}$ = Stock solution of Sucrose at 2 M

After adjustment, the homogenate was transferred to a tube SW28 tube, and the following sucrose gradient was made: 12 – 14 ml of 37% (w/w) sucrose-homogenates at the bottom, followed by 15 ml of 35% (w/w) overlaid carefully on the homogenate, and 9 ml of 29% (w/w) sucrose on the top. The gradient was centrifuged at 4°C 25,000 rpm for 2.5 hrs. The Golgi membranes floated as an opalescent band at the interface between 29% and 35% while ER fraction at the interface between 35% and 37%. Golgi fractions were collected as much as 2 – 3 ml for each gradient and all the fractions were combined. Separated aliquots of 200 µl to 500 µl were stored at 4°C for protein determination. The rest of the aliquots were frozen in liquid nitrogen and stored at -80°C.

8.1.2 Isolation of Golgi membranes from rat liver

Solution Buffers I	10 mM Tris-HCL pH7.4 0.5 M Sucrose
	100 mM EDTA pH7.4
Sucrose Solutions:	30.5% (w/w) Sucrose in 10 mM Tris-HCl pH7.4
	35% (w/w) Sucrose in 10 mM tris-HCl pH7.4
	37% (w/w) Sucrose in 10 mM Tris-HCl pH7.4

The liver from a rat was removed and based on its weight 4 times in buffer I was added, and the EDTA concentration was adjusted to 5mM final concentration. The tissue was minced using scissors and then homogenized on ice with a Dounce homogenizer. The homogenate was centrifuged at 2500 rpm for 10min, and the post nuclear supernatant (PNS) was filtered through 4 layers of cheesecloth. In a SW28 rotor tube, 30 ml of PNS were added and overlaid on 8 ml of 37% (w/w) sucrose solution. The sample was centrifuged at 25000 rpm (83000 *xg*) for 1.5 hrs. A band was collected at the interface 37% - 16% (w/w) of sucrose, and 4 ml were collected per sample. The sucrose concentration was adjusted to 37% (w/w) using either a 55% (w/w) sucrose solution or 10 mM Tris-HCl pH7.4 (see formula on section 9.1.1). 14 ml of membranes adjusted to 37% (w/w) sucrose were poured into a SW28 tube, and overlaid with 10 ml of 35% (w/w) sucrose, followed by a 10 ml layer of 30.5% (w/w) sucrose, and 5 ml of 25% (w/w) sucrose. The gradient was centrifuged at 25000 rpm (100.000 *xg*) for 2.5 hrs, and the Golgi membranes collected at the interface 25% - 30% (w/w) sucrose. The membranes were fractionated in aliquots and frozen at -80^{o}C.

8.1.3 Preparation of Golgi-derived detergent insoluble complexes (GICs)

Golgi-derived microdomains were prepared as described by Gkantiragas, I. *et al*. (2001). 7 mg of Golgi membranes were collected by centrifugation at 4°C 100,000 *xg* for 1 hr after dilution with 4 volumes of PEN buffer. The pellet (Golgi membranes) was resuspended in 2 ml of ice-cold PEN buffer containing 1% TX-100, followed by incubation on ice for 30 min. 2 ml of 80%

(w/v) sucrose in PEN buffer (without Triton X-100) were added to the resuspended membranes to obtain a 40% solution. The mixture was transferred into a SW41 tube and sequentially overlaid with 1.3 ml of the following sucrose solutions: 30%, 25%, 20%, 15%, 10% and 5% sucrose (w/v). The gradient was centrifuged for 22 hrs at 4°C 39,000 rpm, and the opalescent band at the interface between 10% and 15% was collected. An aliquot was used for protein and lipid quantification and the other aliquots were at -80°C.

9 Cytosol preparation from Mammalian Cells

9.1 Cytosol preparation from CHO and Hela Cells

CHO or HeLa cells were cultured in suspension as indicated in section 8.1.1. 1.2 L of suspension cultures were spun down at 500 *xg* for 10min. The pellet was washed twice with PBS, and then washed twice with breaking buffer containing 10 mM Tris-HCl, pH7.5, 0.25 M sucrose, followed by dilution 1:5 in breaking buffer (1.2 L of suspension culture yields approximately 5ml of cell pellet). The suspension was homogenized as described in section 8.1.1., and the homogenate was adjusted to a concentration of 0.5 M KCl, and incubated for 1 hr on ice for 30 min. After incubation, the homogenate was centrifuged 1 hr at 55000 rpm (TFT rotor 55.38). The supernatant was dialyzed once against 5 L of PBS, and twice against 50 mM Tris-HCl pH7.5, 50 mM NaCl. The dialyzed cytosol was centrifuged at 100000 *xg* for 2 hrs.

9.2 Cytosol preparation from Rat liver

Solution buffer H:	165 mM KOH
	50 mM HEPES pH7.55 (Acetic acid)
	2 mM $MgCH_3CO_2$
Additional components:	1 mM DTT
(protease inhibitors Solution)	1 µM Leupetin
	10 µM Antipain
	100 µM PMSF

9 g of rat liver from 1.5 months old rats were blended following homogenization by a Dounce homogenizer in buffer H and addition the protease inhibitor solution. The homogenate was centrifuge at 9000 rpm for 10 min. The pellet was discarded and the supernatant was subjected to another round of centrifugation using a TFT rotor (55.38) in a Kontron centrifuge at 33000 rpm (100000 *xg*) for 1 hr. The supernatant was collected and centrifuged again in TFT rotor (55.38) at 44000 rpm (160000 *xg*) for 1.5 hrs. The supernatant was divided in aliquots and frozen at -80^{o}C.

9.3 Cytosol fractionation

A 320 ml Superdex200 prep grade (Amersham Biotech) column was calibrated by loading proteins with known molecular masses, such as Thyroglobulin (669kDa) Alcohol Dehydrogenase (150kDa), Bovine Serum Albumine (66kDa), Carbonic Anhydrase (29kDa) and lysozyme (14kDa) and determination of the elutions pattern and fraction locations in a Biologic workstation (BioRad). To fractionate cytosol of either CHO or HeLa, 10 ml of cytosol containing 20 mg/ml protein were loaded on the pre-equilibrated Superdex200 column. The eluted fractions were separated in a low molecular weight fraction containing proteins below 100kDa (LMW) and a high molecular weight fraction containing proteins above 100kDa (HMW). Both fractions were about 200 ml, and were separately loaded onto a GAPR-1 affinity column to determine whether GAPR-1 binds to a complex of proteins in the cytosol bigger than 100kDa or smaller than 100kDa.

9.4 Cytosolic Protein complex denaturation

200 ml of HeLa cytosol at 1mg/ml were subjected to denaturation by adding 1% SDS followed by incubation at 95^{o}C for 20min. The denaturated solution was quenched by adding 1,8 L of buffer containing Tris-HCl 50 mM pH7.5, 50 mM NaCl, 1% Triton X-100. The solution was then loaded onto a GAPR-1 affinity column, containing either GAPR-1 wild type or GAPR-1 mutant.

10 Large scale purification of GAPR-1

GAPR-1 was over-expressed in M15[RP4] bacteria, containing a GAPR-1-pQE60 vector. An overnight culture was prepared in LB medium containing 100 µg/ml ampicilin (AMP) and 50 µg/ml kanamycin (KAN). 12 L of LB medium, containing AMP and KAN, were inoculated with 30 ml of overnight culture, and incubated until an optical density at 620nm of 0.5 was reached. The overexpression was induced by the addition of 12 ml of 1M IPTG, and the incubation was continued for 3 hrs at 37^{o}C. The 12 L suspension were centrifuged at 7000 rpm for 10 min (preparative centrifuge, Hereaus), and the pellet resuspended in DEAE buffer containing 50 mM Tris-HCl pH7.5 and 50 mM NaCl. The pellet was washed once in DEAE buffer and resuspended in 300 ml of DEAE buffer containing a mix of protease inhibitors (tablets, Boehringer, Mannheim). The suspension was passed 5 times through a cell disruptor (Emulsiflex®, Avestin), or passed 3 times through a French press, and the homogenate was centrifuged at 4000 rpm for 15 min to remove unbroken cells. The supernatant was centrifuged at 100000 *xg* for 1hr (TFT rotor 55.38, Kontron Instruments). After centrifugation, supernatant was diluted ~1:6 in DEAE buffer, giving a total sample volume of approximately 1.8 L. The 1.8 L sample was passed over a DEAE column (Amersham Biotech) (1ml/min) was equilibrated with 50 mM Tris-HCl pH7.5; 50 mM NaCl. The flow through was collected and applied onto a 25 ml cation exchange column (Macroprep High S support, BioRad), pre-equilibrated with DEAE buffer. The column was washed with DEAE buffer until the optical density at 280 nm was below 0.1. To elute the bound proteins from the column, a liner gradient from 50 to 1000 mM NaCl was applied, and fractions of 1 ml were collected, after a dead volume of approximately 16 ml. Fractions containing highest and purest amount of GAPR-1 were combined (4 ml) and applied onto a Superdex200 column 26 mm x 76 cm (Amersham Biotech) for further purification, collecting fraction of 2ml. The peak fractions were analyzed by SDS-PAGE (14% gel). For every step during the purification, samples were collected for analysis, and quality control of the purification process. For large a scale purification of GAPR-1 mutant, the same protocol was followed. GAPR-1 wild type, and mutant proteins purified by this protocol were used for further studies.

10.1 Size exclusion chromatography light scattering (SEC-LS)

The molecular masses of GAPR-1 wild type and mutant proteins were determined using SEC-LS. 200 µl of GAPR-1 (200 µg/ml) was applied to a Superdex200 HR 10/30 (Amersham Biotech) upstream of DAWN DSP LS (Wyatt QELS). The column was equilibrated in Tris-HCl 50 mM pH8.0, 300 mM NaCl at a flow rate of 0.5 ml/min. The average molecular masses (M_w) of GAPR-1 were calculated at peak maxima using three independent analyses, i.e. the two and three-detector method, and the ASTRA analysis. The M_w was estimated throughout the entire eluting peak at 50 µl intervals using ASTRA software.

10.2 Crystal structure determination

The following protocols were used by Dr. Matthew Groves and Audrey Kühn (EMBL) to obtain GAPR-1 crystal. Briefly, the protein products obtained from overexpression were checked by dynamic light scattering, mass spectrometry and equilibrium centrifugation for homogenity and oligomerisation state prior to crystallization. The protein was concentrated using Amicon Centricon 10kDa filters to a concentration of 12.6 mg/ml as estimated by Bradford reagent (BioRad). Initial screening was performed at room temperature (295.5K) by hanging drop vapour diffusion (McPherson, 1982) using the sparse matrix kits from Hampton Research (Hampton Research, Laguna Niguel, CA). Drops were prepared on siliconized cover slips and equilibrated against 1ml reservoir solution. Screens were prepared by combining equal volumes of reservoir solution with protein solution. Conditions producing crystals from the initial screens were refined to produce crystals suitable for X-ray diffraction analysis.

10.2.1 Data Collection

After transferring to a cryoprotectant solution (reservoir solution with an additional 15% v/v glycerol), crystals were picked up using a fiber loop and flash frozen in a stream of nitrogen gas at 100K. In-house diffraction data were collected from a single crystal on a Mar345 (Mar Research) image-plate detector using Cu Kα radiation from a rotating-anode X-ray generator

operating at 50kV and 100mA. A higher resolution data set was collected at the ID14 EH-2 ESRF beamline on a MarCCD detector. The programs MOSFLM (Leslie, A 1992), SCALA (Evans, P. 1997), SHARP (Fortelle, E. de la,. Bricogne, G. 1997), O (Jones, T. *et al*. 1991) and CNS (Brünger. A. *et al*. 1998) were used for data processing and analysis.

10.3 Circular Dichroism of GAPR-1

CD spectra were recorded on a Jasco J720 spectrophotometer. The instrument was calibrated with 10 mM sodium phosphate buffer. Cell path lengths 1 mm and 2 mm were used. GAPR-1 wild type and mutant were dialyzed twice against 10 mM sodium phosphate buffer prior to measurement. Spectra were acquired at a scan speed of 100 nm/min with a 1-nm slit and 1-second response time, averaging 20 scans, and corrected by subtraction of the solvent spectrum obtained under identical conditions. To carry out the Far U.V spectra measurements 5.8 µM of protein was used both GAPR-1 wild type and mutant, and for the Near-UV spectra measurements 588 µM were used, respectively.

10.4 Coupling of GAPR-1 to CNBr-activated Sepharose 4B

Swelling Buffer	HCl 1 mM cold
Coupling buffer	$NaHCO_3$ 0.1 M, pH8.3; NaCl 0.5 M
Blocking buffer	Ethanolamine 1 M pH8.0
Washing buffer	Acetate buffer 0.1 M, pH4.0

0.5g of CNBr-activated Sepharose 4B (Amersham Biotech) were washed and swelled 5 min in 300ml of cold HCl 1mM by centrifuging 5 times with 50 ml at 1000 rpm. 5 mg of purified GAPR-1 (wild type or mutant) were dialyzed in coupling buffer prior to mixing with the swelled resin. The mix was incubated overnight at 4^{o}C with gentle agitation, followed by centrifugation at 1000 rpm for 5 min. The supernatant was concentrated using amicon concentration units to 1 ml, and a protein determination was carried out to estimate the coupling efficiency. The gel was transferred to a solution of ethanolamine (1 M) to block the remaining active groups for 16 hrs at 4^{o}C. The gel was

washed with coupling buffer followed by acetate buffer, and again coupling buffer to wash away excess adsorbed protein. The protein-coupled-agarose beads were ready to use at this point.

11 GAPR-1 affinity Chromatography

200 ml of CHO cytosol (1 mg/ml) were prepared (section 9.1) and loaded onto 1ml GAPR-1 affinity columns, either GAPR-1wt or GAPR-1mut columns, at a flow rate of 0.5 ml/min. After loading, the columns were washed with wash buffer (Tris-HCl 50 mM pH7.5, 50 mM NaCl), and coupled to a SMART® FPLC system (Amersham Biotech). When the optical density at 280nm reached 0.05, a NaCl gradient 50-1000 mM was applied (0.5 ml/min) to elute the proteins bound to GAPR-1. The system collected 48 samples of 250 µl each. The fractions were analyzed by SDS-PAGE (Novex®, Invitrogen), and the protein composition of the samples was identified by mass spectrometry fingerprinting (MALDI-TOF). The columns were also used with HeLa cytosol and Rat liver cytosol.

12 GAPR-1 Ligand Overlay

50 µg of proteins from cytosol were separated by 12% SDS-PAGE (Novex® Invitrogen) and transferred to a nitrocellulose membrane (BA 85, Schleicher and Schuell). The proteins transferred to the membrane were renaturated by incubation at 4^{o}C for 1 to 2 days in renaturation buffer containing 50mM HEPES/KOH pH7.2, 5 mM magnesium acetate, 100 mM potassium acetate, 3 mM DTT, 10mg/ml BSA, 0.1% (w/v) triton X-100, and 0.3% (w/v) Tween 20. After renaturation, the membrane was incubated at room temperature for 1hr in binding buffer containing 12.5 mM HEPES/KOH, pH7.4, 1.5 mM magnesium acetate, 75 mM potassium acetate, 10 mM $ZnSO_4$, 1 mM DTT, 2 mg/ml BSA, 0.005% (w/v) triton X-100, 4 mM n-octylglycopyranoside, and 0.5 µM of GAPR-1. The filter was then washed several times with washing buffer composed of 20 mM Tris-HCl pH7.4, 100 mM NaCl, 20 mM $MgCl_2$, and 0.005% Triton X-100.

After washing, the membrane was incubated with antibody against GAPR-1 (α-1852) and developed using secondary antibody anti-rabbit HRP-conjugated.

13 SDS-PAGE and Western Blot analysis

13.1 SDS-PAGE for separation of proteins

Gels for SDS-PAGE were prepared according to the guidelines of Molecular Cloning (3rd ed.). 12% and 14% separation gels were used in this experimental work or 12% and 4-12% pre-cast separation gels commercially available from Invitrogen. After electrophoresis, the gels were stained in coomassie blue solution and destained. For radioactive gels, after staining, the gels were dried and exposed to a film. Other gels were used for western blot analysis of the proteins of interest.

13.2 Transfer proteins from SDS-PAGE to a PVDF membrane or Nitrocellulose

After performing SDS-PAGE, the proteins were electro-transferred to PVDF membranes (Immobilon-P® Milipore). The PVDF-membrane was submerged in methanol prior to soaking in the Anode buffer II. In semi-dry blotting discontinuous buffer system is used, composed of two anode buffers and one cathode buffer. The SDS-PAGE gel and PVDF membrane were arranged as follows: 2 sheets of Whatman 3MM filter paper pre-soaked in Anode buffer I were placed on the platinum anode, followed by 2 sheets of Whatman paper pre-soaked in Anode buffer II, the PVDF-membrane, the gel, and firmly 3 sheets of Whatman paper pre-soaked in Cathode buffer on top. The air was removed carefully by rolling out the air bubbles either by using a pipette or a 50ml tube. The cathode was placed on the stack and the blotting was executed at 24V for 1.5 hrs.

13.3 Incubation of PVDF membranes with antibodies

Once the transfer was completed, the PDVF membrane was rinsed in water and stained with a Ponseau S solution. Excess of Ponseau S dye was washed away with water until protein marker bands appeared on the membrane and their positions could be marked on the membrane. The

markers used throughout most of the thesis were broad range protein marker from Bio-Rad™. The size of the protein markers is outlined in Table 8.

Table 8. Protein standards (Broad Range)

Protein	Molecular mass (kD)
Myosin	200
β-galactosidase	116
Phosphorylase-b	97
Serum albumin	66
Ovalbumin	45
Carbonic anhydrase	31
Trypsin inhibitor	21
Lysozyme	14
Aprotinin	6.5

The PVDF membrane was blocked with 50 ml of 5% BSA in PBS for 1 hr at room temperature or overnight at 4°C. The blot was rinsed for 1min in PBS to remove BSA and incubated with the diluted primary antibodies (in 1% BSA PBS-T) for 1 hr at room temperature, followed by washing 3 times with PBST for 15 min. The blot was incubated with the HRP-conjugated secondary antibodies (1/1000 dilution) or HRP-conjugated Protein-G (1/1000 dilution) in 50 ml 1% BSA in PBST for 1 hr at room temperature. The blot was washed 3 times with PBST for 15 min and developed using ECL® western blotting detection system (Amersham-Biotech).

14 Protein Determination

14.1 Protein Determination by BCA

For soluble protein determination the BCA protein assay was employed (Pierce). All samples, including a set of standards (BSA: 2.5 µg, 5.0 µg, 10 µg, 15 µg, 20 µg, 25 µg, 30 µg and 35 µg), were prepared in aqueous solution. For 10 µl of each sample 200 µl of working reagent was added. The solution was prepared by mixing 50 parts of Reagent A with 1 part of Reagent B. The

samples, including standards and blanks, were incubated at 37°C for 30 min, followed by measurement of absorbance at 562nm on a plate reader.

14.2 Protein determination by Lowry

Lowry Solution A:	2 g Na_2-tartrate	Dissolved in 500 ml 1N NaOH,
	100 g N_2CO_3	adjusted to 1 L with MiliQ water
Lowry Solution B:	2 g Na_2-tartrate	Dissolved in 90 ml H_2O, 10ml NaOH
	1 g $CuSO_4x\ 5H_2O$	adjusted to 500 ml with MiliQ water
Lowry Solution C:	Folin-Cicocalteus.	Reagent prepared prior to use by diluting 1/10 with MiliQ water

Protein determination for membrane protein was performed according to Lowry. The protein standards were prepared with BSA (2.5 µg, 5.0 µg, 10 µg, 15 µg, 20 µg, 25 µg, 30 µg and 35 µg) dissolved in water. The samples and standards were prepared by adding 10 µl of deoxycholate stock solution (Stock solution: Sodium deoxycholate 2 mg/ml) to 50 ul of sample. 150 µl of TCA (10%) (TriChloroacetic acid) were added to the sample, vortexed and centrifuged for 10 min at 14000 rpm. The supernatant was removed, and 10 µl of SDS were added, followed by 50 µl of Lowry solution A. The sample was incubated at 50^{o}C for 10min, and cooled down for 3min to room temperature. 10 µl of Lowry solution B was added, and the sample incubated for 15min at room temperature. 150 µl of Lowry solution C were added, and the sample was placed at 50^{o}C for 10 min. Once the sample was at room temperature again, the absorbance was measured at 620nm on a plate reader.

15 Protein Precipitation

15.1 Chloroform-Methanol Precipitation

Chloroform-Methanol Solution 1:2	20 ml $CHCl_3$: 40 ml CH_3OH

One volume of sample was mixed with 3 volumes of Chloroform-Methanol solution. The mix was vortexed until the solution was clear (1 or 2 drops of methanol were added when the solution did not become clear). The sample

was centrifuged 14000 rpm for 15min at 15^{o}C. The supernatant was discarded and the pellet was dried for 1hr at 37^{o}C or overnight at room temperature. The pellet was dissolved by adding Sample cocktail I. Once dissolved, the sample was suitable for protein determination and/or protein electrophoresis.

15.2 TCA precipitation

TCA solution 72% (w/v)	72 g of trichloacetic acid dissolved in 100 ml H_2O
Sodium deoxycholate 2%	2 g of Sodium deoxycholate in 100 ml H_2O
Acetone	kept at -20^{o}C

The protein sample was diluted to a final volume of 1ml with MilliQ water, followed by addition of 16.7 µl of 2% sodium deoxycholate. The sample was vortexed and incubated for 15min at room temperature. 100 µl of TCA solution 72% was added to the sample and vortexed, and then centrifuged for 7 min at 14000 rpm. The supernatant was aspirated and 1ml of acetone at -20 added to wash the pellet. The sample was centrifuged as described above, and the pellet was allowed to dry.

References

Anderson, R.G. (1998). The caveolae membrane system. *Annu Rev Biochem* **67**, 199-225.

Antoniw, J.F., Dunkley, A.M., White, R.F., and Wood, J. (1980). Soluble leaf proteins of virus-infected tobacco (Nicotiana tabacum) cultivars. *Biochem Soc Trans* **8**, 70-71.

Bacon, D.,Anderson, W. (1988). A Fast Algorithm for Rendering Space-Filling Molecule Pictures. *Journal of Molecular Graphics* **6**, 219-220.

Bagnat, M., and Simons, K. (2002). Cell surface polarization during yeast mating. *Proc Natl Acad Sci U S A* **99**, 14183-14188.

Balch, W.E., Dunphy, W.G., Braell, W.A., and Rothman, J.E. (1984). Reconstitution of the transport of protein between successive compartments of the Golgi measured by the coupled incorporation of N-acetylglucosamine. *Cell* **39**, 405-416.

Baumann, C.A., Chokshi, N., Saltiel, A.R., and Ribon, V. (2000). Cloning and characterization of a functional peroxisome proliferator activator receptor-gamma-responsive element in the promoter of the CAP gene. *J Biol Chem* **275**, 9131-9135.

Belenguer, P., Baldin, V., Mathieu, C., Prats, H., Bensaid, M., Bouche, G., and Amalric, F. (1989). Protein kinase NII and the regulation of rDNA transcription in mammalian cells. *Nucleic Acids Res* **17**, 6625-6636.

Block, M.R., Glick, B.S., Wilcox, C.A., Wieland, F.T., and Rothman, J.E. (1988). Purification of an N-ethylmaleimide-sensitive protein catalyzing vesicular transport. *Proc Natl Acad Sci U S A* **85**, 7852-7856.

Bouton, C., and Demple, B. (2000). Nitric oxide-inducible expression of heme oxygenase-1 in human cells: Translation-independent stabilization of the mRNA and evidence for direct action of NO. *J Biol Chem*.

Bretscher, M.S., and Munro, S. (1993). Cholesterol and the Golgi apparatus. *Science* **261**, 1280-1281.

Brown, D.A., and London, E. (1998). Functions of lipid rafts in biological membranes. *Annu Rev Cell Dev Biol* **14**, 111-136.

Brown, D.A., and London, E. (2000). Structure and function of sphingolipid- and cholesterol-rich membrane rafts. *J Biol Chem* **275**, 17221-17224.

Brown, R.L., Haley, T.L., West, K.A., and Crabb, J.W. (1999). Pseudechetoxin: a peptide blocker of cyclic nucleotide-gated ion channels. *Proc Natl Acad Sci U S A* **96**, 754-759.

Brown, D. (2002). Structure and function of membrane rafts. *Int J Med Microbiol* **291**, 433-437.

Brown, D.A., and Rose, J.K. (1992). Sorting of GPI-anchored proteins to glycolipid-enriched membrane subdomains during transport to the apical cell surface. *Cell* **68**, 533-544.

Brünger, A. T and Warren, G.L. (1998) Crystallography and NMR system: a new software suite for macromolecular structure determination. *Acta Crystallogr.* D54, 905-921.

Burd, C.G., Dreyfuss, G. (1994). Conserved Structures and Diversity of Functions of RNA-Binding Proteins. *Science* **265**, 615-621.

Buser, C.A., Kim, J., McLaughlin, S., and Peitzsch, R.M. (1995). Does the binding of clusters of basic residues to acidic lipids induce domain formation in membranes? *Mol Membr Biol* **12**, 69-75.

Cary, L.A., and Cooper, J.A. (2000). Molecular switches in lipid rafts. *Nature* **404**, 945, 947.

Cervoni, N., Detich, N., Seo, S.B., Chakravarti, D., and Szyf, M. (2002). The oncoprotein Set/TAF-1beta, an inhibitor of histone acetyltransferase, inhibits active demethylation of DNA, integrating DNA methylation and transcriptional silencing. *J Biol Chem* **277**, 25026-25031.

Conboy, I.M., Manoli, D., Mhaiskar, V., and Jones, P.P. (1999). Calcineurin and vacuolar-type H+-ATPase modulate macrophage effector functions. *Proc Natl Acad Sci U S A* **96**, 6324-6329.

Conrath, U., Pieterse, C.M., and Mauch-Mani, B. (2002). Priming in plant-pathogen interactions. *Trends Plant Sci* **7**, 210-216.

Cooper, S. (1998). On the proposal of a G0 phase and the restriction point. *Faseb J* **12**, 367-373.

Cooper, S. (2003). Reappraisal of serum starvation, the restriction point, G0, and G1 phase arrest points. *Faseb J* **17**, 333-340.

Curran, R.D., Ferrari, F.K., Kispert, P.H., Stadler, J., Stuehr, D.J., Simmons, R.L., and Billiar, T.R. (1991). Nitric oxide and nitric oxide-generating compounds inhibit hepatocyte protein synthesis. *Faseb J* **5**, 2085-2092.

Daniely, Y., and Borowiec, J.A. (2000). Formation of a complex between nucleolin and replication protein A after cell stress prevents initiation of DNA replication. *J Cell Biol* **149**, 799-810.

De Matteis, M.A., and Morrow, J.S. (1998). The role of ankyrin and spectrin in membrane transport and domain formation. *Curr Opin Cell Biol* **10**, 542-549.

Derenzini, M., Sirri, V., Trere, D., and Ochs, R.L. (1995). The quantity of nucleolar proteins nucleolin and protein B23 is related to cell doubling time in human cancer cells. *Lab Invest* **73**, 497-502.

Dermine, J.F., Duclos, S., Garin, J., St-Louis, F., Rea, S., Parton, R.G., and Desjardins, M. (2001). Flotillin-1-enriched lipid raft domains accumulate on maturing phagosomes. *J Biol Chem* **276**, 18507-18512.

Drevot, P., Langlet, C., Guo, X.J., Bernard, A.M., Colard, O., Chauvin, J.P., Lasserre, R., and He, H.T. (2002). TCR signal initiation machinery is pre-assembled and activated in a subset of membrane rafts. *Embo J* **21**, 1899-1908.

Donaldson, J.G., Finazzi, D., and Klausner, R.D. (1992). Brefeldin A inhibits Golgi membrane-catalysed exchange of guanine nucleotide onto ARF protein. *Nature* **360**, 350-352.

Dumler, I., Stepanova, V., Jerke, U., Mayboroda, O.A., Vogel, F., Bouvet, P., Tkachuk, V., Haller, H., and Gulba, D.C. (1999). Urokinase-induced mitogenesis is mediated by casein kinase 2 and nucleolin. *Curr Biol* **9**, 1468-1476.

Duronio, R.J., Jackson-Machelski, E., Heuckeroth, R.O., Olins, P.O., Devine, C.S., Yonemoto, W., Slice, L.W., Taylor, S.S., and Gordon, J.I. (1990). Protein N-myristoylation in Escherichia coli: reconstitution of a eukaryotic protein modification in bacteria. *Proc Natl Acad Sci U S A* **87**, 1506-1510.

Dykstra, M., Cherukuri, A., Sohn, H.W., Tzeng, S.J., and Pierce, S.K. (2003). LOCATION IS EVERYTHING: Lipid Rafts and Immune Cell Signaling. *Annu Rev Immunol* **21**, 457-481.

Eberle, H.B., Serrano, R.L., Fullekrug, J., Schlosser, A., Lehmann, W.D., Lottspeich, F., Kaloyanova, D., Wieland, F.T., and Helms, J.B. (2002). Identification and characterization of a novel human plant pathogenesis-related protein that localizes to lipid-enriched microdomains in the Golgi complex. *J Cell Sci* **115**, 827-838.

Eisenberg, I., Barash, M., Kahan, T., and Mitrani-Rosenbaum, S. (2002). Cloning and characterization of a human novel gene C9orf19 encoding a conserved putative protein with an SCP-like extracellular protein domain. *Gene* **293**, 141-148.

Emoto, K., Kuge, O., Nishijima, M., and Umeda, M. (1999). Isolation of a Chinese hamster ovary cell mutant defective in intramitochondrial transport of phosphatidylserine. *Proc Natl Acad Sci U S A* **96**, 12400-12405.

Eu, J.P., Liu, L., Zeng, M., and Stamler, J.S. (2000). An apoptotic model for nitrosative stress. *Biochemistry* **39**, 1040-1047.

Evans, P.R., Scaling of MAD Data", Proceedings of CCP4 Study Weekend, 1997, on Recent Advances in Phasing.
http://www.ccp4.ac.uk/proceedings/1997/p_evans/main.html

Farazi, T.A., Waksman, G., and Gordon, J.I. (2001). The biology and enzymology of protein N-myristoylation. *J Biol Chem* **276**, 39501-39504.

Fernandez, C., Szyperski, T., Bruyere, T., Ramage, P., Mosinger, E., and Wuthrich, K. (1997). NMR solution structure of the pathogenesis-related protein P14a. *J Mol Biol* **266**, 576-593.

Fielding, C.J., and Fielding, P.E. (2003). Relationship between cholesterol trafficking and signaling in rafts and caveolae. *Biochim Biophys Acta* **1610**, 219-228.

Fortelle, E. de la,. Bricogne, G. (1997). Maximum-Likelihood Heavy-Atom Parameter Refinement for Multiple Isomorphous Replacement and Multiwavelength Anomalous Diffraction Methods. In *Methods Enzymol*, **276**. Macromolecular Crystallography Part A. C.W. Carter and R.M. Sweet ed. Academic Press, San Diego, pp. 472-494.

Gustavsson, J., Parpal, S., Karlsson, M., Ramsing, C., Thorn, H., Borg, M., Lindroth, M., Peterson, K.H., Magnusson, K.E., and Stralfors, P. (1999). Localization of the insulin receptor in caveolae of adipocyte plasma membrane. *Faseb J* **13**, 1961-1971.

Galbiati, F., Volonte, D., Liu, J., Capozza, F., Frank, P.G., Zhu, L., Pestell, R.G., and Lisanti, M.P. (2001). Caveolin-1 expression negatively regulates cell cycle progression by inducing G(0)/G(1) arrest via a p53/p21(WAF1/Cip1)-dependent mechanism. *Mol Biol Cell* **12**, 2229-2244.

Galbiati, F., Volonte, D., Engelman, J.A., Scherer, P.E., and Lisanti, M.P. (1999b). Targeted down-regulation of caveolin-3 is sufficient to inhibit myotube formation in differentiating C2C12 myoblasts. Transient activation of p38 mitogen-activated protein kinase is required for induction of caveolin-3 expression and subsequent myotube formation. *J Biol Chem* **274**, 30315-30321.

Gansauge, S., Nussler, A.K., Beger, H.G., and Gansauge, F. (1998). Nitric oxide-induced apoptosis in human pancreatic carcinoma cell lines is associated with a

G1-arrest and an increase of the cyclin-dependent kinase inhibitor p21WAF1/CIP1. *Cell Growth Differ* **9**, 611-617.

Garcia-Cardena, G., Martasek, P., Masters, B.S., Skidd, P.M., Couet, J., Li, S., Lisanti, M.P., and Sessa, W.C. (1997). Dissecting the interaction between nitric oxide synthase (NOS) and caveolin. Functional significance of the nos caveolin binding domain in vivo. *J Biol Chem* **272**, 25437-25440.

Ghisolfi-Nieto, L., Joseph, G., Puvion-Dutilleul, F., Amalric, F., and Bouvet, P. (1996). Nucleolin is a sequence-specific RNA-binding protein: characterization of targets on pre-ribosomal RNA. *J Mol Biol* **260**, 34-53.

Gilchrist, J.S., Abrenica, B., DiMario, P.J., Czubryt, M.P., and Pierce, G.N. (2002). Nucleolin is a calcium-binding protein. *J Cell Biochem* **85**, 268-278.

Ginisty, H., Sicard, H., Roger, B., and Bouvet, P. (1999). Structure and functions of nucleolin. *J Cell Sci* **112** (Pt 6), 761-772.

Gkantiragas, I., Brugger, B., Stuven, E., Kaloyanova, D., Li, X.Y., Lohr, K., Lottspeich, F., Wieland, F.T., and Helms, J.B. (2001). Sphingomyelin-enriched microdomains at the Golgi complex. *Mol Biol Cell* **12**, 1819-1833.

Haluska, P., Jr., and Rubin, E.H. (1998). A role for the amino terminus of human topoisomerase I. *Adv Enzyme Regul* **38**, 253-262.

Hantschel, O., Nagar, B., Guettler, S., Kretzschmar, J., Dorey, K., Kuriyan, J., and Superti-Furga, G. (2003). A myristoyl/phosphotyrosine switch regulates c-Abl. *Cell* **112**, 845-857.

Heil, M., and Bostock, R.M. (2002). Induced systemic resistance (ISR) against pathogens in the context of induced plant defences. *Ann Bot (Lond)* **89**, 503-512.

Helms, J.B., Helms-Brons, D., Brugger, B., Gkantiragas, I., Eberle, H., Nickel, W., Nurnberg, B., Gerdes, H.H., and Wieland, F.T. (1998). A putative heterotrimeric G protein inhibits the fusion of COPI-coated vesicles. Segregation of heterotrimeric G proteins from COPI-coated vesicles. *J Biol Chem* **273**, 15203-15208.

Henriksen, A., King, T.P., Mirza, O., Monsalve, R.I., Meno, K., Ipsen, H., Larsen, J.N., Gajhede, M., and Spangfort, M.D. (2001). Major venom allergen of yellow jackets, Ves v 5: structural characterization of a pathogenesis-related protein superfamily. *Proteins* **45**, 438-448.

Higuchi, H., Yamashita, T., Yoshikawa, H., and Tohyama, M. (2003). PKA phosphorylates the p75 receptor and regulates its localization to lipid rafts. *Embo J* **22**, 1790-1800.

Hofmann, B., Hecht, H.J., and Flohe, L. (2002). Peroxiredoxins. *Biol Chem* **383**, 347-364.

Hovanessian, A.G., Puvion-Dutilleul, F., Nisole, S., Svab, J., Perret, E., Deng, J.S., and Krust, B. (2000). The cell-surface-expressed nucleolin is associated with the actin cytoskeleton. *Exp Cell Res* **261**, 312-328.

Hresko, R.C., and Mueckler, M. (2002). Identification of pp68 as the Tyrosine-phosphorylated Form of SYNCRIP/NSAP1. A cytoplasmic RNA-binding protein. *J Biol Chem* **277**, 25233-25238.

Ilangumaran, S., Arni, S., van Echten-Deckert, G., Borisch, B., and Hoessli, D.C. (1999). Microdomain-dependent regulation of Lck and Fyn protein-tyrosine kinases in T lymphocyte plasma membranes. *Mol Biol Cell* **10,** 891-905.

Jamora, C., Takizawa, P.A., Zaarour, R.F., Denesvre, C., Faulkner, D.J., and Malhotra, V. (1997). Regulation of Golgi structure through heterotrimeric G proteins. *Cell* **91**, 617-626.

Johnson, G.L., and Lapadat, R. (2002). Mitogen-activated protein kinase pathways mediated by ERK, JNK, and p38 protein kinases. *Science* **298**, 1911-1912.

Jones, T.A., Zou, j.Y., Cowan, S.W., Kjeldgaard, M (1991). Improved methods for the building of protein models in electron density maps and the location of errors in the models. In *Crystallographic Computing*. (Moras, D., Podany, A.D., Thiery, J.C. eds). pp. 413-432. Oxford University Press. Oxford. U.K.

Kasahara, M., Gutknecht, J., Brew, K., Spurr, N., and Goodfellow, P.N. (1989). Cloning and mapping of a testis-specific gene with sequence similarity to a sperm-coating glycoprotein gene. *Genomics* **5**, 527-534.

Kawase, H., Okuwaki, M., Miyaji, M., Ohba, R., Handa, H., Ishimi, Y., Fujii-Nakata, T., Kikuchi, A., and Nagata, K. (1996). NAP-I is a functional homologue of TAF-I that is required for replication and transcription of the adenovirus genome in a chromatin-like structure. *Genes Cells* **1**, 1045-1056.

Kelly, S.M., and Price, N.C. (2000). The use of circular dichroism in the investigation of protein structure and function. *Curr Protein Pept Sci* **1**, 349-384.

Kilsdonk, E.P., Yancey, P.G., Stoudt, G.W., Bangerter, F.W., Johnson, W.J., Phillips, M.C., and Rothblat, G.H. (1995). Cellular cholesterol efflux mediated by cyclodextrins. *J Biol Chem* **270**, 17250-17256.

Kim, J., Mosior, M., Chung, L.A., Wu, H., and McLaughlin, S. (1991). Binding of peptides with basic residues to membranes containing acidic phospholipids. *Biophys J* **60**, 135-148.

Kim, Y.M., Son, K., Hong, S.J., Green, A., Chen, J.J., Tzeng, E., Hierholzer, C., and Billiar, T.R. (1998). Inhibition of protein synthesis by nitric oxide correlates with cytostatic activity: nitric oxide induces phosphorylation of initiation factor eIF-2 alpha. *Mol Med* **4**, 179-190.

Kirchhausen, T. (1999). Adaptors for clathrin-mediated traffic. *Annu Rev Cell Dev Biol* **15**, 705-732.

Klessig, D.F., Durner, J., Noad, R., Navarre, D.A., Wendehenne, D., Kumar, D., Zhou, J.M., Shah, J., Zhang, S., Kachroo, P., Trifa, Y., Pontier, D., Lam, E., and Silva, H. (2000). Nitric oxide and salicylic acid signaling in plant defense. *Proc Natl Acad Sci U S A* **97**, 8849-8855.

Kratzschmar, J., Haendler, B., Eberspaecher, U., Roosterman, D., Donner, P., and Schleuning, W.D. (1996). The human cysteine-rich secretory protein (CRISP) family. Primary structure and tissue distribution of CRISP-1, CRISP-2 and CRISP-3. *Eur J Biochem* **236**, 827-836.

Kraulis, P (1991) MOLSCRIPT: a program to produce both detailed and schematic plots of protein structure. *J. Appl. Crystallogr*. **24**, 946-950.

Kurzchalia, T.V., and Parton, R.G. (1999). Membrane microdomains and caveolae. *Curr Opin Cell Biol* **11**, 424-431.

Ladinsky, M.S., Mastronarde, D.N., McIntosh, J.R., Howell, K.E., and Staehelin, L.A. (1999). Golgi structure in three dimensions: functional insights from the normal rat kidney cell. *J Cell Biol* **144**, 1135-1149.

Langlet, C., Bernard, A.M., Drevot, P., and He, H.T. (2000). Membrane rafts and signaling by the multichain immune recognition receptors. *Curr Opin Immunol* **12**, 250-255.

Leslie, A. G.W. (1992). Joint CCP4 and ESF-EACMB. *Newsletteer on Protein Crystallography*. No. 26. Daresbury Laboratory, Warrington, U.K.

Lisanti, M.P., Scherer, P.E., Vidugiriene, J., Tang, Z., Hermanowski-Vosatka, A., Tu, Y.H., Cook, R.F., and Sargiacomo, M. (1994). Characterization of caveolin-rich membrane domains isolated from an endothelial-rich source: implications for human disease. *J Cell Biol* **126**, 111-126.

Lischwe, M.A., Cook, R.G., Ahn, Y.S., Yeoman, L.C., and Busch, H. (1985). Clustering of glycine and NG,NG-dimethylarginine in nucleolar protein C23. *Biochemistry* **24,** 6025-6028.

Lu, G., Villalba, M., Coscia, M.R., Hoffman, D.R., and King, T.P. (1993). Sequence analysis and antigenic cross-reactivity of a venom allergen, antigen 5, from hornets, wasps, and yellow jackets. *J Immunol* **150**, 2823-2830.

Melkonian, K.A., Ostermeyer, A.G., Chen, J.Z., Roth, M.G., and Brown, D.A. (1999). Role of lipid modifications in targeting proteins to detergent-resistant membrane rafts. Many raft proteins are acylated, while few are prenylated. *J Biol Chem* **274,** 3910-3917.

Malhotra, V., Serafini, T., Orci, L., Shepherd, J.C., and Rothman, J.E. (1989). Purification of a novel class of coated vesicles mediating biosynthetic protein transport through the Golgi stack. *Cell* **58**, 329-336.

Mannick, J.B., Asano, K., Izumi, K., Kieff, E., and Stamler, J.S. (1994). Nitric oxide produced by human B lymphocytes inhibits apoptosis and Epstein-Barr virus reactivation. *Cell* **79**, 1137-1146.

McCabe, J.B., and Berthiaume, L.G. (2001). N-terminal protein acylation confers localization to cholesterol, sphingolipid-enriched membranes but not to lipid rafts/caveolae. *Mol Biol Cell* **12**, 3601-3617.

McLaughlin, S., and Aderem, A. (1995). The myristoyl-electrostatic switch: a modulator of reversible protein-membrane interactions. *Trends Biochem Sci* **20**, 272-276.

Mellor, A.L., and Munn, D.H. (1999). Tryptophan catabolism and T-cell tolerance: immunosuppression by starvation?. *Immunol Today* **20**, 469-473.

Mencinger, M., Panagopoulos, I., Contreras, J.A., Mitelman, F., and Aman, P. (1998). Expression analysis and chromosomal mapping of a novel human gene, APRIL, encoding an acidic protein rich in leucines. *Biochim Biophys Acta* **1395**, 176-180.

Mettouchi, A., Klein, S., Guo, W., Lopez-Lago, M., Lemichez, E., Westwick, J.K., and Giancotti, F.G. (2001). Integrin-specific activation of Rac controls progression through the G(1) phase of the cell cycle. *Mol Cell* **8**, 115-127.

Meuwly, P., Molders, W., Buchala, A., and Metraux, J.P. (1995). Local and Systemic Biosynthesis of Salicylic Acid in Infected Cucumber Plants. *Plant Physiol* **109**, 1107-1114.

Mi, Y., Thomas, S.D., Xu, X., Casson, L.K., Miller, D.M., and Bates, P.J. (2003). Apoptosis in leukemia cells is accompanied by alterations in the levels and localization of nucleolin. *J Biol Chem* **278**, 8572-8579.

Mineo, C., James, G.L., Smart, E.J., and Anderson, R.G. (1996). Localization of epidermal growth factor-stimulated Ras/Raf-1 interaction to caveolae membrane. *J Biol Chem* **271**, 11930-11935.

Mizutani, A., Fukuda, M., Ibata, K., Shiraishi, Y., and Mikoshiba, K. (2000). SYNCRIP, a cytoplasmic counterpart of heterogeneous nuclear ribonucleoprotein R, interacts with ubiquitous synaptotagmin isoforms. *J Biol Chem* **275**, 9823-9831.

Moffet, S.B., Deborah; Linder, Maurine. (2000). Lipid-dependent targeting of G proteins into Rafts. *J Bio Chem* **275**, 2191-2198.

Morrissette, J., Kratzschmar, J., Haendler, B., el-Hayek, R., Mochca-Morales, J., Martin, B.M., Patel, J.R., Moss, R.L., Schleuning, W.D., Coronado, R., and et al. (1995). Primary structure and properties of helothermine, a peptide toxin that blocks ryanodine receptors. *Biophys J* **68**, 2280-2288.

Mukherjee, S., and Maxfield, F.R. (2000). Role of membrane organization and membrane domains in endocytic lipid trafficking. *Traffic* **1**, 203-211.

Muller, G., and Frick, W. (1999). Signalling via caveolin: involvement in the cross-talk between phosphoinositolglycans and insulin. *Cell Mol Life Sci* **56**, 945-970.

Murphy, E.V., Zhang, Y., Zhu, W., and Biggs, J. (1995). The human glioma pathogenesis-related protein is structurally related to plant pathogenesis-related proteins and its gene is expressed specifically in brain tumors. *Gene* **159**, 131-135.

Nagar, B., Hantschel, O., Young, M.A., Scheffzek, K., Veach, D., Bornmann, W., Clarkson, B., Superti-Furga, G., and Kuriyan, J. (2003). Structural basis for the autoinhibition of c-Abl tyrosine kinase. *Cell* **112**, 859-871.

Nagata, K., Kawase, H., Handa, H., Yano, K., Yamasaki, M., Ishimi, Y., Okuda, A., Kikuchi, A., and Matsumoto, K. (1995). Replication factor encoded by a putative oncogene, set, associated with myeloid leukemogenesis. *Proc Natl Acad Sci U S A* **92**, 4279-4283.

Nagata, K., Saito, S., Okuwaki, M., Kawase, H., Furuya, A., Kusano, A., Hanai, N., Okuda, A., and Kikuchi, A. (1998). Cellular localization and expression of template-activating factor I in different cell types. *Exp Cell Res* **240**, 274-281.

Nathan, C. (2003). Specificity of a third kind: reactive oxygen and nitrogen intermediates in cell signaling. *J Clin Invest* **111**, 769-778.

Nathan, C., and Shiloh, M.U. (2000). Reactive oxygen and nitrogen intermediates in the relationship between mammalian hosts and microbial pathogens. *Proc Natl Acad Sci U S A* **97**, 8841-8848.

Nicholls, A., Bharadwaj, R., Honig, M. (1993). GRASP: graphical representation and analysis of surface properties*. Biophys. J*. **64**, A166

Nickel, W., Brugger, B., and Wieland, F.T. (1998). Protein and lipid sorting between the endoplasmic reticulum and the Golgi complex. *Semin Cell Dev Biol* **9**, 493-501.

Nilsson, T., and Warren, G. (1994). Retention and retrieval in the endoplasmic reticulum and the Golgi apparatus. *Curr Opin Cell Biol* **6**, 517-521.

Nisole, S., Krust, B., and Hovanessian, A.G. (2002). Anchorage of HIV on permissive cells leads to coaggregation of viral particles with surface nucleolin at membrane raft microdomains. *Exp Cell Res* **276**, 155-173.

Oh, P., and Schnitzer, J.E. (2001). Segregation of heterotrimeric G proteins in cell surface microdomains. G(q) binds caveolin to concentrate in caveolae, whereas G(i) and G(s) target lipid rafts by default. *Mol Biol Cell* **12**, 685-698.

Okamoto, T., Schlegel, A., Scherer, P.E., and Lisanti, M.P. (1998). Caveolins, a family of scaffolding proteins for organizing "preassembled signaling complexes" at the plasma membrane. *J Biol Chem* **273**, 5419-5422.

Oktay, M., Wary, K.K., Dans, M., Birge, R.B., and Giancotti, F.G. (1999). Integrin-mediated activation of focal adhesion kinase is required for signaling to Jun NH2-terminal kinase and progression through the G1 phase of the cell cycle. *J Cell Biol* **145**, 1461-1469.

Okuwaki, M., and Nagata, K. (1998). Template activating factor-I remodels the chromatin structure and stimulates transcription from the chromatin template. J *Biol Chem* **273**, 34511-34518.

Pagano, R.E., Puri, V., Dominguez, M., and Marks, D.L. (2000). Membrane traffic in sphingolipid storage diseases. *Traffic* **1**, 807-815.

Parpal, S., Karlsson, M., Thorn, H., and Stralfors, P. (2001). Cholesterol depletion disrupts caveolae and insulin receptor signaling for metabolic control via insulin receptor substrate-1, but not for mitogen-activated protein kinase control. *J Biol Chem* **276**, 9670-9678.

Peitzsch, R.M., and McLaughlin, S. (1993). Binding of acylated peptides and fatty acids to phospholipid vesicles: pertinence to myristoylated proteins. *Biochemistry* **32**, 10436-10443.

Pelkmans, L., Kartenbeck, J., and Helenius, A. (2001). Caveolar endocytosis of simian virus 40 reveals a new two-step vesicular-transport pathway to the ER. *Nat Cell Biol* **3**, 473-483

Pervin, S., Singh, R., and Chaudhuri, G. (2001). Nitric oxide-induced cytostasis and cell cycle arrest of a human breast cancer cell line (MDA-MB-231): potential role of cyclin D1. *Proc Natl Acad Sci U S A* **98**, 3583-3588.

Peter, M., Nakagawa, J., Doree, M., Labbe, J.C., and Nigg, E.A. (1990). Identification of major nucleolar proteins as candidate mitotic substrates of cdc2 kinase. *Cell* **60**, 791-801.

Pfeffer, S. (2003). Membrane domains in the secretory and endocytic pathways. *Cell* **112**, 507-517.

Pike, L.J., and Miller, J.M. (1998). Cholesterol depletion delocalizes phosphatidylinositol bisphosphate and inhibits hormone-stimulated phosphatidylinositol turnover. *J Biol Chem* **273**, 22298-22304.

Prior, I.A., and Hancock, J.F. (2001). Compartmentalization of Ras proteins. *J Cell Sci* **114**, 1603-1608.

Prior, I.A., Harding, A., Yan, J., Sluimer, J., Parton, R.G., and Hancock, J.F. (2001). GTP-dependent segregation of H-ras from lipid rafts is required for biological activity. *Nat Cell Biol* **3**, 368-375.

Rao, S.V., Mamrack, M.D., and Olson, M.O. (1982). Localization of phosphorylated highly acidic regions in the NH2-terminal half of nucleolar protein C23. *J Biol Chem* **257**, 15035-15041.

Resh, M.D. (1999). Fatty acylation of proteins: new insights into membrane targeting of myristoylated and palmitoylated proteins. *Biochim Biophys Acta* **1451**, 1-16.

Rich, T., Chen, P., Furman, F., Huynh, N., and Israel, M.A. (1996). RTVP-1, a novel human gene with sequence similarity to genes of diverse species, is expressed in tumor cell lines of glial but not neuronal origin. *Gene* **180**, 125-130.

Roper, K., Corbeil, D., and Huttner, W.B. (2000). Retention of prominin in microvilli reveals distinct cholesterol-based lipid micro-domains in the apical plasma membrane. *Nat Cell Biol* **2**, 582-592.

Roy, S., Luetterforst, R., Harding, A., Apolloni, A., Etheridge, M., Stang, E., Rolls, B., Hancock, J.F., and Parton, R.G. (1999). Dominant-negative caveolin inhibits H-Ras function by disrupting cholesterol-rich plasma membrane domains. *Nat Cell Biol* **1**, 98-105.

Ruano, M.J., Hernandez-Hernando, S., Jimenez, A., Estrada, C., and Villalobo, A. (2003). Nitric oxide-induced epidermal growth factor-dependent phosphorylations in A431 tumour cells. *Eur J Biochem* **270**, 1828-1837.

Said, E.A., Krust, B., Nisole, S., Svab, J., Briand, J.P., and Hovanessian, A.G. (2002). The anti-HIV cytokine midkine binds the cell surface-expressed nucleolin as a low affinity receptor. *J Biol Chem* **277**, 37492-37502.

Sawai, T., Negishi, M., Nishigaki, N., Ohno, T., and Ichikawa, A. (1993). Enhancement by protein kinase C of prostacyclin receptor-mediated activation of adenylate cyclase through a calmodulin/myristoylated alanine-rich C kinase substrate (MARCKS) system in IC2 mast cells. *J Biol Chem* **268**, 1995-2000.

Scheel, J., Srinivasan, J., Honnert, U., Henske, A., and Kurzchalia, T.V. (1999). Involvement of caveolin-1 in meiotic cell-cycle progression in Caenorhabditis elegans. *Nat Cell Biol* **1**, 127-129.

Schmidt, H.H., and Walter, U. (1994). NO at work. *Cell* **78**, 919-925.

Schmidt-Zachmann, M.S., and Nigg, E.A. (1993). Protein localization to the nucleolus: a search for targeting domains in nucleolin. *J Cell Sci* **105** (Pt 3), 799-806.

Schneider, D.S. (2002). Plant immunity and film Noir: what gumshoe detectives can teach us about plant-pathogen interactions. *Cell* **109**, 537-540.

Schnitzer, J.E., McIntosh, D.P., Dvorak, A.M., Liu, J., and Oh, P. (1995). Separation of caveolae from associated microdomains of GPI-anchored proteins. *Science* **269**, 1435-1439.

Schreiber, M.C., Karlo, J.C., and Kovalick, G.E. (1997). A novel cDNA from Drosophila encoding a protein with similarity to mammalian cysteine-rich secretory proteins, wasp venom antigen 5, and plant group 1 pathogenesis-related proteins. *Gene* **191**, 135-141.

Schuren, F.H., Asgeirsdottir, S.A., Kothe, E.M., Scheer, J.M., and Wessels, J.G. (1993). The Sc7/Sc14 gene family of Schizophyllum commune codes for extracellular proteins specifically expressed during fruit-body formation. *J Gen Microbiol* **139**, 2083-2090.

Seo, S.B., McNamara, P., Heo, S., Turner, A., Lane, W.S., and Chakravarti, D. (2001). Regulation of histone acetylation and transcription by INHAT, a human cellular complex containing the set oncoprotein. *Cell* **104**, 119-130.

Serafini, T., Orci, L., Amherdt, M., Brunner, M., Kahn, R.A., and Rothman, J.E. (1991). ADP-ribosylation factor is a subunit of the coat of Golgi-derived COP-coated vesicles: a novel role for a GTP-binding protein. *Cell* **67**, 239-253.

Shorter, J., and Warren, G. (2002). Golgi architecture and inheritance. *Annu Rev Cell Dev Biol* **18**, 379-420.

Simons, K., and Ikonen, E. (1997). Functional rafts in cell membranes. *Nature* **387**, 569-572.

Singer, S.J., and Nicolson, G.L. (1972). The fluid mosaic model of the structure of cell membranes. *Science* **175**, 720-731.

Smart, E.J., Graf, G.A., McNiven, M.A., Sessa, W.C., Engelman, J.A., Scherer, P.E., Okamoto, T., and Lisanti, M.P. (1999). Caveolins, liquid-ordered domains, and signal transduction. *Mol Cell Bio*l **19**, 7289-7304.

Sohn, K., Orci, L., Ravazzola, M., Amherdt, M., Bremser, M., Lottspeich, F., Fiedler, K., Helms, J.B., and Wieland, F.T. (1996). A major transmembrane protein of Golgi-derived COPI-coated vesicles involved in coatomer binding. *J Cell Biol* **135**, 1239-1248.

Song, K.S., Li, S., Okamoto, T., Quilliam, L.A., Sargiacomo, M., and Lisanti, M.P. (1996). Co-purification and direct interaction of Ras with caveolin, an integral membrane protein of caveolae microdomains. Detergent-free purification of caveolae microdomains. *J Biol Chem* **271**, 9690-9697**.**

Srivastava, M., and Pollard, H.B. (1999). Molecular dissection of nucleolin's role in growth and cell proliferation: new insights. *Faseb J* **13**, 1911-1922.

Stamler, J.S. (1994). Redox signaling: nitrosylation and related target interactions of nitric oxide. *Cell* **78**, 931-936.

Sternberg, P.W., and Schmid, S.L. (1999). Caveolin, cholesterol and Ras signalling [news; comment]. *Nat Cell Biol* **1**, E35-37.

Sutterlin, C., Doering, T.L., Schimmoller, F., Schroder, S., and Riezman, H. (1997). Specific requirements for the ER to Golgi transport of GPI-anchored proteins in yeast. *J Cell Sci* **110**, 2703-2714.

Suzuki, N., Saito, T., and Hosoya, T. (1987). In vivo effects of dexamethasone and cycloheximide on the phosphorylation of 110-kDa proteins and the protein kinase activities of rat liver nucleoli. *J Biol Chem* **262**, 4696-4700.

Szyperski, T., Fernandez, C., Mumenthaler, C., and Wuthrich, K. (1998). Structure comparison of human glioma pathogenesis-related protein GliPR and the plant pathogenesis-related protein P14a indicates a functional link between the human immune system and a plant defense system*. Proc Natl Acad Sci U S A* **95**, 2262-2266.

Thiede, B., Dimmler, C., Siejak, F., and Rudel, T. (2001). Predominant identification of RNA-binding proteins in Fas-induced apoptosis by proteome analysis. *J Biol Chem* **276**, 26044-26050.

Thomma, B., Eggermont, K., Penninckx, I., Mauch-Mani, B., Vogelsang, R., Cammue, B.P.A., and Broekaert, W.F. (1998). Separate jasmonate-dependent and salicylate-dependent defense-response pathways in arabidopsis are essential for resistance to distinct microbial pathogens. *Proc Natl Acad Sci U S A* **95**, 15107-15111.

Vainio, S., Heino, S., Mansson, J.E., Fredman, P., Kuismanen, E., Vaarala, O., and Ikonen, E. (2002). Dynamic association of human insulin receptor with lipid rafts in cells lacking caveolae. *EMBO Rep* **3**, 95-100.

van Meer, G. (1989). Lipid traffic in animal cells. *Annu Rev Cell Biol* **5**, 247-275.
van't Hof, W., and Resh, M.D. (1997). Rapid plasma membrane anchoring of newly synthesized p59fyn: selective requirement for NH2-terminal myristoylation and palmitoylation at cysteine-3. *J Cell Biol* **136**, 1023-1035.

Vieira, O.V., Botelho, R.J., and Grinstein, S. (2002). Phagosome maturation: aging gracefully. *Biochem J* **366**, 689-704.

Vincent, J.P. (2003). Membranes, trafficking, and signaling during animal development. *Cell* **112**, 745-749.

Volonte, D., Galbiati, F., Li, S., Nishiyama, K., Okamoto, T., and Lisanti, M.P. (1999). Flotillins/cavatellins are differentially expressed in cells and tissues and form a hetero-oligomeric complex with caveolins in vivo. Characterization and epitope-mapping of a novel flotillin-1 monoclonal antibody probe. *J Biol Chem* **274**, 12702-12709.

Volonte, D., Zhang, K., Lisanti, M.P., and Galbiati, F. (2002). Expression of caveolin-1 induces premature cellular senescence in primary cultures of murine fibroblasts. *Mol Biol Cell* **13**, 2502-2517.

Wakasugi, K., and Schimmel, P. (1999). Two distinct cytokines released from a human aminoacyl-tRNA synthetase. *Science* **284**, 147-151.

Wang, Y., Thiele, C., and Huttner, W.B. (2000). Cholesterol is required for the formation of regulated and constitutive secretory vesicles from the trans-Golgi network. *Traffic* **1**, 952-962.

Wang, Y., Guan, J., Wang, H., Leeper, D., and Iliakis, G. (2001). Regulation of dna replication after heat shock by replication protein a-nucleolin interactions. *J Biol Chem* **276**, 20579-20588.

Ward, T.H., Polishchuk, R.S., Caplan, S., Hirschberg, K., and Lippincott-Schwartz, J. (2001). Maintenance of Golgi structure and function depends on the integrity of ER export. *J Cell Biol* **155**, 557-570.

Warren, G., and Malhotra, V. (1998). The organisation of the Golgi apparatus. *Curr Opin Cell Biol* **10**, 493-498.

Wary, K.K., Mariotti, A., Zurzolo, C., and Giancotti, F.G. (1998). A requirement for caveolin-1 and associated kinase Fyn in integrin signaling and anchorage-dependent cell growth. *Cell* **94**, 625-634.

Weiner, A.M., and Maizels, N. (1999). A deadly double life. *Science* **284**, 63-64.

Weiss, O., Holden, J., Rulka, C., and Kahn, R.A. (1989). Nucleotide binding and cofactor activities of purified bovine brain and bacterially expressed ADP-ribosylation factor. *J Biol Chem* **264**, 21066-21072.

Yamaguchi, T., Nagahama, M., Itoh, H., Hatsuzawa, K., Tani, K., and Tagaya, M. (2000). Regulation of the golgi structure by the alpha subunits of heterotrimeric G proteins. *FEBS Lett* **470**, 25-28.

Yamakawa, T., Miyata, S., Ogawa, N., Koshikawa, N., Yasumitsu, H., Kanamori, T., and Miyazaki, K. (1998). cDNA cloning of a novel trypsin inhibitor with similarity to pathogenesis-related proteins, and its frequent expression in human brain cancer cells. *Biochim Biophys Acta* **1395**, 202-208.

Yamazaki, Y., Koike, H., Sugiyama, Y., Motoyoshi, K., Wada, T., Hishinuma, S., Mita, M., and Morita, T. (2002). Cloning and characterization of novel snake venom proteins that block smooth muscle contraction. *Eur J Biochem* **269**, 2708-2715.

Yanagida, M., Shimamoto, A., Nishikawa, K., Furuichi, Y., Isobe, T., and Takahashi, N. (2001). Isolation and proteomic characterization of the major proteins of the nucleolin-binding ribonucleoprotein complexes. *Proteomics* **1**, 1390-1404.

Yang, T.H., Tsai, W.H., Lee, Y.M., Lei, H.Y., Lai, M.Y., Chen, D.S., Yeh, N.H., and Lee, S.C. (1994). Purification and characterization of nucleolin and its identification as a transcription repressor. *Mol Cell Biol* **14**, 6068-6074.

Zetterberg, A., and Larsson, O. (1985). Kinetic analysis of regulatory events in G1 leading to proliferation or quiescence of Swiss 3T3 cells. *Proc Natl Acad Sci U S A* **82**, 5365-5369.

Zheng, J., Knighton, D.R., Xuong, N.H., Taylor, S.S., Sowadski, J.M., and Ten Eyck, L.F. (1993). Crystal structures of the myristylated catalytic subunit of cAMP-dependent protein kinase reveal open and closed conformations. *Protein Sci* **2**, 1559-1573.

Zhou, W., Parent, L.J., Wills, J.W., and Resh, M.D. (1994). Identification of a membrane-binding domain within the amino-terminal region of human immunodeficiency virus type 1 Gag protein which interacts with acidic phospholipids. *J Virol* **68**, 2556-2569.

Acknowledgments

I want to thank Dr. Bernd Helms for all his support, endurance and understanding during the development of this work, and for his encouragement under the difficult circumstances

My deep gratitude goes to Prof. Dr. Felix T. Wieland for allowing me to carry out my thesis work in his lab and for his advices.

Maribel quiero agradecerte por tu amistad y tu apoyo. Me disté la fuerza y la confianza que necesité en los momentos difíciles. También te agradezco por los tiempos de alegría y felicidad. No puedo dejar pasar todo el apoyo científico que me brindaste en el desarrollo de este trabajo.

Susana te agradezco por comprenderme y escucharme en lo bueno y lo malo, y por tu amistad incondicional.

I thank Dr. Britta Brügger for all the kindly and honest support during many difficult moments.

To my friend Holger Kühn who offered a hand during some of the most important struggles of my life, for bringing hope, understanding, and for his patience in listening my ramblings.

To Phillipp Milkereit who always was willing to wander through many matters. Our moments together opened up hope for believing that good things are always possible.

Claudia Seleenmeyer, sharing living and life with you has been a meaningful, wonderful and great task. I thank you for our time together, for your friendship, and your trust. You deserve the best.

To Dora Kaloyanova who always challenged my views in science and life. You are a friend that is very critical but supportive in all moments. I am missing many of the things we shared during my time in Germany.

Xueyi Li for his invaluable scientific help during this time we share and for his friendship in the moments of confusion, conflict and despair.

Pablo Hess, a good friend who gave me some of the best and great moments in Germany.

Ari Satyagraha, you are always being a good and meaningful friend. We shared great moments in Germany. Thanks for your trust and care.

Hatim for sharing good moments during the time we spent in the lab, the respect and the brotherhood developed in the moments of struggle.

To Julien who was always a good listener, willing to say the right word at the right time.

To Sandra, Thilo and Raphael for bringing freshness and joy in the moments I needed the most.

To Martina Bremser who was willing to give unconditional help and care.

To Gabi Weiss who provided the technical experience, time and extra help in cell culture.

To Matthew Groves who provided me with excellent advices and interesting ideas during the preparation and writing of this thesis, as well for his contribution in making the graphic representations of GAPR-1 used in this thesis.

To Valérie Paneels, my deep gratitude goes for all her kindness and unrestricted help during the preparation of the circular dichroism experiments. Without her commitment and enthusiasm this task would not have been accomplished.

To Manuela de La Paz (Manoli) who was willing to discuss my data, and her kindness to provide advice and suggestions.

To all past and present BZH members for their kindness, Andreas, Daniel, Heike, Peter, Armin, Jörg, Sun Zhe, André, Boyan, Klaus, Sabine, Dominik, Ibrahim, Connie, Jutta, Stephan, Marisa, Fatima.